CAPACITANCE OF PLANAR CAPACITORS AND DISCONTINUOUS METAL FILMS

A THESIS SUBMITTED BY

ADEL GIRGIS BISHAY

FOR THE DEGREE OF DOCTOR OF PHILOSOPHY

THE CITY UNIVERSITY
DEPARTMENT OF PHYSICS
NORTHAMPTON SQUARE
LONDON

JUNE 1985

THIS THESIS IS DEDICATED

LOVINGLY

TO MY WIFE [redacted]

Contents

ACKNOWLEDGEMENTS

I would like to express my deep thanks and gratitude to Dr. D.W. Stops for supervising this project and his stimulating advice during the different phases of the undertaken research.

My thanks are also due to Dr. [redacted], a visitor to the Electrical Engineering Department, for his guidance on the measurement of very small capacitance.

My gratitude to Mr. [redacted] for taking the electron micrographs. Also, I thank Mr. [redacted] and Mr. [redacted] for their technical help during the experimental work.

I would also like to express my thanks and appreciation to my wife, [redacted], for her encouragement and patience during my studies.

Finally, I am grateful to the Egyptian government for the financial support without which this research could not have been accomplished.

ABSTRACT

The planar capacitors were prepared by depositing two co-planar electrodes of relatively thick aluminium films on one side of two different substrates, namely, Corning glass (7059) and "Melinex" which is the trade name of plastic sheets (polyethelene terephthalate). The length and width of the electrodes are 25mm and 4mm respectively while the width of the gap between them is 2mm. The capacitance of these capacitors was (i) calculated (ii) measured at different frequencies in the frequency range (1-100)Kc. The calculated values of the planar capacitance are slightly larger than the measured ones; but they could be considered in reasonable agreement if we allow, qualitatively, for the reduction in two of the contributions to the calculated capacitance, namely, the contribution from the medium above the electrodes and the contribution from the medium underneath the substrate. The reduction is due to the presence of the lid and the bottom of the shield box which enclosed the capacitors during the measurements. The in situ monitoring of the changes in the planar capacitance and the dissipation factor of the capacitors, which used as sensing devices, as a consequence of depositing discontinuous gold and aluminium films across their gaps enabled us to (i) measure (deduce) the capacitance of the films (ii) see the factors which affect the dissipation factor after laying down the films. It was found that the capacitance of the films and the dissipation factor depends on the d.c. resistance of the films at the moment of halting the deposition, the operating frequency and time. Also the measured capacitance of our films was compared with (i) the calculated capacitance under certain conditions and not for the films themselves (ii) the

reported values in the literature for the measured capacitance of discontinuous metal films and in this context it is very important to focus on the fact that the reported values were not the outcome of investigations conducted with the intention of measuring the capacitance of the films (Pd, Mn) but only mentioned as a by-product of the main enquiries. The comparison has revealed that the measured capacitance is larger than the calculated one and much smaller than those reported of Pd and Mn films.

CHAPTER 1 INTRODUCTION

1.1 Thin film microelectronics

In the past, most major advances in electronic technology have been associated with a reduction in the size of new devices compared with those in general use at the time. The prime example of this is the general replacement of vacuum tubes by semiconductor devices. In more recent years the space programme has required the development of smaller circuits to ease the problems associated with pay-load limitations and this represents one of the motivations behind the present widespread interest in thin film microelectronics which primarily exists for the purpose of micro-miniaturization with consequent high component packing densities.

1.2 Thin film resistors

Before the design of a thin film resistor can begin, it is necessary to choose the most appropriate film and substrate material for the particular application under consideration and once these have been chosen, the design problem consists of establishing a geometrical pattern of a given thickness which meets the resistor requirements of stability, power rating, size, resistance value and frequency response.

Generally, the pattern that evolves will resemble one of the two shown in Fig. (1.1). The straight line pattern on the left is normally used for low-value resistors, and the meandering-line pattern on the right is used for larger values. A major part of the resistor design problem is the specification of the dimensions indicated in the figure. The resistance of the straight line resistor can be expressed as

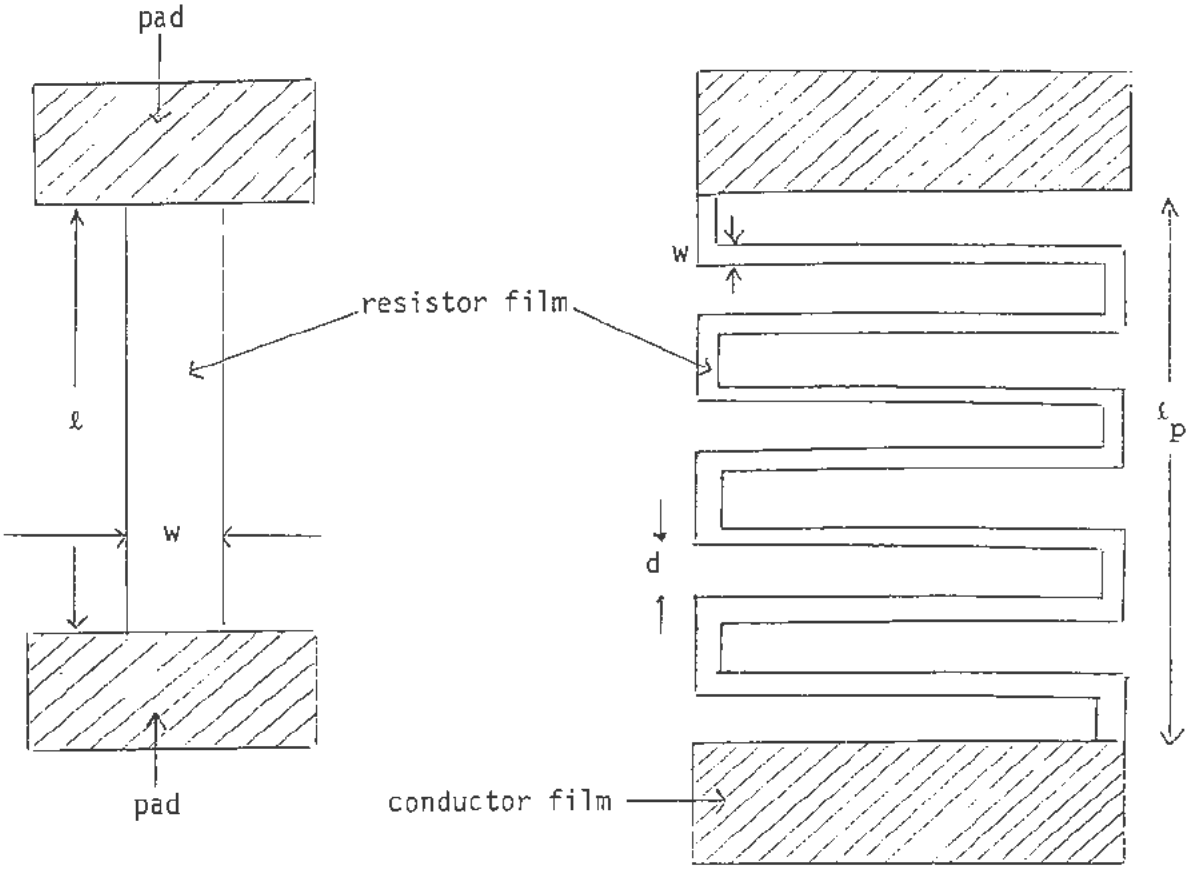

Fig. (1.1) Thin film resistor patterns

$$R = \frac{\rho}{t_f} \frac{\ell}{w} = R_{\square} \frac{\ell}{w} \qquad (1.1)$$

where ρ and t_f are the resistivity and thickness of the film respectively, $\frac{\ell}{w}$ is the aspect ratio of the film and $R_{\square}$ is the surface resistivity or the sheet resistance of the film, which is expressed in $\Omega/\square$.

From the capacitance point of view (1), the straight line resistor pattern has very little capacitance associated with the resistor path itself. In fact, the termination areas (the two electrodes) provide considerably more shunting capacitance than the path does. In the meandering-line pattern there is a shunting capacitance between adjacent meanders that can be significant, particularly when the substrate material has a high dielectric constant. It is clear that the resistor lines are connected at one end so that the capacitance of interest is actually distributed along the resistor path. This makes the lump-equivalent model only an approximation, particularly at high frequencies where the shunting capacitance effects are most important. An equivalent circuit of the meandering-line resistor, which includes the distributed nature of the capacitance, is shown in Fig. (1.2). This equivalent circuit also includes the series inductance effects, and is drawn to represent the meandering line resistor shown in Fig. (1.1).

Measurements have been made on tantalum nitride film resistors with different meandering patterns. The total shunting capacitance was found to be about 0.1pF and the series inductance was about 5nH. Resistors of value above 1000Ω are limited in performance by shunting capacitance effects, whilst those of smaller values are more affected by the series inductance. In the region of

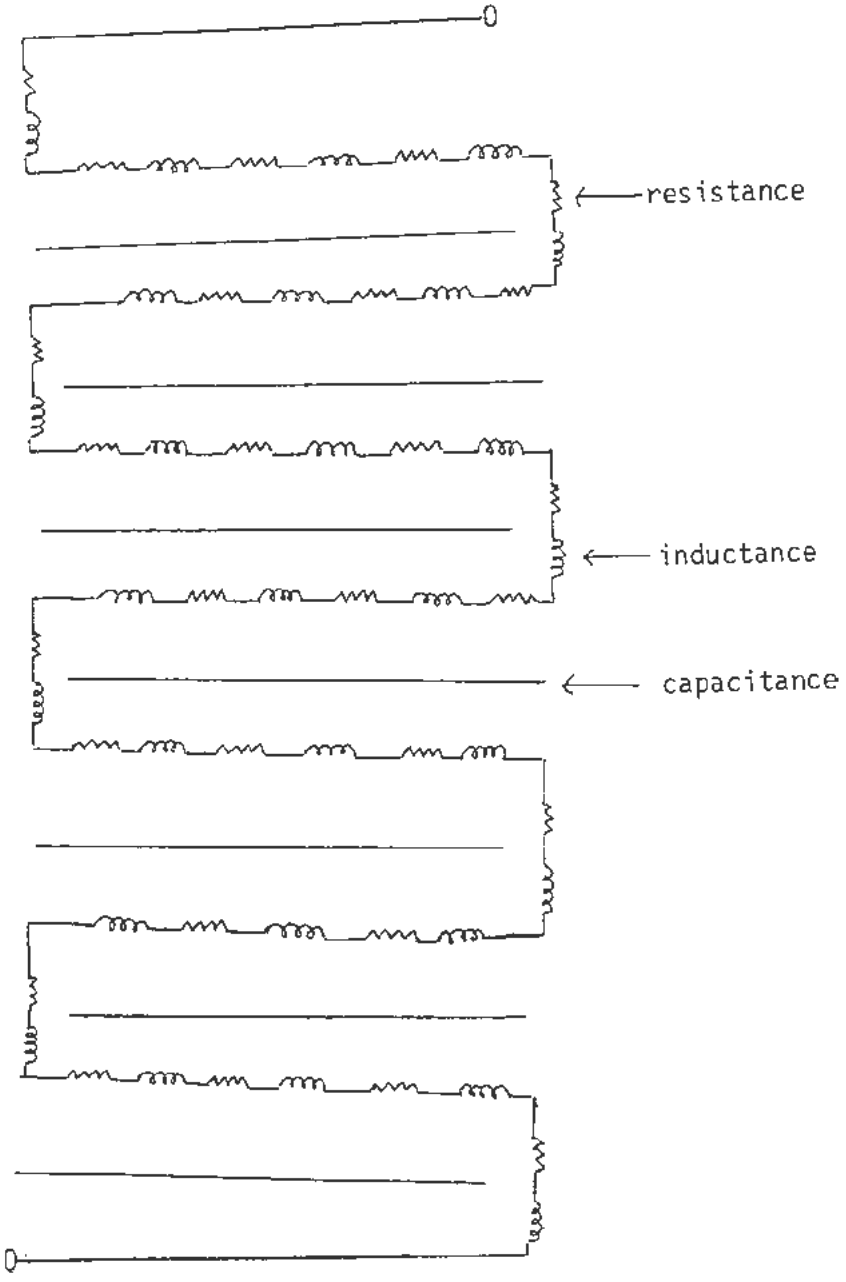

Fig. (1.2) Schematic diagram of thin film resistor including distributed parasitics

1000Ω, the impedance is essentially a pure resistance to frequencies above 100MHz. To appreciably improve the high frequency performance, it is necessary to reduce the shunting capacitance.

1.3 Planar capacitors

As already mentioned in Section 1.2 there is always capacitance between any two metallic paths deposited on one side of dielectric substrate. It will be appropriate at this stage to illustrate the different contributions to such capacitance and hence the factors which affect its magnitude.

1.3.a Theoretical calculation of planar capacitance

The capacitance betwen two metallic electrodes deposited on one side of dielectric substrate as in Fig. (1.3) was calculated by different researchers (1-3), who reported that there are two main contributions to such a capacitance:

(i) Contribution from the medium above the electrodes, which may be any dielectric, and whose value (C_I) depends on W, d, L and the dielectric constant of the medium.

$$C_I = \frac{\varepsilon_0}{2} \frac{K(k_1')}{K(k_1)} L \qquad (1.2)$$

where K(k) is the complete elliptical integral of the first kind,

$\varepsilon_0 = 8.85 \times 10^{-12} \frac{F}{m}$ and

$$k_1 = \frac{d}{2W + d} \quad , \quad k_1' = \sqrt{1 - k_1^2}$$

(ii) Contribution from the medium below the electrodes namely the

substrate contribution C_{II} whose value depends on T, E_r, W, d and L where T, E_r are the thickness and dielectric constant of the substrate respectively. The value of the substrate contribution can be calculated by comparing this contribution with that of an equivalent capacitance of parallel plate capacitor as in Fig. (1.4)

$$C'_{II} = \frac{C_{II}}{L} = 0.886\ E_r \frac{t_0}{d_0}\ \text{pF/cm} \qquad (1.3)$$

By conformal transformation an exact relationship between t_0 and d_0 in terms of W, T and d can be obtained. The Schwarz-Christoffel transform yields a solution in terms of elliptic integrals. Numerical values of these integrals K are available from standard reference tables.

$$d'_0 = 2K(\cos\theta,\ \pi/2) \qquad \text{with } d'_0 = \frac{\pi d_0}{4T}$$

$$t'_0 = K(\sin\theta,\ \pi/2) \qquad \text{with } t'_0 = \frac{\pi t_0}{4T}$$

$$\text{Cos}\theta = \frac{\tanh d'}{\tanh(2W' + d')} \qquad \text{with } W' = \frac{\pi W}{4T},\ d' = \frac{\pi d}{4T}$$

In fact there is a contribution from the medium underneath the substrate (C_{IV}) but this can be ignored if $E_r >> 1$ and $T >> 2W + d$. In view of this presentation we have to ask why the capacitance (C_{III}) between faces 1 and 2 in Fig. (1.3) was not involved. Generally speaking, to calculate (C_{III}) the thickness of the electrodes (t_e) and the dielectric constant (ϵ) of the medium separating them must be known according to the following equation

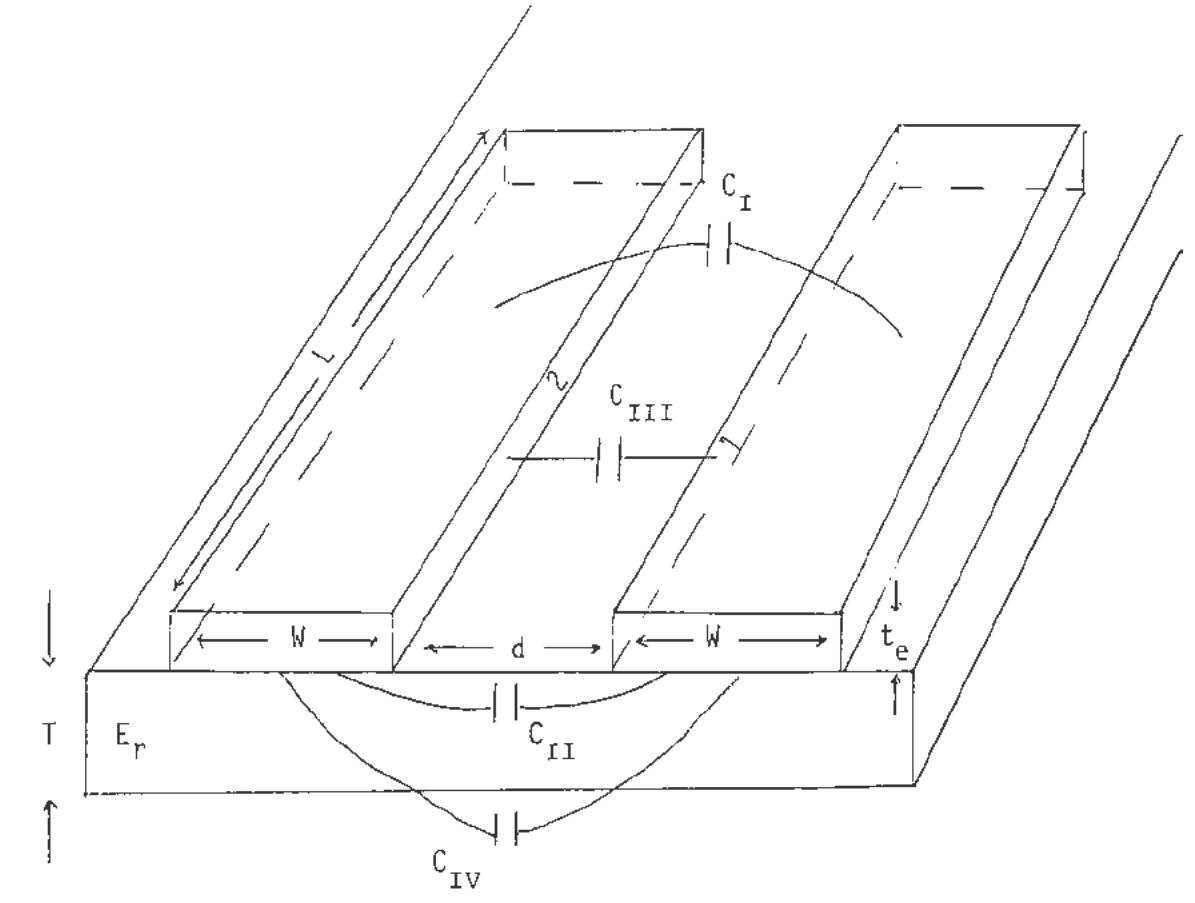

Fig. (1.3) Different contributions to the planar capacitance (not to scale)

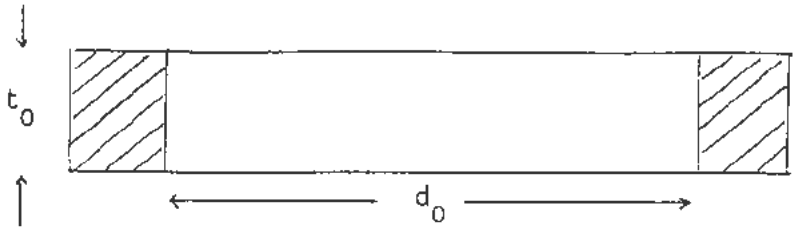

Fig. (1.4)

$$C_{III} = \varepsilon_0 \varepsilon \frac{t_e L}{d} \qquad (1.4)$$

ε can be taken as that of air (unity) (4)

To have an idea about the magnitudes of (C_I) and (C_{II}) we will quote an example already published in the literature (1) if $L = 2.54 \times 10^{-2}$m, $W = d = 2.54 \times 10^{-4}$m, $T = 12.7 \times 10^{-4}$m, $E_r = 5.8$

$C_I = 0.18$pF , $C_{II} = 1$pf

to calculate (C_{III}) for such dimensions, we put $t_e = 10^3$A°, $\varepsilon = 1$ in equation (1.4), $C_{III} = 8.8 \times 10^{-5}$pF.

It is clear that (C_{III}) is much smaller than C_I and C_{II} and this explains why it was not involved.

1.3.b Literature survey related to planar capacitors

From the published literature it appears that there is only one relevant paper and that is by Kaiser and Castro (3) who calculated and measured the capacitance between two metallic paths (electrodes) deposited on $BaTiO_3$ with very high dielectric constant ($E_r = 1770$, T = 0.02 inch). Their calculations were carried out for $\frac{W}{T}$ ranges from 0.2 to infinity corresponding to $\frac{d}{T}$ from 1 to 7 while the measurements were performed only for $\frac{W}{T} = 1$. It is very important to emphasise that the motivation behind their investigation was not interest in planar capacitors in the sense illustrated in Section 1.3 for they were really concerned with how to avoid the harmful effects on thin film circuits performance resulting when the size of the capacitance between the various conductive paths is no longer negligible compared with circuit components. As a matter of fact, it is not necessary for all the planar capacitors to be prepared as in Fig. (1.3)

but the two metallic electrodes could be of interdigitated nature and in this context, Keister and Scapple (5) have used planar quartz capacitors, with deposited aluminium electrodes etched to the appropriate comb pattern by means of the conventional photo-resist etching technique, to determine the thickness and rate of deposition of silicon monoxide films by observing the change in capacitance as a result of depositing these films on the quartz capacitors. Also, Binotto and Picicentini (6) have studied the effect of varying the geometrical dimensions and frequency (10^3Hz - 100MHz) on the loss factor and capacitance of interdigitated planar capacitors with 96% alumina glazed as substrate (T = 0.03 inch, E_r = 9.6). Interdigitated planar capacitors were also used in the investigation conducted by Channon and Barnwell (7) to develop humidity sensitive thick film paste which can help in the fabrication of humidity transducers using standard thick film processing equipment.

1.3.c Representation of planar capacitors

The capacitor is the only element which can be made to approach the ideal (8) very closely, that is, to have the least amount of unwanted residual properties. Nevertheless, actual capacitors do not have ideal behaviour not only because of internal losses, but also because connections must be made by means of leads which introduce series resistance (r_s) and inductance (L') as shown in Fig. (1.5). At low frequencies the effects of (r_s) and (L') (9,10) are negligible provided that external connections are kept very short. However internal losses (dielectric losses) (11) occur in all solid and liquid dielectrics due to (i) conduction currents (ii) hystersis. The conduction current is due to the imperfect insulating qualities of the dielectric and is calculated by the application of Ohm's

law; it is in phase with the applied voltage and results in a power loss in the material and is dissipated as heat. The dielectric hysteresis is defined as the lagging of the electric flux behind the electric force producing it, so that under a varying electric field a further dissipation of energy as heat occurs. The mechanisms responsible for the hysteresis (12) will depend on the ways in which a substance may be polarized; there are various forms of electrical polarization like electronic, ionic, structural dipole, point defect dipole and interfacial polarization at crystallites. Dielectric hysteresis cannot be measured as a separate quantity and in practice only the total dielectric losses are measured usually by means of an a.c. bridge. Consequent to these losses the current through such an imperfect capacitor will not lead the applied voltage by $\frac{\pi}{2}$ but will differ therefrom by an angle δ called the loss angle of the capacitor. The angle δ is a measure of the imperfection of the capacitor. A perfect capacitor is one in which there is no energy loss so that $\delta = 0$; this ideal is most nearly obtained in a capacitor with air or other gas as a dielectric. So far as its effect in an a.c circuit is concerned, an imperfect capacitor (13) can be represented by a perfect capacitance in combination with a resistance. The equivalent capacitance and resistance can be most simply arranged either in series or in parallel. The resistance is chosen to dissipate the same power as the imperfect capacitor, and in combination with the capacitance to give the same loss angle. The equivalent series arrangement (the capacitor being considered as an impedance) is usually more convenient in practice, but the parallel arrangement (the capacitor being considered as an admittance) is sometimes useful, particularly for h.f. measurements; both are illustrated in Fig. (1.6).

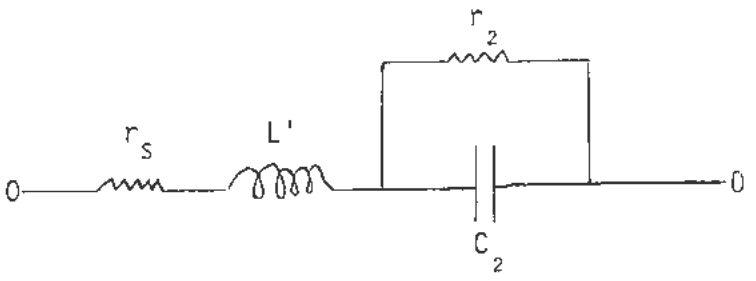

Fig. (1.5) Equivalent circuit capacitor to emphasise the losses due to r_s and L'

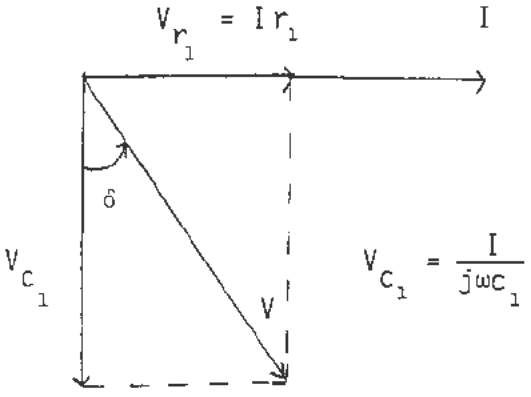

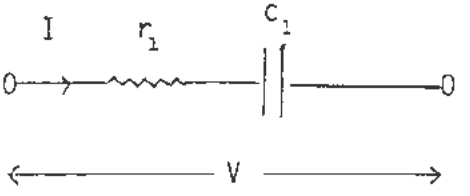

$$\tan\delta = \omega r_1 c_1$$

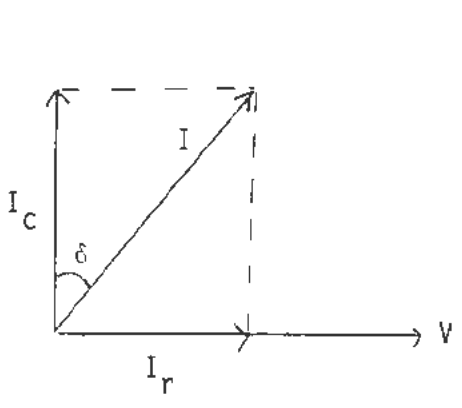

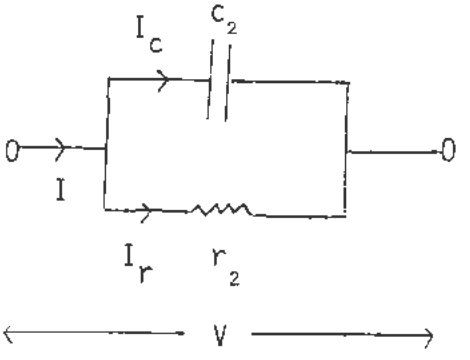

$$\tan\delta = \frac{1}{\omega r_2 c_2}$$

Fig. (1.6) Circuits equivalent to an imperfect capacitor

By straightforward circuit analysis, the following relations can be deduced

$$C_2 = \frac{C_1}{1 + \tan^2\delta} \qquad (1.5) \quad , \quad \frac{r_2}{r_1} = \frac{\tan^2\delta + 1}{\tan^2\delta} \qquad (1.6)$$

if $\tan\delta << 1 \therefore C_2 = C_1$ and if $\tan^2\delta >> 1 \therefore r_2 = r_1$.

It will be appropriate in the present context to find expression for $\tan\delta$ in terms of the real (E_r') and imaginary (E_r'') parts of the dielectric constant (E_r) of any dielectric material. From the definition of dielectric hysteresis already mentioned, E_r can be described as complex quantity (14)

$$E_r = E_r' - jE_r'' \qquad (1.7)$$

If a sinusoidal voltage ($V = V_0 e^{j\omega t}$) is applied to a capacitor, the relation between current I and voltage V may be written

$$I = C\frac{dV}{dt} = j\omega VC = j\omega VE_rC_0$$

$$I = j\omega V(E_r' - jE_r'')C_0 = \omega VE_r''C_0 + j\omega VE_r'C_0 \qquad (1.8)$$

where C is the capacitance with the dielectric between the electrodes and C_0 is the capacitance without it. The current (I) may be resolved into two components (15): a charging current ($j\omega VE_r'C_0$) in quadrature with the voltage, and a conduction current ($\omega VE_r''C_0$) in phase with the voltage as shown in Fig. (1.6). Using the conduction component, the effective conductivity (σ) of the dielectric can be written as

$$\sigma = \omega E_r''\varepsilon_0 \qquad (1.9)$$

and consequently $\tan\delta = E_r''/E_r' = \dfrac{\sigma}{\omega\varepsilon_0 E_r'}$ (1.10)

1.4 Discontinuous metal films

Swann (16) drew the analogy between rain falling on a pavement and the growth of a metal film on a supporting layer. It is generally an appreciable time from the start of rain fall before a continuous film of water on concrete is formed, and so it is also with the formation of a metal film. In general when a film is deposited on substrate in vacuum by evaporation or sputtering the nucleation of the deposited film begins at many different nucleation sites, usually at imperfections in the substrate surface as a result of the loss of the high mobility of arriving atoms at such sites (17). Additional particles (arriving atoms) agglomerate around the nuclei, and an island structured film is formed. As the deposition is continuous, islands coalesce decreasing the island density. The islands then grow until contact is made with neighbours, and gradually the voids between the agglomerates are filled producing a filamentary network. Eventually, a macroscopically uniform thin film is obtained. To sum up, a discontinuous metal film consists of a two-dimensional array of microparticles (islands) separated from each other by distances of the order of a few to about 100A° (18). The aggregates are of different sizes and ranging from few atoms per island to 10^4 or more (19). For electrical conduction to occur, electrons have to be transferred from one island to the next across the gaps, and it is the mechanism of this transfer which determines the resistance of the film. Several mechanisms have been proposed to account for the electron transport between separate islands, for example thermionic emission (20), field emission (21), tunnelling and activated tunnelling (22,23), substrate-assisted tunnelling (24) and space-charge limited current flow across the substrate surface (25). As discussed by Neugebauer (26) and

by Hill (27,28) the parameters involved in the conduction mechanism are the island size, the distance between conducting islands, the nature of the substrate surface and in special cases the thermal expansion coefficients of the thin film and the substrate.

1.4.a Factors affecting the island size and inter-island spacing

Most of the detailed information on thin film properties is organized according to the film deposition process used rather than the film material. However the patterns of behaviour of discontinuous films, irrespective of the ways of their production, are reasonably consistent; for example films laid down as continuous and then argon ion etched to become discontinuous have similar electrical and ageing characteristics to those formed directly by deposition. In general there are five factors that determine the island size and inter-island spacing (29): thermal effects at the substrate, the kinetic energy of the arriving vapor, the arriving vapor flux density, the angle of incidence of arriving vapor, and electrostatic effects at the substrate. Increasing the substrate temperature increases the mobility of arriving vapor resulting in larger islands and greater inter-island separation. Increasing the kinetic energy of the arriving vapor has the same effect since more energy must be dissipated by lateral motion of the arriving vapor. Increasing the arriving vapor flux density imparts more momentum at the surface and has the same effect. Increasing the angle of incidence of the vapor stream from normal to glancing incidence imparts a higher velocity component parallel to the substrate surface, also resulting in greater lateral mobility and increased agglomeration. The electrostatic effects at the substrate are less well established but study of Pt, Au, Ag and Ni nucleation on 25A° thick SiO_2 films on n- and p-type Si

has shown that the metals carrying a positive charge (Pt, Ni) resulted in smaller, more closely spaced islands on n-type substrates, while the reverse was true on p-type substrates (30). The opposite appears to be true of Au and Ag, which apparently carry negative charges. Less agglomeration has been observed when d.c. electric field is applied in the plane of the substrate (31-36) or when the substrate is charged by electron or ion bombardment (37). Hill (27,28) identified four types of discontinuous films and classified them according to particle size and spacings. He assigned various conduction mechanisms as being the dominant mode of intergranular charge transfer. Type (i) films consist of small particles separated by small gaps, leading to high activation energies and short tunnelling path lengths. Type (ii) films (small particles separated by large gaps) typically show high activation energies and the dominant conduction mode is predicted to be thermionic emission into the substrates. Type (iii) films (large particles and small gaps) should exhibit low activation energy and negligible resistivity within the metallic grains. Type (iv) films (large particles and large gaps) should be characterized by small intergranular resistance and thermionic emission and/or bulk conduction through the substrate.

1.4.b Representation of discontinuous metal films

For this purpose it is assumed that the film is a matrix made up of islands (38), all identical in size as in Fig. (1.7a). If R_1 is the inter-island resistance, C' is the capacitance between two neighbouring islands and R_2 is the resistance associated with each island [Fig. (1.7b)], the whole matrix can be represented by three frequency independent components: a resistance R_b in series with a resistance R_g in parallel with capacitance C_g as in Fig. (1.7c).

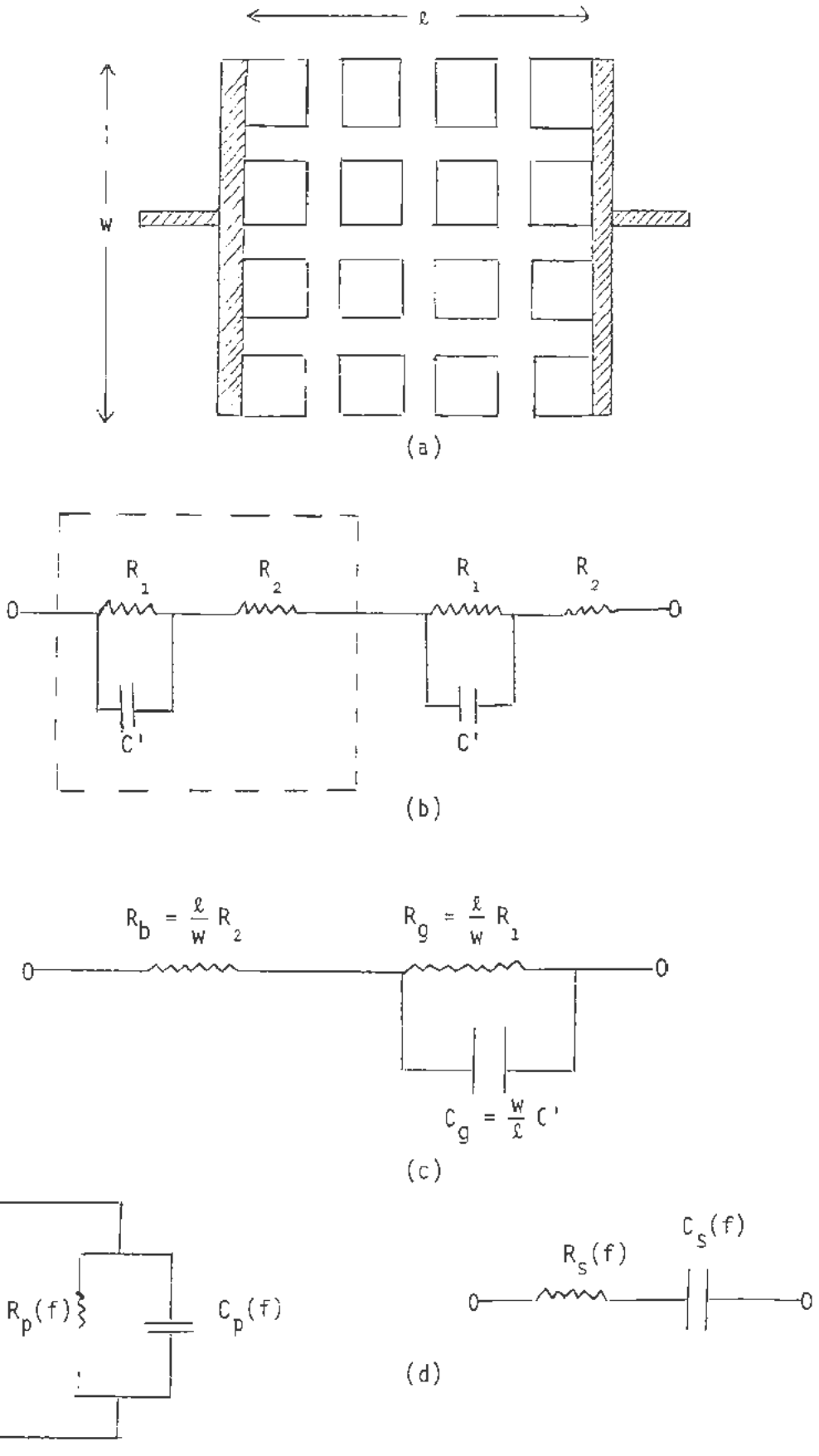

Fig. (1.7) The structure and equivalent electrical circuits representing an island film: (a) the matrix of islands; (b) & (c) the equivalent electrical circuit of the film allowing for the inter-island capacitances; (d) parallel and series representation of the equivalent circuit

Again the impedance of an island film can be regarded as either parallel or series combination of a resistance and capacitance both are frequency dependent [Fig (1.7d)]. By straight forward circuit analysis the following relations emerge

$$R_p(f) = \frac{\ell}{w}\left[\frac{(R_1+R_2)^2 + R_2^2\,(R_1\omega C')^2}{R_1 + R_2 + R_2\,(R_1\omega C')^2}\right] \tag{1.11}$$

$$R_s(f) = \frac{\ell}{w}\left[\frac{R_1 + R_2 + R_2\,(R_1\omega C')^2}{1 + (R_1\omega C')^2}\right] \tag{1.12}$$

$$C_p(f) = \frac{w}{\ell}\left[\frac{R_1^2 C'}{(R_1+R_2)^2 + \omega^2 C'^2 R_1^2 R_2^2}\right] \tag{1.13}$$

$$C_s(f) = \frac{w}{\ell} C'\left[1 + \frac{1}{(\omega R_1 C')^2}\right] \tag{1.14}$$

At low frequencies, the current is largely blocked by the capacitance (C') (39), thus, it flows through the resistance (R_1) and consequently (R_p) and (R_s) will be $\frac{\ell}{w}(R_1+R_2)$ which is the d.c. resistance of the film. On the other hand, at high frequencies the current flows through the capacitance, since the impedance of the capacitor is much lower than the resistance (R_1) and the net resistance will be $\frac{\ell}{w} R_2$.

1.4.c <u>The capacitance between two neighbouring islands (C')</u>

In view of the fact that the island metal film is a matrix of islands dispersed on the surface of the dielectric substrate, it is expected that the presence of these aggregates will affect the potential and charge of any selected one in the matrix. Let

the total number of islands be n, if V_i and Q_i are the potential and charge of the ith island respectively, then the following equations (40) can be written

$$\begin{aligned}
V_1 &= S_{11}Q_1 + S_{21}Q_2 + \ldots\ldots\ldots + S_{n1}Q_n \\
V_2 &= S_{12}Q_1 + S_{22}Q_2 + \ldots\ldots\ldots + S_{n2}Q_n \\
&\vdots \\
V_n &= S_{1n}Q_1 + S_{2n}Q_2 + \ldots\ldots\ldots + S_{nn}Q_n
\end{aligned} \tag{1.15}$$

The coefficients S_{ij} are called the coefficients of potential or the mutual susceptances. This set of equations can also be solved for the charge on the conductors (islands) in terms of the potentials of the conductors as

$$\begin{aligned}
Q_1 &= C_{11}V_1 + C_{21}V_2 + \ldots\ldots\ldots + C_{n1}V_n \\
Q_2 &= C_{12}V_1 + C_{22}V_2 + \ldots\ldots\ldots - C_{n2}V_n \\
&\vdots \\
Q_n &= C_{1n}V_1 + C_{2n}V_2 + \ldots\ldots\ldots + C_{nn}V_n
\end{aligned} \tag{1.16}$$

The quantity C_{rr} is called the coefficient of capacitance or the self capacitance, and C_{ij} is called the coefficient of induction or the

mutual capacitance. For the sake of calculation, consider that the system consists of two spherical islands completely immersed in a dielectric as shown in Fig. (1.8). To calculate the capacitive coefficients as given by equations (1.16) for this system, it can be assumed that sphere 1 is at unit potential by placing a charge $4\pi\varepsilon_0 E_r a$ at its center, if sphere 2 is at ground potential, a charge will be induced of magnitude $\frac{-4\pi\varepsilon_0 E_r a^2}{D}$ at distance $\frac{a^2}{D}$ to the left of the center of sphere 2 by the method of charge images in spheres. This charge in sphere 2 will have its image inside sphere 1, which in turn will have its image inside sphere 2, etc. The charges inside sphere 1 can be added and will be C_{11} since sphere 1 was held at unit potential. By symmetry this will also be C_{22}. The total charge induced in sphere 2 is C_{12} $(= C_{21})$. This can be shown to give (41)

$$C_{11} = C_{22} = 4\pi\varepsilon_0 E_r a \sinh\beta \sum_{n=1}^{\infty} \mathrm{Csch}(2n-1)\beta \qquad (1.17)$$

$$C_{12} = C_{21} = -4\pi\varepsilon_0 E_r a \sinh\beta \sum_{n=1}^{\infty} \mathrm{Csch}\, 2n\beta \qquad (1.18)$$

$$\beta = \tfrac{1}{2} \cosh^{-1}\left[\frac{D^2 - 2a^2}{2a^2}\right]$$

Equation (1.18) could also be written as (42)

$$C_{12} = C_{21} = \frac{4\pi\varepsilon_0 E_r a}{2}\,[1 + f(m)] \qquad (1.19)$$

$$f(m) = m + m^2 + m^3 + 2m^4 + \ldots\ldots$$

$$m = \frac{a}{D} = \frac{a}{2a + S} \quad \text{if } 2a \gg S \quad \therefore\ m = \tfrac{1}{2}$$

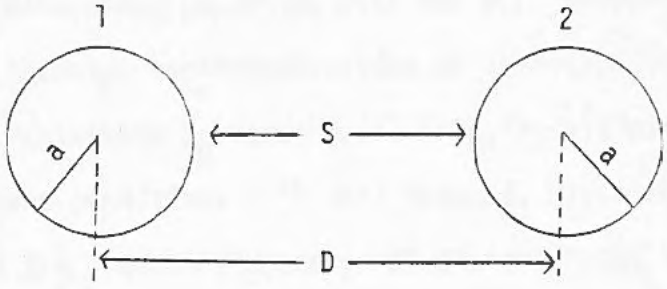

Fig. (1.8) Two islands immersed in a dielectric

$$C_{12} = C_{21} = 4\pi\varepsilon_0 E_r a \qquad (1.20)$$

For example if $E_r = 10$, $a = 10^3 A^\circ$; $C_{12} = C_{21} = 1.1 \times 10^{-4} pF$

1.4.d Literature survey related to a.c properties of discontinuous metal films

From a survey of the literature, it is evident that much of the experimetnal and theoretical work has been devoted to studies of the d.c. conductivity of discontinuous metal films whilst little attention has been paid to the behaviour of these films in alternating electric fields. There is a common feature in most of the limited number of publications concerned with the a.c. properties of discontinuous metal films, namely, the concentration on investigating the variation of the a.c. resistance $R_p(f)$ or $R_s(f)$ [Fig. (1.7d)] with frequency under different conditions. In this respect, Hirsh and Bazian (43) have studied the frequency response of discontinuous Ni films in the frequncy range (0 - 2MHz) at a number of temperatures between 4.2°K and 297°K. They found that the decrease in resistance with frequency was more pronounced in the films possessing a larger d.c. resistance. Also Joglekar (38) has investigated, in situ, the resistance/frequency behaviour of vacuum-evaporated discontinuous Bi films deposited on glass in the 50KHz - 40MHz range and reported that the behaviour changed markedly with film thickness and temperature. Recently Angadi and Ashrit (44) have reported, for the first time, the frequency response of discontinuous Samarium (rare-earth metal) films in the frequency range 100Hz - 1MHz, for different film thicknesses. In 1983, Angadi and Shivaprasad (45) studied the frequency response of discontinuous (Mn, Pd) films in the frequency range 100Hz - 1MHz

for different film thicknesses. In fact none of the aforementioned investigators mentioned anything related to C_p or C_s (Fig. (1.7d)] of the studied films. Other researchers have taken another route in their studies by trying to find the best-fit for their experimental results. In this context, Deshpand and Crowell (46) studied, in situ, the variation of R_p [Fig. (1.7d)] for discontinuous Mo films in the frequency range 0.1MHz - 50MHz upon exposure to oxygen at 10^{-7} to 10^{-4} torr. From their findings and equation (1.11) they were able to estimate values for R_b, R_g, C_g [Fig. (1.7c)] which gave the best fit. In the same way, Wlicznerski (47) has conducted researches on the variation of the conductance ($\frac{1}{R_p}$) for discontinuous Cr films in the frequency range 10^{-1}Hz to 10^{7}Hz and deduced values for R_b, R_g, C_g. Regarding the capacitance of the Cr films, he failed in determining exactly its change with frequency. Last but not least, Morris (48) has studied the variation of admittance against frequency (0.01Hz to 10MHz) for five metal films. Only films 1,2 were discontinuous as deposited while films 3,4 were originally continuous and became discontinuous by Joule heating but film 5 was semi-continuous. From the admittance measurements he was able to evaluate the equivalent gap capacitance C_g [Fig. (1.7c)] and the surprising thing was its large value (C_g~10pF) for all the films. He claimed that massive aggregates (films 3,4) or very long filaments (film 5) can develop such large gap capacitance but it cannot possibly apply to the fine island structure of films 1,2.

Up to this stage of the survey, it is clear that there have been no definitive attempts to study the capacitive chracteristics of discontinuous metal films; nevertheless there are two papers where some information about the capacitance of films was reported.

The first is by Castro and Beynon (49) who studied the variation of the a.c. resistance with frequency for Mn and Mn-SiO thin films at a number of temperatures between -180 and 100°C. The frequency range extended from 100Hz to 1MHz; a Wayne-Kerr universal bridge was used up to 20KHz and a Wayne-Kerr r.f. bridge above that frequency. They reported that the capacitance was less than 2pF for all the films studied. The second is by Tick and Fehlner (50) who were concerned with the behaviour of composite discontinuous films of gold-rich islands grown on palladium nuclei. At first the chracteristics of Pd films, which were eventually used as the nucleating layer for the gold films, was examined. An a.c. bridge was used to measure the capacitance of the Pd films at 40KHz and it was approximately 2pF. Secondly, gold was deposited in incremental amounts and the variation of the resistance with frequency was studied and nothing related to the capacitance was reported apart from the fact that it was essentially constant with frequency.

1.5 Two-dimensional artificial dielectrics

The so-called "artificial dielectrics" comprise arrays of metallic elements within a supporting dielectric material. The effect of the metallic insertions is to afford a medium having an effective dielectric constant in excess of that of the supporting medium. The excess can be adjusted by suitable choice of the shape, distribution and concentration of the elements. Kock (51) discussed theoretically the properties of cubical arrays of spheres, discs and strips with reference to the condition where the linear dimensions and separation of the metallic elements are small compared with the wave length of the incident radiation; he pointed out to the possibility of using artificial dielectrics as lenses for microwave radiation. Riddle (52)

exploited the idea of artificial dielectrics to measure the rate of evaporation of metals by sensing the change in capacitance between two parallel electrodes which span the stream of evaporating atoms. Generally, the metallic elements can be arranged within the supporting medium either in two or three dimensional arrays and the emphasis here will be on the first case since it is relevant to discontinuous metal films remembering that the latter are two-dimensional arrays of metallic elements (islands). In the work of Kharadly and Jackson (53), theoretical and experimental studies were conducted on artificial dielectrics composed of two-dimensional array of infinitely long perfect conducting circular cylinders and thin strips arranged with their axes normal to the electric field. For two-dimensional array of parallel elements supported and distributed within a medium of permittivity $\varepsilon\varepsilon_0$ where ε is the dielectric constant of the medium and ε_0 is the free space permittivity, (in our case the medium will be the air or space between the two faces 1,2 in Fig. 1.3) the effective permittivity of the system $\varepsilon_1\varepsilon_0$ is given by

$$\varepsilon_1\varepsilon_0 = \varepsilon\varepsilon_0 + N\alpha \tag{1.21}$$

where N is the number of elements per unit area; α is the polarizability per unit length in the direction of the electric field and it depends on the shape of the element and on the nature of the supporing medium; α is related to α_0 which is the polarizability of the element in free space by the expression $\alpha = \varepsilon\alpha_0$ and eqn. (1.21) may therefore be written

$$\varepsilon_1 = \varepsilon \left(1 + \frac{\alpha_0 N}{\varepsilon_0}\right) \tag{1.22}$$

We have considered the medium between the two faces 1, 2 in Fig. (1.3), after depositing the discontinuous film, as a two-dimensional artificial dielectric but in the same time the islands (elements) are located on the surface of another supporting medium (substrate) and we may have another two-dimensional artificial dielectric if the presence of the islands will enhance the dielectric constant of the substrate and according to Leaver (54) this will be the case. He derived the following equations

$$E_r'/E_r = \frac{1 + 2\nu A/3}{1 - \nu A/3} \tag{1.23}$$

$$A = 8(2 + \frac{s}{a})^{-2} \left[(1 + \frac{s}{a})^{-2} + 0.5(3 + \frac{2s}{a})^{-2} + 0.077(2 + \frac{s}{a})^{-2} \right] \tag{1.24}$$

where E_r, E_r' are the dielectric constants of the substrate before and after laying down the islands, A is a constant for certain array characterized by separation (s) between the islands, each with radius a, and ν is a factor related to the ellipticity of the islands.

1.6 Statement of the problem

As already mentioned in Section 1.4.c, it is clear that no attention has been given so far to explicit studies of the capacitance of discontinuous metal films and accordingly it is of interest and value to conduct researches which will throw light on this ignored aspect of island films i.e. its capacitance (C_p or C_s in Fig. 1.7d). The achievement of this main goal requires, among other things, the presence of sensing devices, namely, the planar capacitors and the preparation of such capacitors in the present work was of twofold use (i) to measure and calculate their capacitances. The importance

of this step stems from the fact that there is only one publication in this domain as illustrated in Section 1.3.b and so work directed toward the study of planar capacitors in its own right is required.
(ii) the in situ monitoring of the changes in the planar capacitance and dissipation factor of the capacitors as a consequence of depositing discontinuous gold and aluminium films across their gaps will enable us to measure (deduce) the capacitance of the films.

CHAPTER 2 EXPERIMENTAL WORK

2.1 Choice of the metals

Gold and aluminium were chosen because gold island films would be chemically stable and free from multilayer oxidation (55), while aluminium granular films have great susceptibility to oxidation (56,57), even if they are kept under vacuum (58), which may lend them to exhibit different properties from those of gold. These two metals can be evaporated easily since their melting points are 1063°C and 659°C respectively.

2.2 Choice of the substrates

Corning (7059) glass and "Melinex" were used as substrates in the present work. The first is especially made for supporting thin films both commercially and for studying basic electrical properties. Generally speaking, if a glass substrate contains a considerable amount of alkali ions (59), these ions will migrate to the surface and react with some metallic films resulting in complete disintegration of the films. This process is accelerated in the presence of an electric field. Corning (7059) is considered as alkali-free since the percentage of the alkali content is less than 0.2% by weight. The second is the trade name of plastic films (polyethylene terephthalate) produced by I.C.I. in England. This polymer was selected because it is infrequently used as substrate for thin metallic films and is substantially inert to most chemicals whilst having good thermal properties (60,61).

2.3 Cleaning of the substrates

There has been a great deal of emphasis in the literature on the importance of substrate cleanliness (62-64) for (a) reproducibility of results and (b) the validity of applying simple nucleation theory to experiments. Recommended procedures for glass substrates vary but generally involve (i) removal of the surface grease by ultrasonic cleaning in acetone or washing in hot detergent solution, (ii) washing in water, (iii) washing in de-ionized water, (iv) drying in isopropyl alcohol vapour. In the present work the following procedure was adopted; the substrates were placed in glass rack and then immersed in a solution of a detergent and de-ionized water (3c.c Decon 90 in 100c.c water). This solution was brought to the boiling point and held there for about one minute; after that the rack was rinsed twice with de-ionized water to remove any detergent remaining on the substrates. Once the substrates are roughly dried, they were transferred to isopropyl vapour tower for about 20 minutes. Melinex was cleaned by washing in Xylene (60).

2.4 Deposition of the two planar electrodes on the surface of substrates

Each of the dielectric substrates (Corning or Melinex 76mm x 25mm) was transferred immediately after cleaning to the vacuum chamber which is promptly evacuated for depositing, by thermal evaporation, two relatively thick aluminium films (W = 4mm, L = 25mm) separated by a gap (d = 2mm) as shown in Fig. (2.1). Aluminium was used as electrodes on account of its low resistivity (56) and satisfactory adherence to substrates without the need for an intermediate bonding layer. The importance of using a relatively large gap (2mm) is

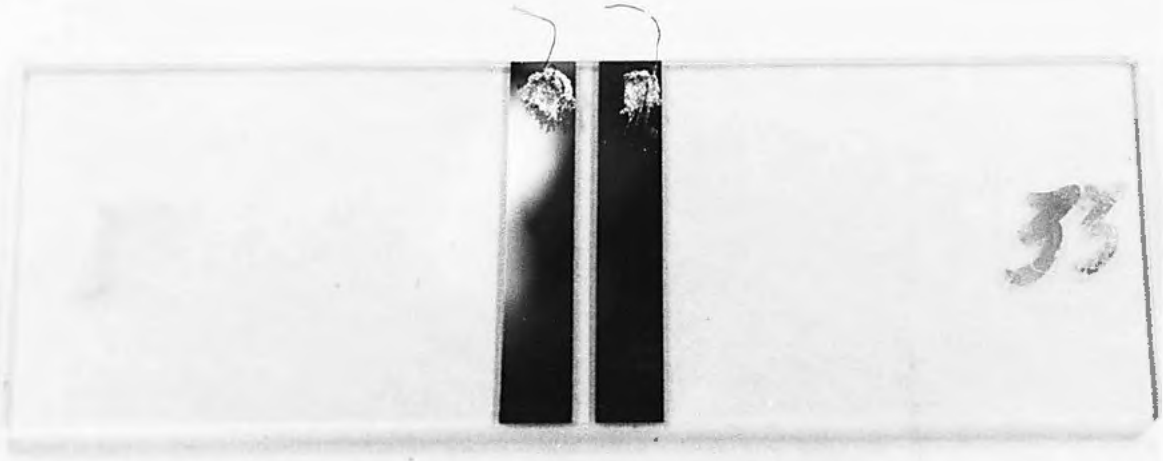

Fig. (2.1) Photograph of the planar capacitor

to avoid bridging the two electrodes by dust particles which could influence the losses of the planar capacitor (65,66). The substrate was placed on the chamber baseplate and a helical tungsten filament, loaded with aluminium, located above it. A simple masking system was used to achieve the aforementioned dimensions, a metallic strip of 2mm width was mounted very close to the substrate to get the required gap with sharp boundaries (67,68), while another two metallic sheets were used to mask the rest of the substrate except for the areas specified for the two electrodes as illustrated in Fig. (2.2). The thickness of the aluminium films was not monitored during deposition but they appeared to be thick from visual tests. The pumping system used to evacuate the chamber consists of an oil diffusion pump and a single stage mechanical oil-sealed rotary backing pump which also "roughs" down the coating plant to about 10^{-2} torr. The oil diffusion pump was connected to the coating plant chamber via a high-vacuum isolating valve which permits the diffusion pump to be kept under vacuum and at operating temperature when the coating chamber is at atmospheric pressure. The pressure in the vacuum system was monitored with Penning and Pirani gauges.

2.5 Attachment of leads to the electrodes

Leads must be made to the planar capacitor in order either to use or to measure its capacitance (69). In this respect, two fine (0.1mm in diameter), short (1.5cm) and bare copper wires were bonded to the aluminium electrodes with thermosetting silver preparation FSP43 which is an epoxy based resin containing silver in the form of flake. It is suitable for application to different types of materials provided that they will withstand the minimum stoving

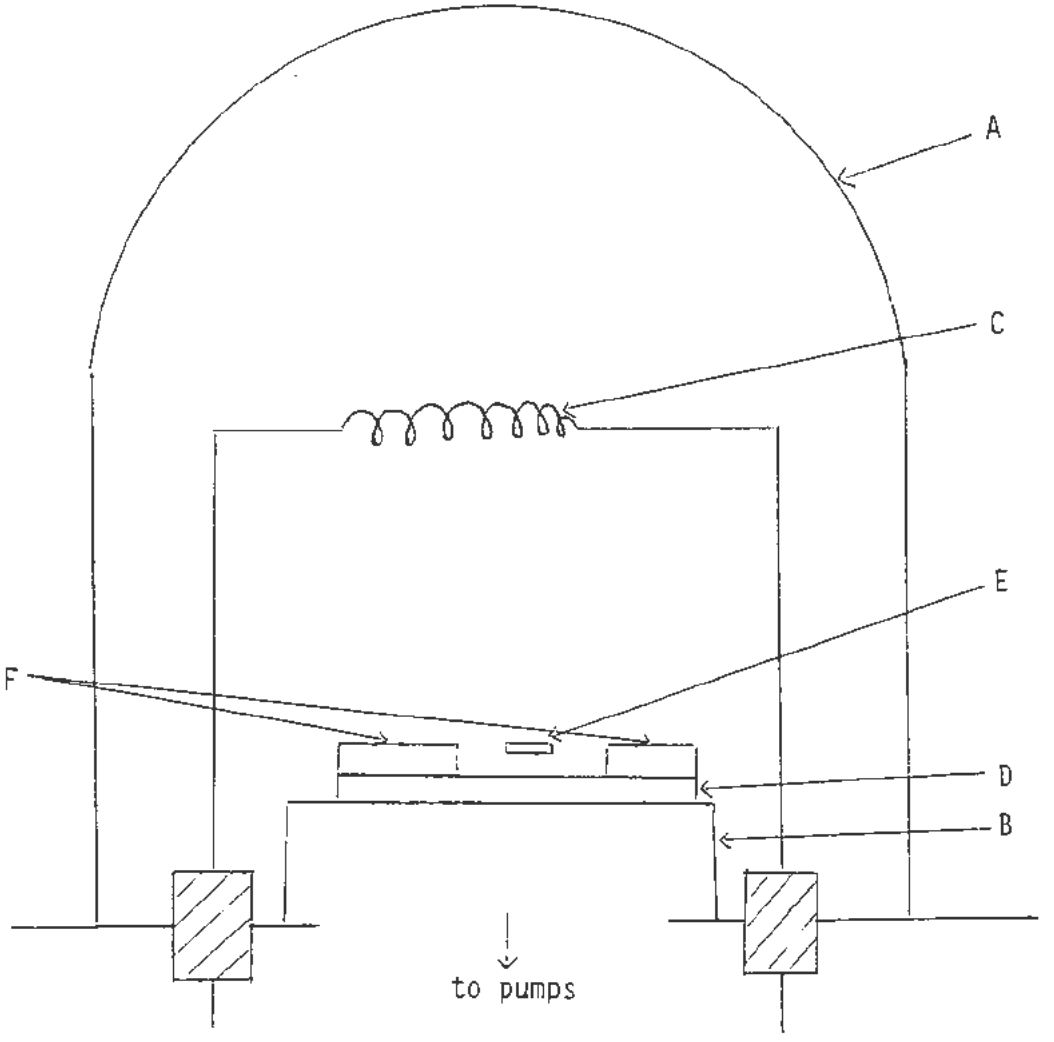

Fig. (2.2) Deposition of two aluminium electrodes

A coating chamber; B baseplate; C tungsten filament; D substrate;

E metallic strip 2mm width; F two masking metallic sheets

temperature of 80°C necessary for curing the preparation. Silver preparation, FSR43 is supplied as two separate components, FSP43R and FSR43H, which are mixed together in the ratio by weight of two parts of the first to one part of the second components.

2.6 Shielding of the planar capacitors

It is well known that the capacitance between two electrodes is only definite if one conductor completely surrounds the other (70); consequently the capacitance between the two planar aluminium electrodes will suffer a lack of definition due to the dependance of such capacitance on the position and motion of neighbouring objects. This lack of definition can be eliminated if the planar capacitor is completely enclosed within a shield which in this case is a die-cast metal box held at ground potential. In doing so, the total (working) capacitance is generally dependent on the capacitance between the individual electrodes and ground (metal case) C_{13}, C_{23} as well as the direct capacitance between the electrodes themselves C_{12} as shown in Fig. (2.3). The working capacitance of the system C will be given by the following equation

$$C = C_{12} + \frac{C_{13} C_{23}}{C_{13} + C_{23}} \qquad (2.1)$$

Despite the fact that C_{12} is now independent of the surroundings outside the shield, the latter has added an extra unwanted capacitance $\frac{C_{13} C_{23}}{C_{13} + C_{23}}$ to C_{12}. It should be noted that the two aluminium electrodes were insulated from the shield and brought out to external terminals via two BNC socket installed in the wall of the metal case.

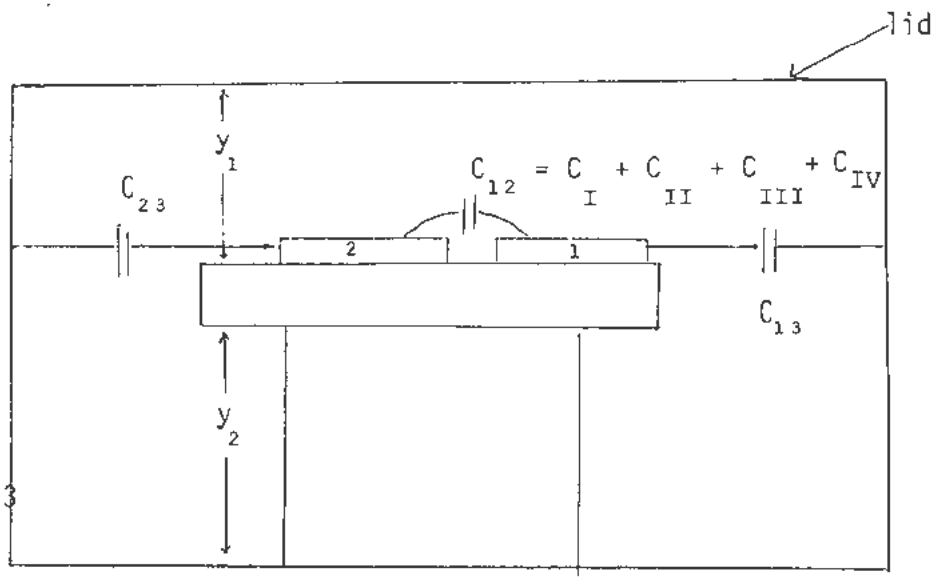

Fig. (2.3) Planar capacitor shielded in die-cast metal box

Generally speaking, if a separate terminal is provided for the shield, the arrangement will be known as a three-terminal capacitor (65) as distinguished from a two terminal capacitor, which, if shielded, has the shield permanently connected electrically to one of the electrodes.

2.7 Measurement of small capacitance

In general the measurements of capacitance, particularly those of high accuracy, are made by a null method which uses some form of the basic ratio bridge, shown in Fig. (2.4). The capacitance of the unknown, C_X, is balanced by a calibrated, variable, standard capacitor, C_N, or by a fixed standard capacitor and a variable ratio arms, such as R_A. Such bridges with resistive ratio arms and with calibrated variable capacitors or resistors can be used over a wide range of both capacitance and frequency and with a direct-reading accuracy which seldom exceeds 0.1%. For higher accuracy, resolution, and stability in capacitance measurements at audio frequencies, a bridge with inductively-coupled or transformer ratio arms has many advantages, and increasing use of transformer-ratio-arm bridges is being made in the measurements of many types and sizes of capacitors.

2.7.a Transformer ratio arms

The advantages of transformer ratio arms in a bridge are that accuracies within a few parts per million are not difficult to obtain over a wide range of integral values, even for ratios as high as 1000 to 1, and that these ratios are almost unaffected by age, temperature, or voltage. The low impedance of the transformer ratio arm also makes it easy to measure direct impedances and to exclude the ground impedances in a three-terminal measurement without the use of guard

circuits and auxiliary balances. To illustrate these characteristics, a simple capacitance bridge with transformer ratio arms is shown in Fig. (2.5). On the toroidal core, a primary winding, connected to the generator, serves only to excite the core; the number of primary turns, N_p, determines the load on the generator but does not influence the bridge network. If all the magnetic flux is confined to the core - as it is to high degree in a symmetrically wound toroid with a high-permeability core - the ratio of the open-circuit voltages induced in the two secondary windings will be exactly equal to the ratio of the number of turns. The ratio can be changed by the use of taps along the two secondaries, but when the number of turns between taps is fixed, the voltage is highly invariant. Changes in the core permeability with time and temperature have only a second order effect on the ratio, because they modify only the very small amount of leakage flux that is not confined to the core in a practical transformer. The ratio is, therefore, both highly accurate and highly stable. In Fig. (2.5), the two transformer secondary windings are used as the ratio arms of the capacitance bridge with the standard capacitor, C_N, and the unknown, C_X, as the other two arms in a conventional four-arm bridge network. The condition for balance or zero detector current, is easily shown to be that

$$V_N C_N = V_X C_X \quad \text{or} \quad \frac{C_X}{C_N} = \frac{V_N}{V_X} = \frac{N_N}{N_X} \tag{2.2}$$

This balance condition is not affected by the capacitances shown from the H and L terminals of C_N and C_X to the terminal G connected to the junction of the ratio arms. The capacitances between L and G shunt the detector, so that they affect only the bridge sensitivity.

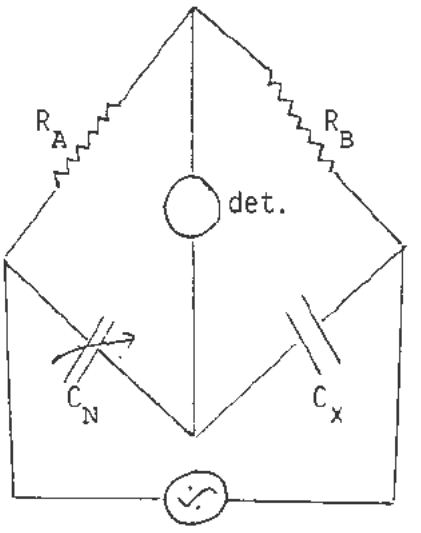

Fig. (2.4) Basic ratio bridge

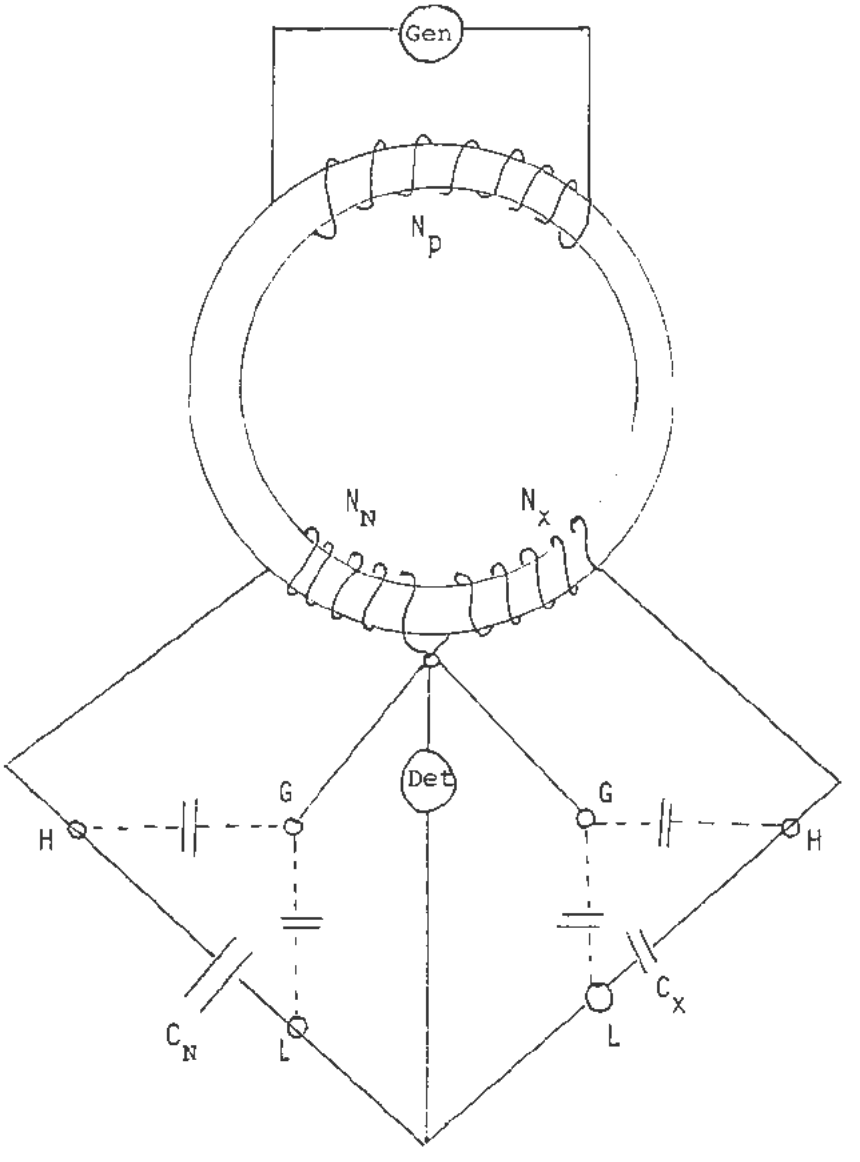

Fig. (2.5) A capacitance bridge with transformer ratio arms

The capacitances between H and G are across the transformer windings. To the extent that the transformer can be assumed ideal, i.e., with no resistance in the secondary windings and with no flux that does not link equally both secondaries, the current drawn by the H-G capacitances does not change the voltages V_N and V_X or the balance conditions. The junction of the ratio arms, G, is therefore a guard point, or at guard potential, in the bridge. All capacitances to G from the H or L corners of the bridge are excluded from the measurement, and in view of this advantage the use of such capacitance bridge will be necessary to measure the direct capacitance C_{12} without being sensitive to the presence of $\frac{C_{13} C_{23}}{C_{13} + C_{23}}$ which is automatically excluded.

2.7.b Assembly used in the present work for measuring the capacitance

When a General Radio capacitance bridge type 1615-A, which has transformer ratio arms as explained in Section (2.7.a), combined with audio oscillator (generator) and null detector type 1232-A the obtained resolution was $\pm 10^{-2}$pF which is far from being satisfactory especially to detect the change in capacitance of the planar capacitor as a result of depositing discontinuous metal film across its gap during in situ measurements. The reason behind this low resolution is the presence of noise; to minimize its effect and hence improve the resolution a phase sensitive detector and phase shifter were added to the aforementioned equipment as illustrated in Figs. (2.6) and (2.7). Such assembly provided a resolution of $\pm 10^{-4}$pF which is considered quite reasonable. Regarding how the bridge will see any unknown capacitor, there are two modes (i) as a series combination of resistance (r_1) and capacitance (c_1) [Fig. (1.6)] and the information available after balancing the bridge is (c_1); the dissipation factor

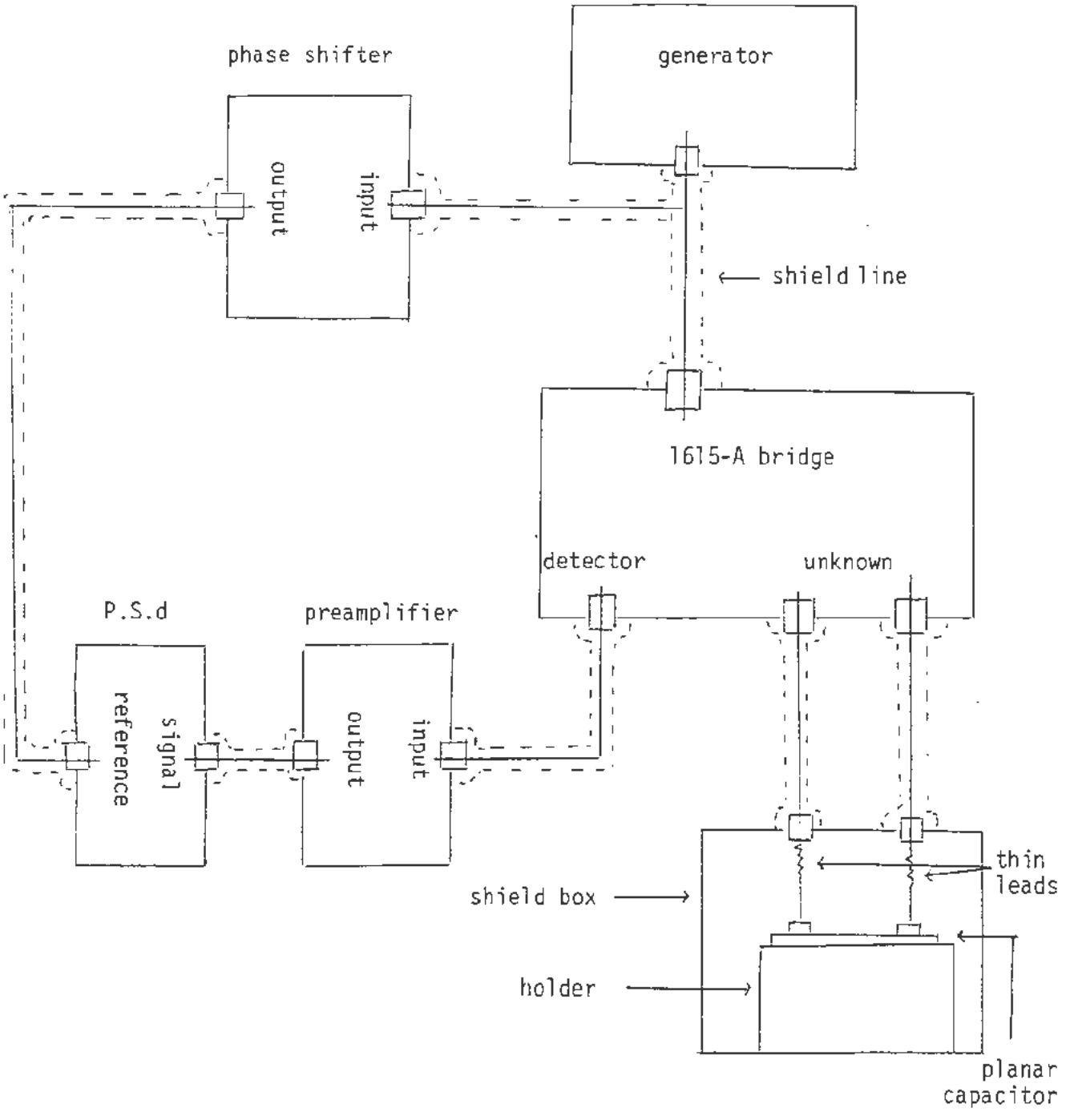

Fig. (2.6) Block diagram of the capacitance measuring circuit

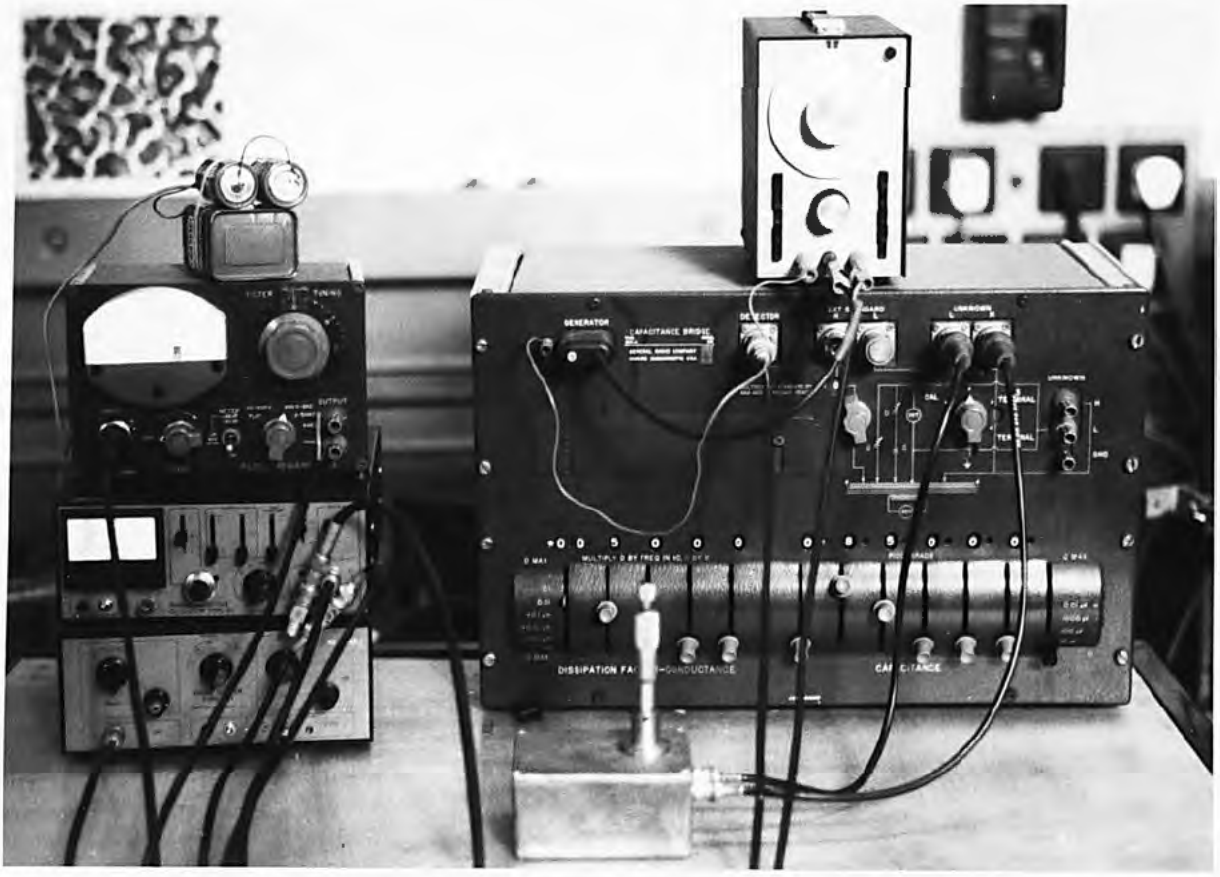

Fig. (2.7) Photograph of the capacitance measuring equipment

D(tanδ). (ii) as a parallel combination of c_2, r_2 [Fig. (1.6)] and the displayed information is (c_2); the conductance $G(\frac{1}{r_2})$. It is the first mode which has been selected in the present work because for most purposes it offers the greater range and convenience (71) while the second mode is useful in some measurements of dielectric materials and is necessary when external standards are added to the bridge and when the loss in the bridge standards exceeds that of the capacitor being measured. With respect to frequency, the bridge can operate up to 100Kc.

2.7.c Measurement of the capacitance of planar capacitors

A batch of 20 capacitors, 10 for each dielectric (Melinex and glass) were prepared as mentioned in Section (2.4) and were kept in a desiccator. Each capacitor was then mounted inside the shield box such that y_1 = 14mm, y_2 = 33mm as in Fig. (2.3) and the two copper leads were bonded, by soldering, to the socket installed in the box. The bridge was balanced at 1, 10, 20, 50, 100kHz and after performing this step for all the capacitors, the average value for the capacitance and dissipation factor were obtained (72). It should be noted that the bridge was balanced first with only the copper leads bonded to the socket, namely, without the planar capacitor to measure the background capacitance and hence, by subtraction, the capacitance between the deposited electrodes alone can be deduced.

2.8 Principle exploited in measuring the capacitance of island films

Since the prime objective in this research is to measure (C_p) [Fig. (1.7d)], it will be necessary to mention the principle exploited to achieve this aim. In theory, if a capacitor is connected to capacitance bridge then its equivalent parallel capacitance (c_2) [Fig. (1.6)]

can be measured. Th bridge will be out of balance when another unknown capacitor, which will be the island film in the present work, shunts the original one and by restoring the balance the capacitance of the unknown can be obtained (73, 74). Keister and Scapple (5) exploited this principle in their work, already mentioned in Section (1.3.b), where they measured the increase in the capacitance of planar capacitors as a result of depositing SiO films with different thicknesses. They reported that after each deposition was completed, the bell jar was opened, the planar capacitor (sensing device) removed and its capacitance measured.

2.9 Concept of mass thickness

It was reported that the thickness of island films cannot be exactly specified because the assumption of homogeneous and plane parallel surfaces does not hold for these films (75,76). To overcome this problem, some investigators described their films by the d.c. resistance at the moment of halting the deposition (18,46,77) while others used the concept of mass thickness (78-80). The mass thickness (d_m) of aggregated film does not represent the true mechanical thickness but it is only a measure of the deposited mass per unit area (M); $d_m = \frac{M}{\rho'}$ where (ρ') is the bulk density of the metal. Generally, quartz crystal oscillators (81,82) are used to measure (M) in the following manner: when an oscillatory quartz crystal with natural resonant frequency f_0 , $f_0 = \frac{N'}{t}$ where $N' = 1.67 \times 10^{13}$ Hz.A° and (t) is the crystal thickness in angstroms (A°), is positioned in the vacuum chamber so that vapour is deposited on the substrate and on defined area of the crystal surface while a second crystal (reference crystal) is housed in an oscillator circuit and the two

frequencies are mixed and the difference frequency then mixed with a variable oscillator to produce a final difference

$$F = f - f_0 \tag{2.3}$$

As deposition proceeds the frequency of the crystal in the coating chamber decreases as a result of evaporant deposited upon it whereas the frequency of the external crystal remains constant. The measurements taken are those of the frequency differences between the two crystals and consequently $\Delta F = -\Delta f_0$.

A deposited mass per unit area (M) will cause a change Δf_0 given by

$$\Delta f_0 = - \frac{N'}{\sigma t^2} M \tag{2.4}$$

where σ is the density of quartz and so

$$d_m = \frac{\sigma t^2}{\rho' N'} \Delta F \tag{2.5}$$

In the present work the films will be described by both the d.c. resistance at the moment of halting the deposition and the mass thickness (d_m); the latter was determined directly in angstroms (A°) by using film thickness monitor (Edward F.T.M.2). It is very important to take into consideration the temperature stability of the monitor crystal because individual crystals are frequency calibrated at one nominal temperature, normally 25°C, but if the operation temperature rises or falls about the nominal, a shift in frequency can be expected by different extents and direction for each crystal. Heat from any source in the chamber can affect the monitor crystal frequency while the reference crystal frequency remains constant. As a result, whether the monitor crystal frequency increases or

or reduces, there is an undesirable shift in the final difference (ΔF). Any change in the monitor crystal frequency before evaporation is initiated can be offset by the zero control, but if the frequency changes due to temperature during evaporation false thickness readings result. To check the effect of heat radiation alone dummy experiments were performed with the monitor crystal well shielded and no remarkable frequency shift was observed.

2.10 Deposition of the island films across the gaps of the planar capacitors

The procedure adopted by Keister and Scapple (5), mentioned in Section (2.8), is inappropriate here since the intention is to deposit island films whose electrical properties vary drastically from the moment of halting the deposition and consequently in situ monitoring of the proposed change in capacitance is required. This implies the use of leadthroughs to connect the sensing device either to the capacitance bridge or to the electrometer which is capable of measuring the d.c. resistances, up to $10^{13}\Omega$, of the deposited films. it is recognized that the use of leadthroughs will introduce a parasitic capacitance which will shunt the sensing device and the deposited film. Regarding the deposition of the island film, each of the planar capacitors was located on the baseplate in the vacuum system while the filament was above and its distance (y) could be changed as shown in Fig. (2.8). The main advantages of such a configuration are (i) to minimize the unwanted capacitance resulted from the leads required to connect the capacitor to the leadthroughs (ii) the offset of capacitor relative to the filament will allow inclined incidence to the evaporated atoms and hence

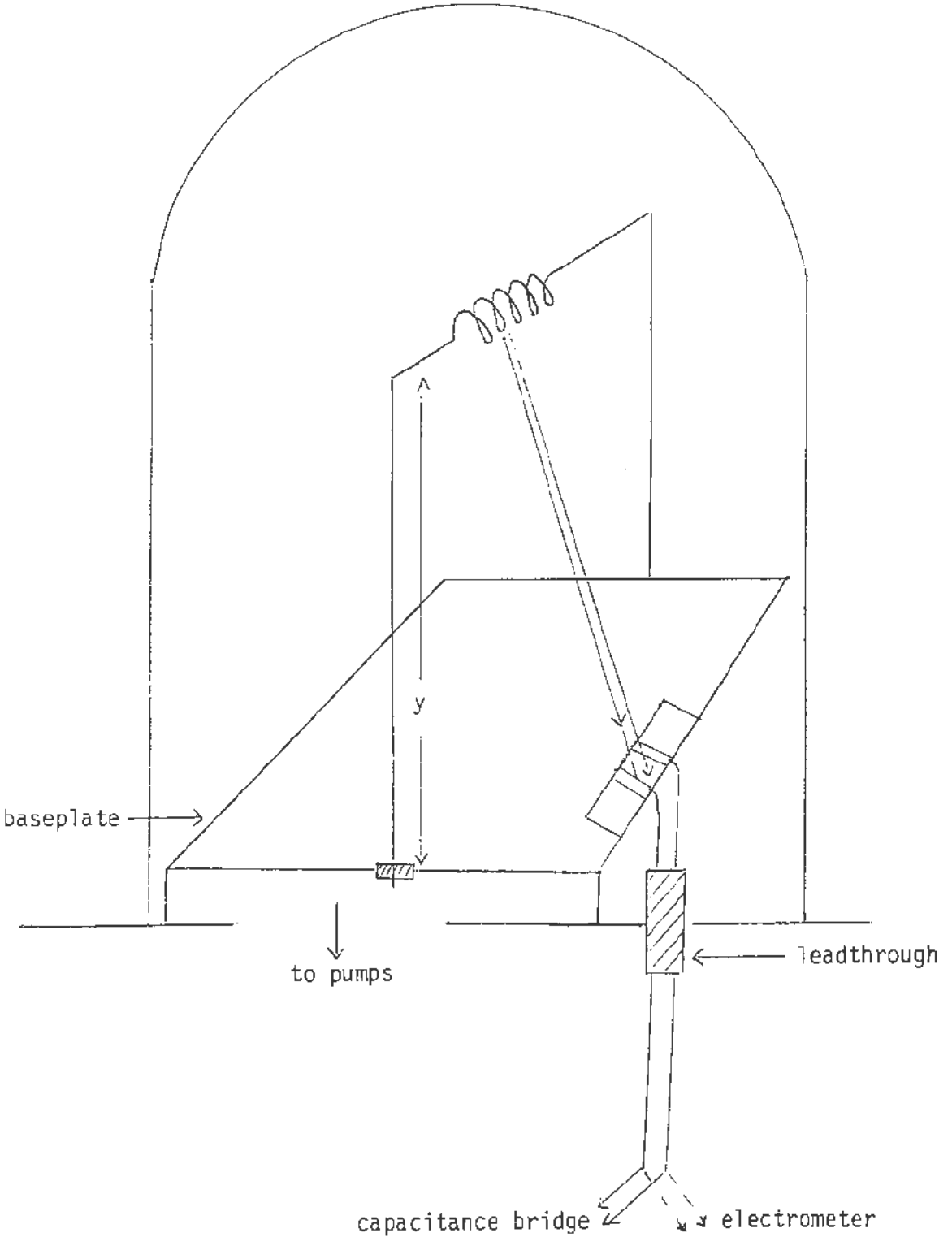

Fig. (2.8) Deposition of island films across the gap of planar capacitors

promote the physical discontinuity in the deposited films as mentioned in Section (1.4.a). A manually controlled shutter was used to serve for (i) protecting the substrate during the outgasing of gold and aluminium (ii) halting the deposition when the desired d.c. resistance was attained (18,46,77) as measured by the electrometer (83) and in the same time the thickness monitor will indicate the mass thickness of the films. The electric field in the plane parallel to the substrate, created from the voltage supplied by the electrometer, was minimized to secure the discontinuity of the deposited films (84).

2.11 Measurement of the capacitance of island films

Immediately before starting the deposition, the capacitance bridge with the planar capacitor in circuit was balanced at 1, 10, 20, 50, 100Kc with the corresponding readings C_1, D_1 where C_1 is the series capacitance and D_1 is the dissipation factor. Depositing the discontinuous film disturbed the balance which could be restored with corresponding C_2, D_2 and by using equation (1.5) the equivalent parallel capacitiances C_1', C_2' could be deduced. The parallel capacitance of the film (C_f) is therefore $C_2' - C_1'$; it was assumed that the out of balance is due only to the presence of the metallic aggregates across the gap of the planar capacitor and to justify this assumption dummy experiments were conducted such that unloaded filament was heated up and as a result a slight momentary out of balance was observed but once the shutter was interposed or the filament power reduced to zero the balance was completely restored which indicated that the heat radiated had no effect on the permanent out of balance which occurred after halting the deposition.

CHAPTER 3 RESULTS

3.1 The measured capacitance of planar capacitors with glass as a dielectric

3.2 The measured capacitance of planar capacitors with "Melinex" as a dielectric

3.3 Calculation of the planar capacitance

3.4 The measured capacitance of discontinuous gold films deposited on glass and "Melinex"

3.5 The measured capacitance of discontinuous aluminium films deposited on glass and "Melinex"

3.6 Post-deposition resistance changes in discontinuous gold and aluminium films

3.7 Calculation of the parallel capacitance of discontinuous metal films

3.8 Determination of the film structure by transmission electron microscopy

3.9 Attempts to produce a larger enhancement in the planar capacitance

3.1 The measured capacitance of planar capacitors with glass as a dielectric

Following the procedure mentioned in Section (2.7.c), the average values of the measured capacitance (C_m) and the dissipation factor (D_m) are presented in Tables (3.1) and (3.2) for the cases of closed and open shield box respectively. In fact it was the event of interrupting the balance by removing the lid of the box which inspired the idea of studying the effect of varying the volume of the shield box on the measured capacitance. To achieve this study without mounting the capacitor in different boxes, the change in the capacitance was observed as a result of moving an earthed metallic sheet over and under the capacitor and this is virtually equivalent to the variation of (y_1) and (y_2) [Fig. (2.3)]. A decrease in the capacitance was observed as the sheet approached the capacitor from either directions as shown in Figs. (3.1) and (3.2).

Table (3.1)

f(Kc)	C_m(pF)	D_m
1	0.7837	0.0012
10	0.7826	0.0012
20	0.7790	0.0012
50	0.7770	0.0012
100	0.7730	0.0012

Table (3.2)

f(Kc)	C_m(pF)	D_m
1	0.8010	0.0012
10	0.7992	0.0012
20	0.7966	0.0012
50	0.7955	0.0012
100	0.7930	0.0012

3.2 The measured capacitance of planar capacitors with "Melinex" as a dielectric

The average values of the measured capacitance (C_m) and the dissipation factor (D_m) are presented in Tables (3.3) and (3.4) for the cases of closed and open box respectively. Figures (3.3)

and (3.4) illustrate the variation of the capacitance with the distance of the earthed sheet as the latter moved over and under the capacitor respectively.

Table (3.3)

f(Kc)	C_m(pF)	D_m
1	0.3664	0.0051
10	0.3656	0.0072
20	0.3633	0.0075
50	0.3628	0.0087
100	0.3620	0.0090

Table (3.4)

f(Kc)	C_m(pF)	D_m
1	0.3795	0.0051
10	0.3785	0.0072
20	0.3763	0.0075
50	0.3750	0.0087
100	0.3720	0.0090

3.3 Calculation of the planar capacitance

The contributions (C_I) and (C_{II}) can be calculated by using the relevant equations in Section 1.3.a; also the contribution (C_{IV}) [Fig. 1.3] must be considered because the condition $E_r \gg 1$, $T \gg 2W + d$ is not valid in the present work. Since our substrates are remarkably thin, we may assume that $C_I \approx C_{IV}$.

i - for Corning glass as a dielectric [W = 4mm, d = 2mm, L = 25mm, T = 0.8mm, E_r = 5.8]

$$C_I = 0.2115\text{pF}, \quad C_{II} = 0.3997\text{pF}$$

$$C = C_I + C_{II} + C_{IV} \approx 0.8227\text{pF} \qquad (3.1)$$

ii - for "Melinex as a dielectric [W = 4mm, d = 2mm, L = 25mm, T = 0.036mm, E_r = 2.95]

$$C_I = C_{IV} = 0.2115\text{pF}$$

(C_{II}) is extremely small compared with (C_I) because d is much larger than T(2) and hence

$$C = C_I + C_{IV} = 0.4230\text{pF} \qquad (3.2)$$

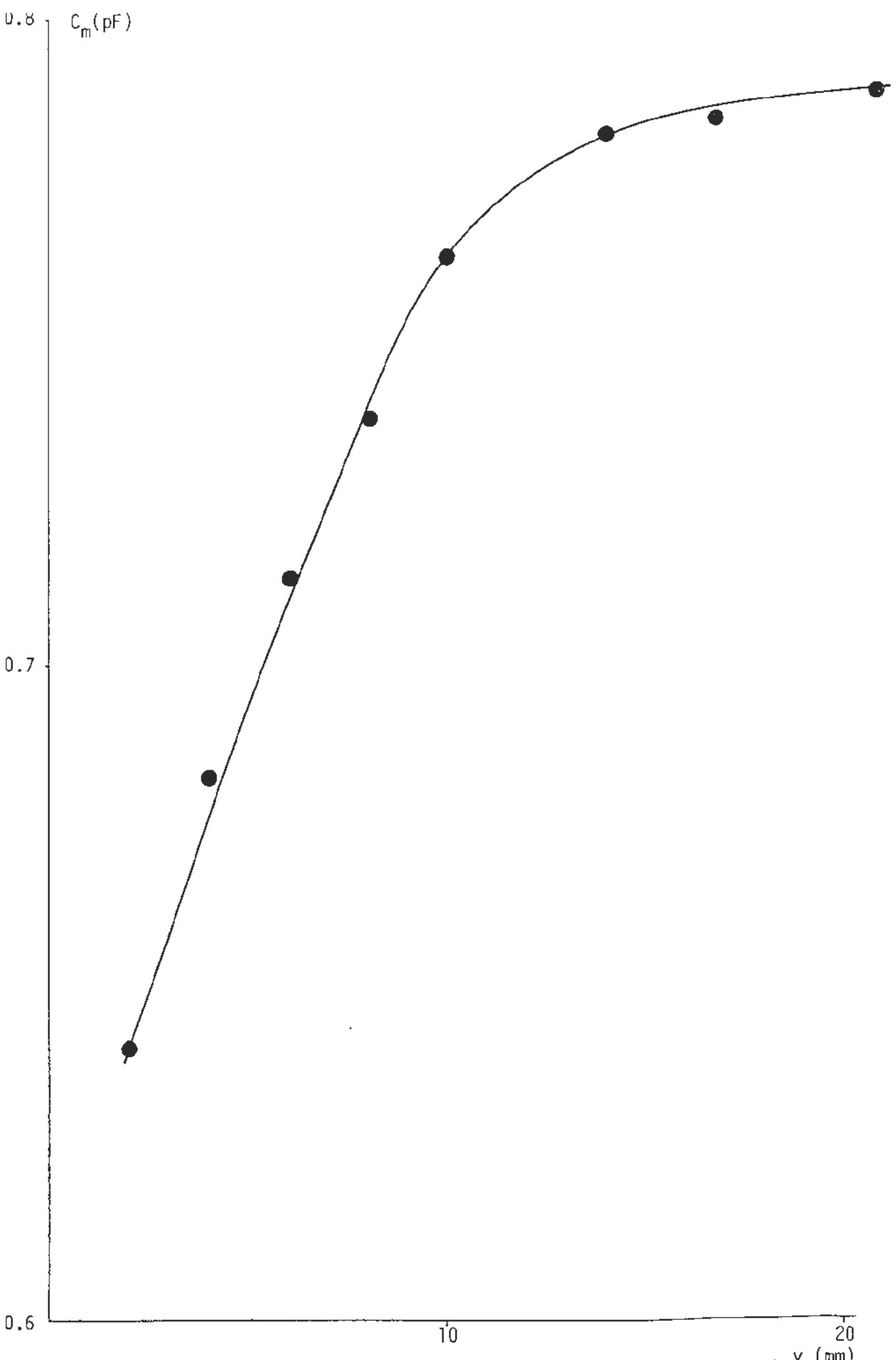

Fig. (3.1) Variation of the capacitance (C_m) with y_1 (y_2 = 33mm)

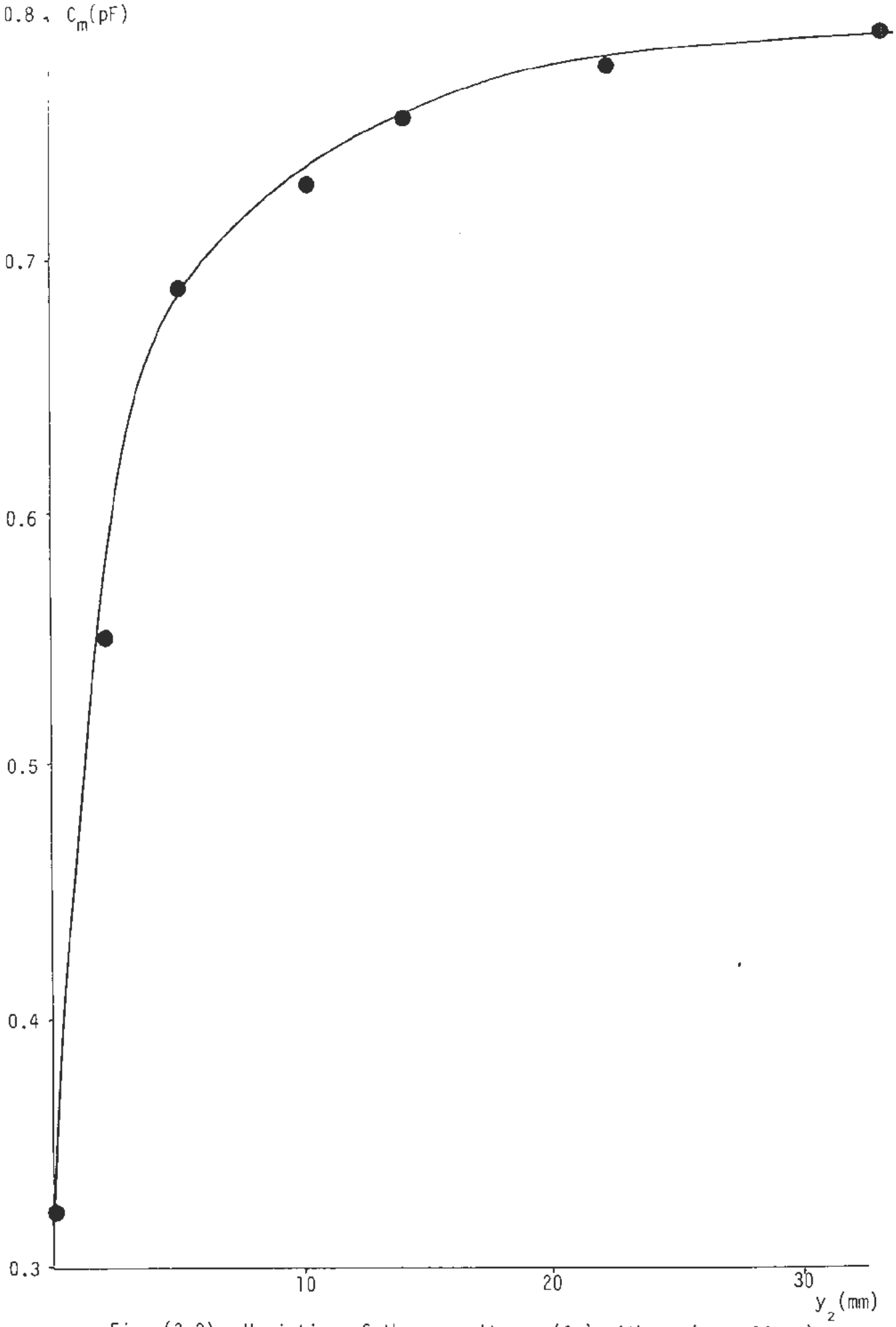

Fig. (3.2) Variation of the capacitance (C_m) with y_2 (y_1 = 14 mm)

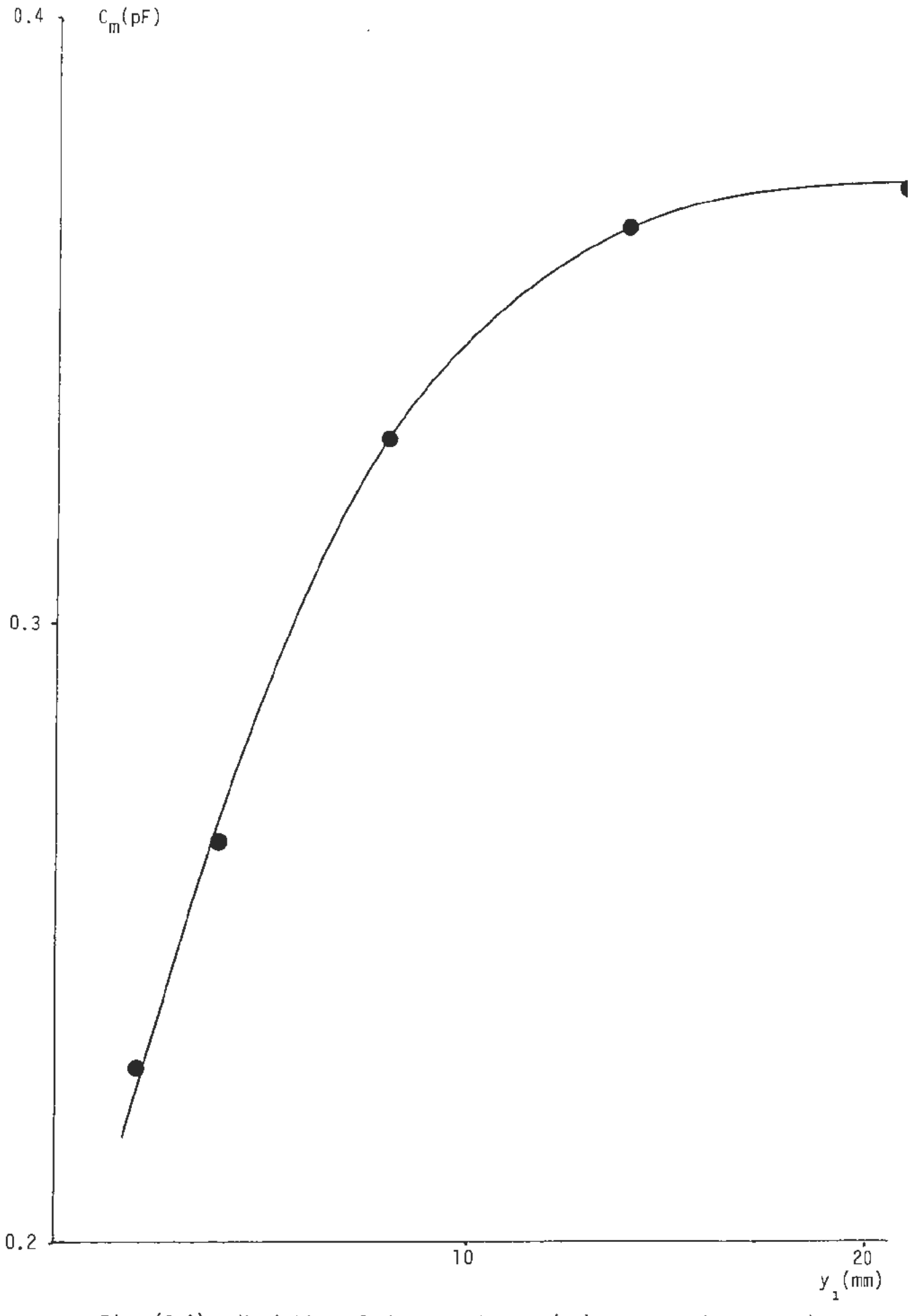

Fig. (3.3) Variation of the capacitance (C_m) with y_1 (y_2 = 33mm)

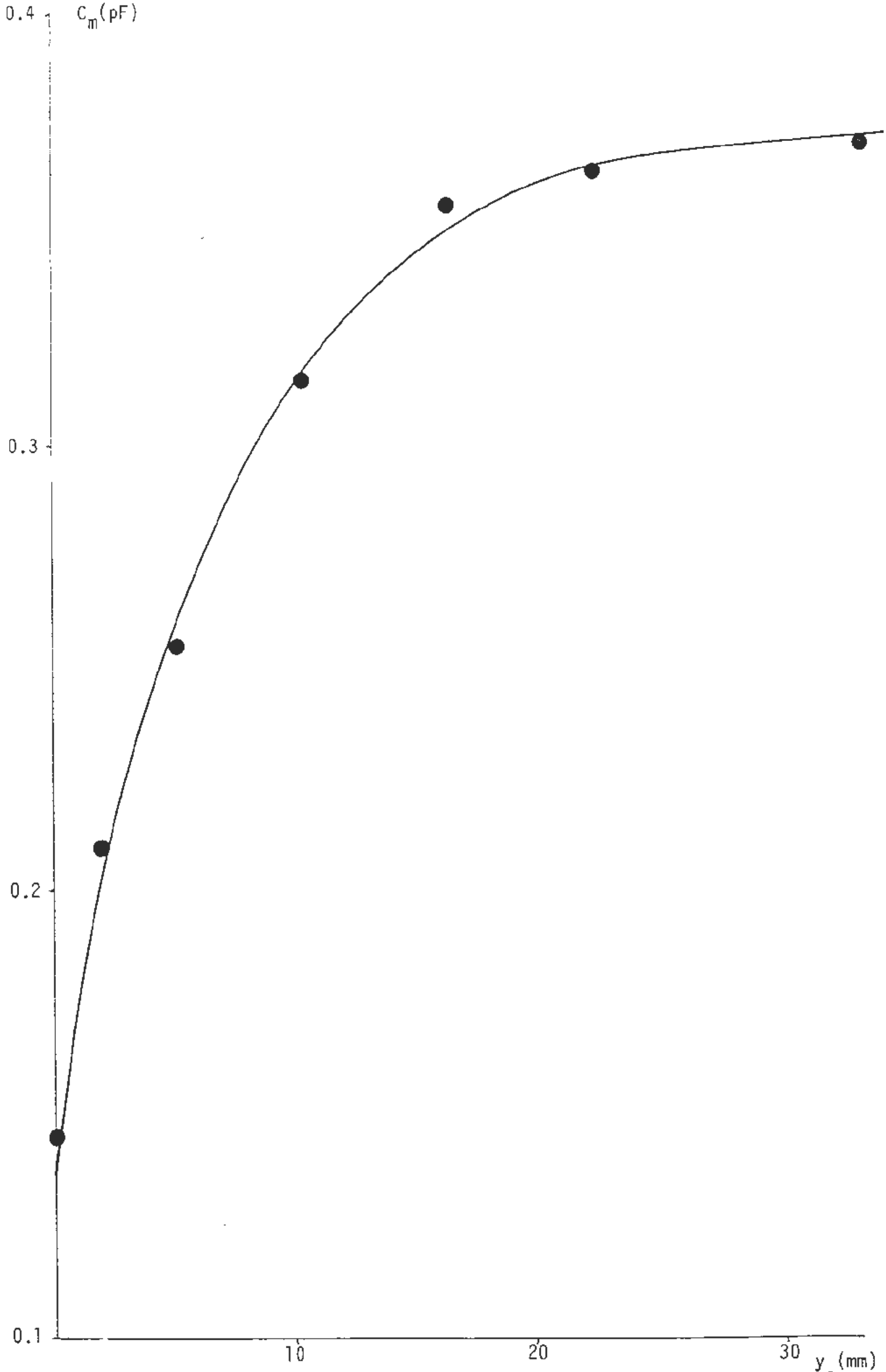

Fig. (3.4) Variation of the capacitance (C_m) with y_2 (y_1 = 14mm)

3.4 The measured capacitance of discontinuous gold films deposited on glass and "Melinex"

The only feasible way, in the present work, to assure the physical discontinuity of the deposited films is to know their d.c. resistances (R_1) at the moment of stopping the deposition; on such a basis and taking into consideration the fact that discontinuous metal films generally have high sheet resistances (85), four gold films with different values of (R_1) and (d_m) were deposited on glass in different evaporation cycles. Immediately after halting the deposition, the sensing device was connected to the capacitance bridge to monitor the changes in the capacitance (C_2) and the dissipation factor (D_2) with time at different frequencies and eventually the capacitance of the deposited films (C_f) was deduced as described in Section (2.10). At the end of the room temperature vacuum annealing period, the d.c. resistances of the films were measured again (R_2) to assess any expected changes. Another four gold films were deposited on "Melinex" and the same steps, as in the case of glass, were followed. The results are presented in Tables(3.5) to (3.12). It should be noted that the values of (C_1), reported in the Tables, were already incorporate the parasitic capacitance introduced by the leadthroughs. This capacitance is 0.4885pF and 0.4780pF at 1Kc and 100Kc respectively. Also, the values of (C_1') were not displayed since (D_1) is less than 0.01 and hence $C_1' = C_1$ (8). For the time being, it is sufficient to observe (i) the dependence of (C_f) on R_1, time and frequency (ii) the more pronounced dependence of (D_2) on the same quantities as shown in Figs. (3.5) to (3.12).

Table (3.5)

In situ monitoring of the changes in the capacitance and dissipation factor as a result of depositing gold film ($R_1 = 5 \times 10^6 \Omega$, $d_m = 60A°$) across the gap of planar capacitor having glass as a dielectric

Before deposition			Immediately after halting the deposition					
f(Kc)	C_1(pF)	D_1	t(mins)	f(Kc)	D_2	C_2(pF)	C_2'(pF)	$C_f = C_2' - C_1'$
1	0.8097	0.005	2	20	0.8	1.3971	0.8519	0.045
10	0.8082	0.005	3	50	0.25	0.8937	0.8411	0.040
20	0.8069	0.005	4	100	0.1	0.8370	0.8287	0.030
50	0.8011	0.005	6	10	1.1	1.9850	0.8982	0.090
100	0.7987	0.005	11	20	0.4	0.9411	0.8113	0.044
			13	50	0.16	0.8256	0.8050	0.039
			15	100	0.07	0.8055	0.8016	0.029
			17	10	0.62	1.1313	0.8172	0.090
			24	10	0.56	1.0735	0.8172	0.090
			25	20	0.26	0.8661	0.8113	0.044
			30	50	0.09	0.8115	0.8050	0.039
			36	100	0.05	0.8070	0.8015	0.028
			38	10	0.43	0.9683	0.8172	0.090
			44	10	0.4	0.9480	0.8172	0.090
			47	20	0.18	0.8376	0.8113	0.044
			60	20	0.16	0.8321	0.8113	0.044
			63	50	0.055	0.8074	0.8050	0.039
			74	10	0.29	0.8858	0.8171	0.089
			85	10	0.27	0.8767	0.8171	0.089
			86	20	0.12	0.8229	0.8112	0.043

Table (3.6)

In situ monitoring of the changes in the capacitance and dissipation factor as a result of depositing gold film ($R_1 = 5 \times 10^7 \Omega$, $d_m = 48A°$) across the gap of planar capacitor having glass as a dielectric

Before deposition			Immediately after halting the deposition					
f(Kc)	C_1(pF)	D_1	t(mins)	f(Kc)	D_2	C_2(pF)	C_2'(pF)	$C_f = C_2' - C_1'$
1	0.8007	0.005	2	20	0.068	0.8034	0.7997	0.075
10	0.8000	0.005	3	10	0.1	0.8206	0.8125	0.125
20	0.7922	0.005	5	1	0.91	1.7950	0.9819	0.1812
50	0.7890	0.005	7	50	0.040	0.8504	0.8490	0.060
100	0.7823	0.005	8	100	0.040	0.8326	0.8313	0.049
			10	20	0.042	0.8667	0.8652	0.073
			12	10	0.069	0.9236	0.9192	0.1192
			13	10	0.067	0.9233	0.9192	0.1192
			14	10	0.065	0.9230	0.9191	0.1191
			16	1	0.63	1.3681	0.9794	0.1787
			18	50	0.020	0.8483	0.8480	0.059
			21	20	0.032	0.8651	0.8642	0.072
			27	10	0.052	0.9207	0.9182	0.1182
			30	10	0.049	0.9204	0.9182	0.1182
			32	1	0.44	1.1677	0.9783	0.1776
			35	50	0.015	0.8472	0.8470	0.058
			37	20	0.028	0.8639	0.8632	0.071
			43	20	0.026	0.8638	0.8632	0.071
			45	10	0.042	0.9197	0.9181	0.1181
			51	10	0.040	0.9196	0.9181	0.1181
			53	1	0.34	1.0902	0.9772	0.1765
			55	20	0.024	0.8627	0.8622	0.070
			65	20	0.022	0.8626	0.8622	0.070
			68	10	0.035	0.9191	0.9180	0.1180
			70	50	0.010	0.8461	0.8460	0.057
			72	1	0.26	1.0429	0.9769	0.1762
			85	20	0.020	0.8625	0.8622	0.070
			87	10	0.032	0.9183	0.9174	0.1174

Table (3.7)

In situ monitoring of the changes in the capacitance and dissipation factor as a result of depositing gold film ($R_1 = 5 \times 10^8 \Omega$, $d_m = 32A°$) across the gap of planar capacitor having glass as a dielectric

Before deposition			Immediately after halting the deposition					
f(Kc)	C_1(pF)	D_1	t(mins)	f(Kc)	D_2	C (pF)	C_2'(pF)	$C_f = C_2' - C_1'$
1	0.8033	0.005	2	1	0.11	1.0263	1.0140	0.2107
10	0.8011	0.005	4	10	0.11	0.9984	0.9983	0.1972
20	0.7992	0.005	5	20	0.008	0.9816	0.9815	0.1823
50	0.7911	0.005	7	50	0.005	0.9623	0.9623	0.1712
100	0.7886	0.005	9	1	0.078	1.0193	1.0131	0.2098
			14	10	0.008	0.9932	0.9931	0.1920
			15	20	0.006	0.9873	0.9873	0.1881
			19	1	0.063	1.0104	1.0064	0.2031
			23	1	0.059	1.0068	1.0033	0.2000
			24	10	0.0065	0.9884	0.9884	0.1873
			26	20	0.004	0.9664	0.9664	0.1672
			29	1	0.054	0.9986	0.9957	0.1924
			36	1	0.050	0.9968	0.9943	0.1910
			37	10	0.006	0.9833	0.9833	0.1822
			45	1	0.045	0.9958	0.9938	0.1905

Table (3.8)

In situ monitoring of the changes in the capacitance and dissipation factor as a result of depositing gold film (R_1 = 5 x $10^9\Omega$, d_m = 22A°) across the gap of planar capacitor having glass as a dielectric

Before deposition			Immediately after halting the deposition					
f(Kc)	C_1(pF)	D_1	t(mins)	f(Kc)	D_2	C_2(pF)	C_2'(pF)	$C_f = C_2' - C_1'$
1	0.8065	0.005	2	1	0.027	1.0320	1.0312	0.2247
10	0.8043	0.005	3	10	0.006	1.0175	1.0175	0.2132
20	0.8001	0.005	4	20	0.006	1.0084	1.0084	0.2083
50	0.7982	0.005	7	1	0.022	1.0280	1.0275	0.2210
100	0.7876	0.005	11	1	0.021	1.0252	1.0247	0.2182
			26	10	0.005	1.0143	1.0143	0.2100
			30	1	0.018	1.0191	1.0188	0.2123

Table (3.9)

In situ monitoring of the changes in the capacitance and dissipation factor as a result of depositing gold film ($R_1 = 5 \times 10^6 \Omega$, $d_m = 63A°$) across the gap of planar capacitor with "Melinex" as a dielectric

Before deposition			Immediately after halting the deposition					
f(Kc)	C_1(pF)	D_1	t(mins)	f(Kc)	D_2	C_2(pF)	C_2'(pF)	$C_f = C_2' - C_1'$
1	0.6339	0.004	2	20	0.84	1.1487	0.6735	0.044
10	0.6310	0.005	3.5	50	0.215	0.6940	0.6633	0.039
20	0.6295	0.006	7	10	1.2	1.7519	0.7180	0.087
50	0.6243	0.007	10	20	0.6	0.9146	0.6725	0.043
100	0.6175	0.007	12	100	0.07	0.6487	0.6455	0.028
			15	10	1.1	1.5824	0.7160	0.085
			18	50	0.15	0.6731	0.6583	0.034
			22	100	0.04	0.6435	0.6425	0.025
			32	20	0.36	0.7515	0.6653	0.041
			34	10	0.75	1.1156	0.7140	0.083
			36	50	0.095	0.6612	0.6553	0.031
			40	100	0.03	0.6401	0.6395	0.022
			42	20	0.3	0.7298	0.6695	0.040
			47	10	0.62	0.9857	0.7120	0.081
			54	50	0.05	0.6549	0.6533	0.029
			60	100	0.02	0.6408	0.6405	0.023
			62	20	0.24	0.7070	0.6685	0.039
			73	10	0.47	0.8668	0.7100	0.079
			89	50	0.04	0.6533	0.6523	0.028
			90	100	0.01	0.6391	0.6385	0.021

Table (3.10)

In situ monitoring of the changes in the capacitance and dissipation factor as a result of depositing gold film ($R_1 = 5 \times 10^7 \Omega$, $d_m = 50A°$) across the gap of planar capacitor with "Melinex" as a dielectric

Before deposition			Immediately after halting the deposition					
f(Kc)	C_1(pF)	D_1	t(mins)	f(Kc)	D_2	C_2(pF)	C_2'(pF)	$C_f = C_2' - C_1'$
1	0.6325	0.004	2	10	0.23	0.7929	0.7531	0.123
10	0.6301	0.005	3	20	0.09	0.7066	0.7009	0.072
20	0.6289	0.006	5	50	0.025	0.6815	0.6811	0.060
50	0.6211	0.007	6	100	0.010	0.6663	0.6662	0.047
100	0.6192	0.007	9	10	0.14	0.7668	0.7521	0.122
			11	20	0.06	0.7024	0.6999	0.071
			13	50	0.02	0.6804	0.6801	0.059
			17	100	0.006	0.6652	0.6652	0.046
			19	10	0.1	0.7586	0.7511	0.121
			23	10	0.095	0.7569	0.7501	0.120
			24	20	0.044	0.7003	0.6989	0.070
			31	20	0.040	0.699	0.6979	0.069
			34	50	0.015	0.6783	0.6781	0.057
			36	10	0.080	0.7539	0.7491	0.119
			50	20	0.032	0.6966	0.6959	0.067
			57	50	0.010	0.6772	0.6771	0.056
			61	1	0.7	1.2026	0.8071	0.1746
			81	10	0.05	0.7490	0.7471	0.117
			82	20	0.024	0.6943	0.6939	0.065
			85	50	0.010	0.6752	0.6751	0.054
			87	1	0.65	1.1465	0.8060	0.1735

Table (3.11)

In situ monitoring of the changes in the capacitance and dissipation factor as a result of depositing gold film ($R_1 = 5 \times 10^8 \Omega$, $d_m = 30A°$) across the gap of planar capacitor with "Melinex" as a dielectric

Before deposition			Immediately after halting the deposition					
f(Kc)	C_1(pF)	D_1	t(mins)	f(Kc)	D_2	C_2(pF)	C_2'(pF)	$C_f = C_2' - C_1'$
1	0.6338	0.004	2	10	0.014	0.8305	0.8303	0.1983
10	0.6320	0.005	4	1	0.090	0.8506	0.8438	0.2100
20	0.6288	0.006	6	20	0.012	0.8091	0.8090	0.1802
50	0.6201	0.007	8	50	0.010	0.7602	0.7601	0.1400
100	0.6188	0.007	11	10	0.011	0.8293	0.8292	0.1972
			12	1	0.055	0.8450	0.8425	0.2087
			14	20	0.010	0.8082	0.8081	0.1793
			24	10	0.010	0.8285	0.8284	0.1964
			26	1	0.042	0.8285	0.8270	0.1932
			34	20	0.008	0.8062	0.8062	0.1774
			45	10	0.009	0.8265	0.8265	0.1945

Table (3.12)

In situ monitoring of the changes in the capacitance and dissipation factor as a result of depositing gold film (R_1 = 5 x $10^9\Omega$, d_m = 19A°) across the gap of planar capacitor with "Melinex" as a dielectric

f(Kc)	C_1(pF)	D_1	t(mins)	f(Kc)	D_2	C_2(pF)	C_2'(pF)	$C_f = C_2' - C_1'$
1	0.6340	0.004	1	1	0.030	0.8585	0.8577	0.2237
10	0.6315	0.005	2	10	0.010	0.8444	0.8443	0.2128
20	0.6291	0.006	3	20	0.009	0.8366	0.8365	0.2074
50	0.6220	0.007	4	1	0.025	0.8580	0.8575	0.2235
100	0.6194	0.007	6	10	0.008	0.8442	0.8441	0.2126
			11	1	0.020	0.8576	0.8573	0.2233
			22	1	0.016	0.8573	0.8571	0.2231
			30	1	0.014	0.8567	0.8567	0.2227

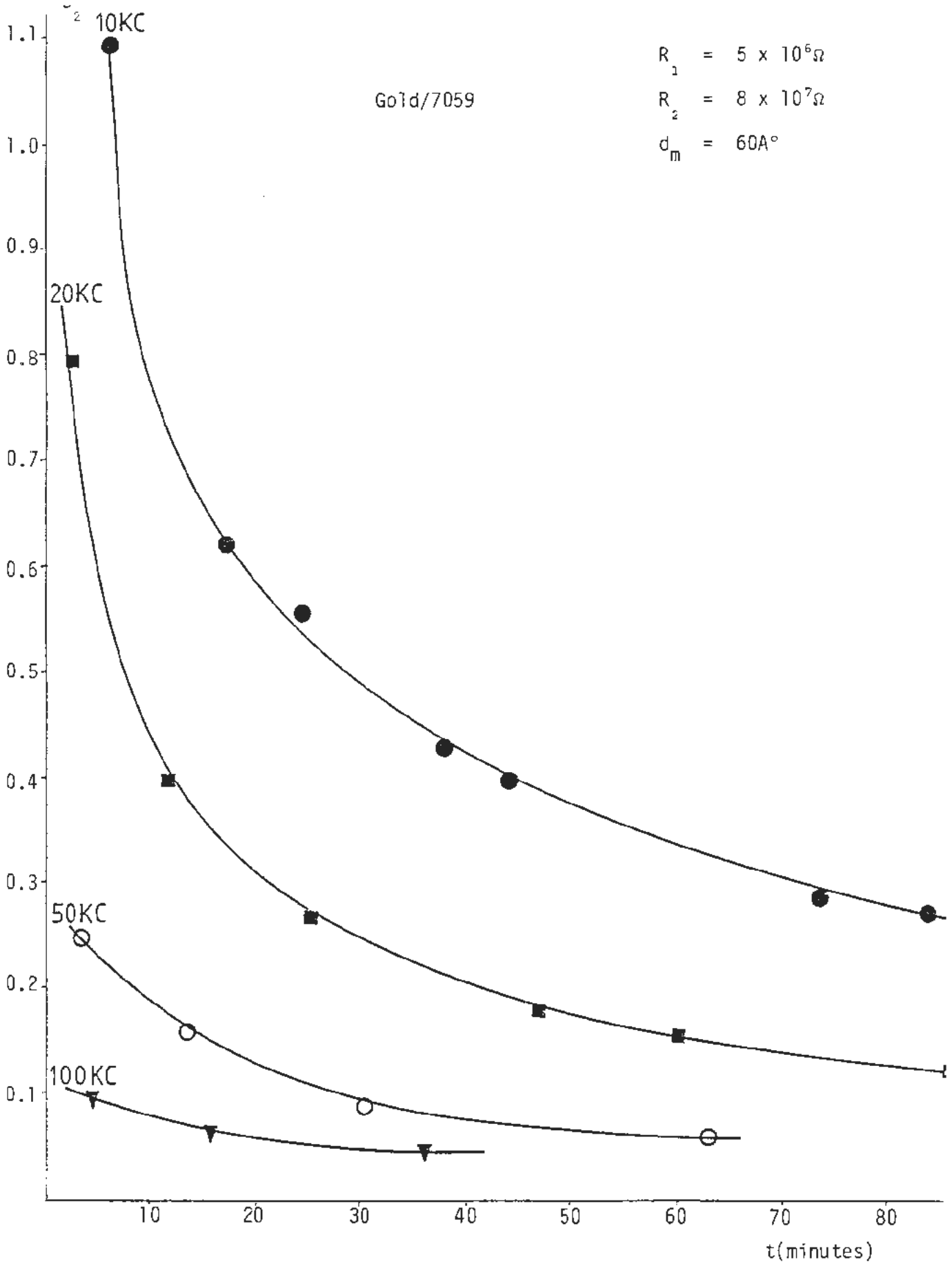

Fig. (3.5) Variation of the dissipation factor (D_2) with time in vacuum

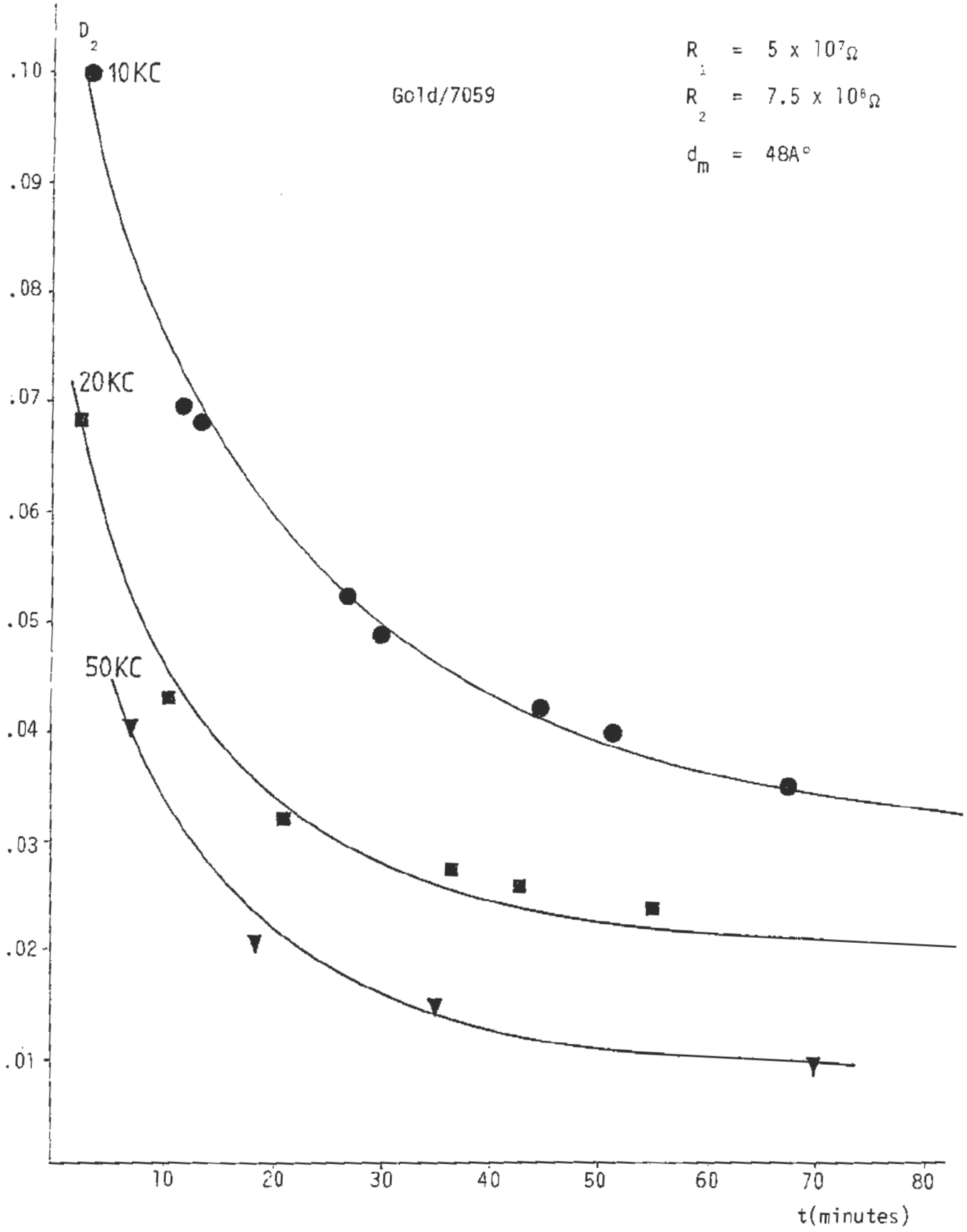

Fig. (3.6) Variation of the dissipation factor (D_2) with time in vacuum

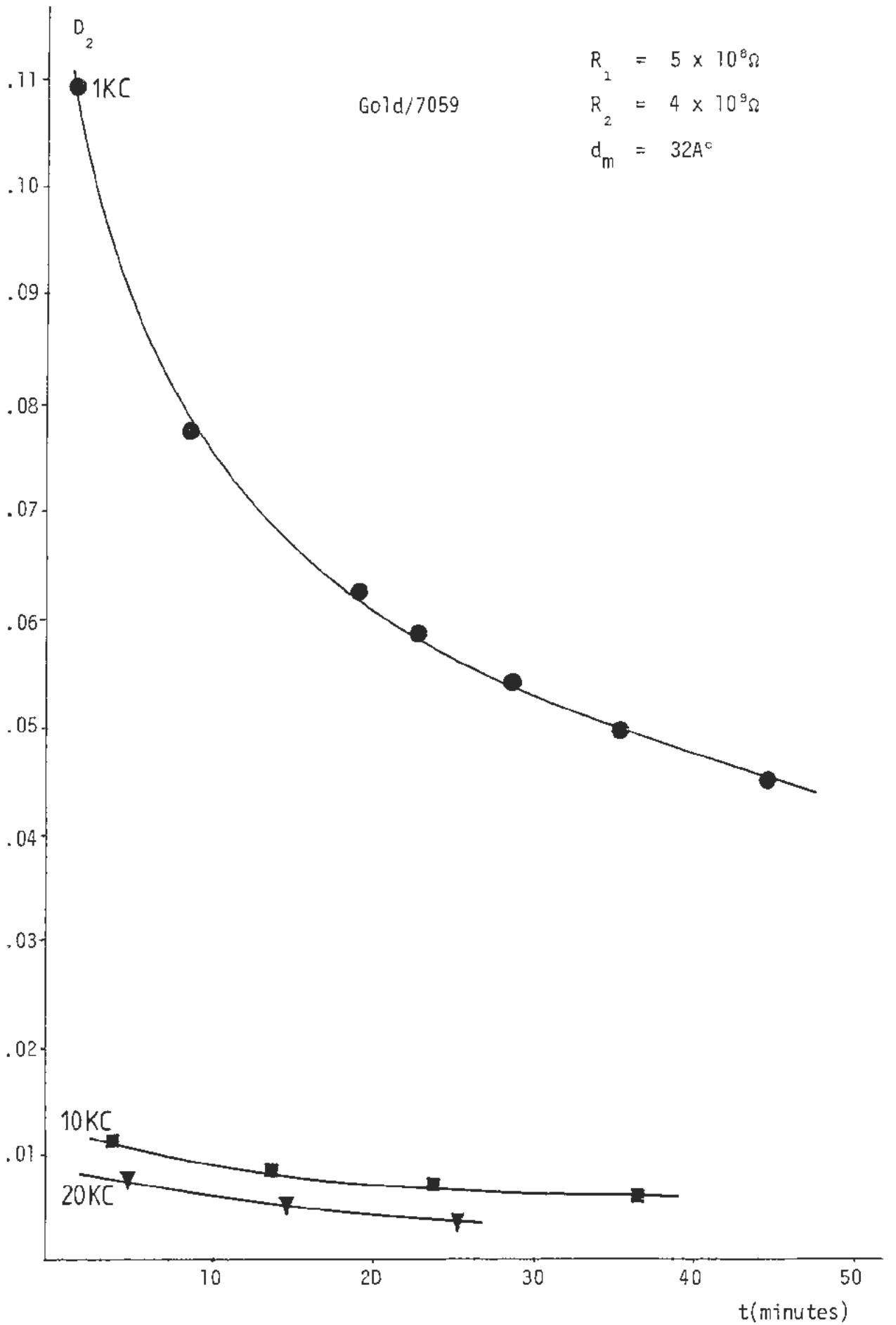

Fig. (3.7) Variation of the dissipation factor (D_2) with time in vacuum

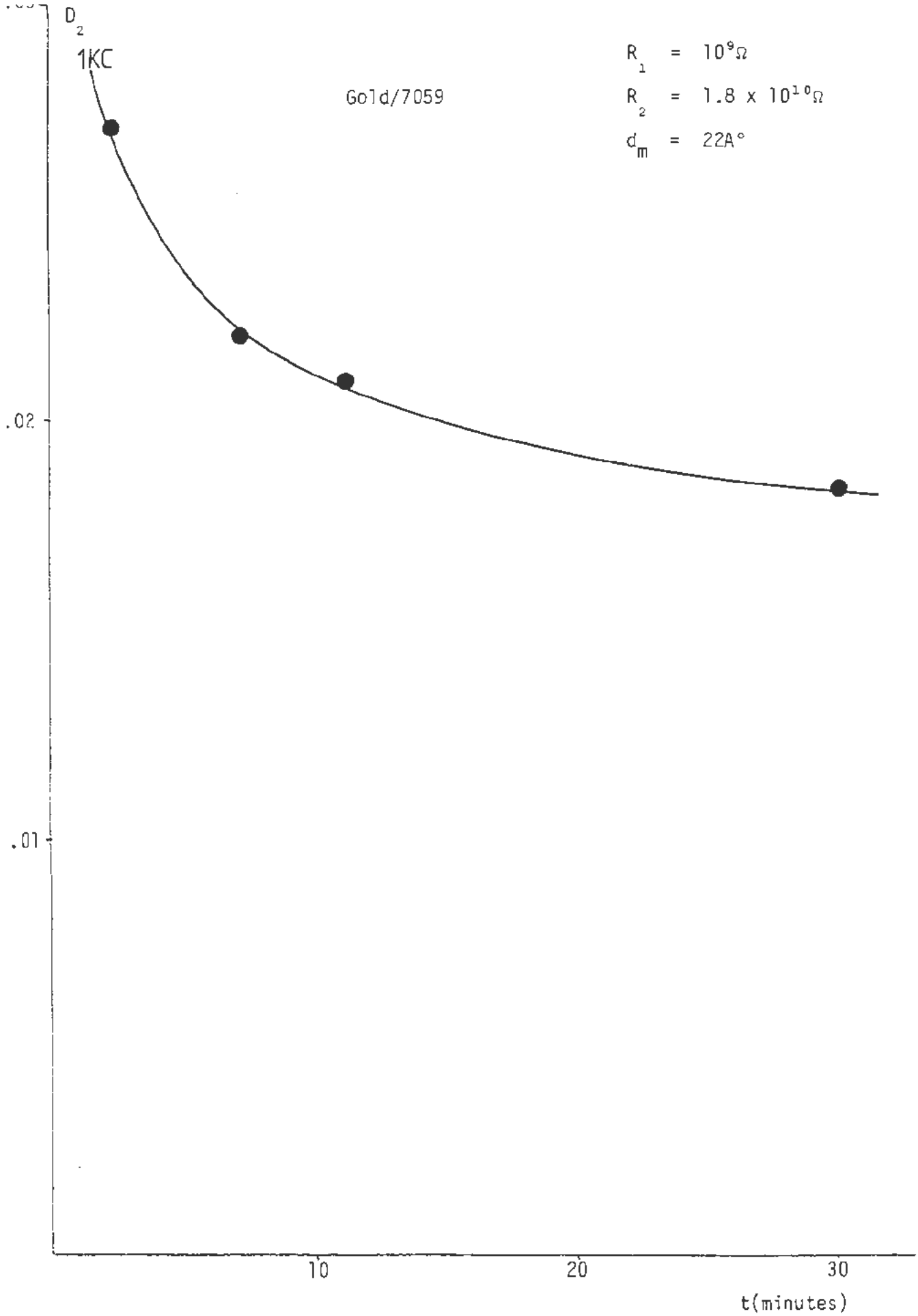

Fig. (3.8) Variation of the dissipation factor (D_2) with time in vacuum

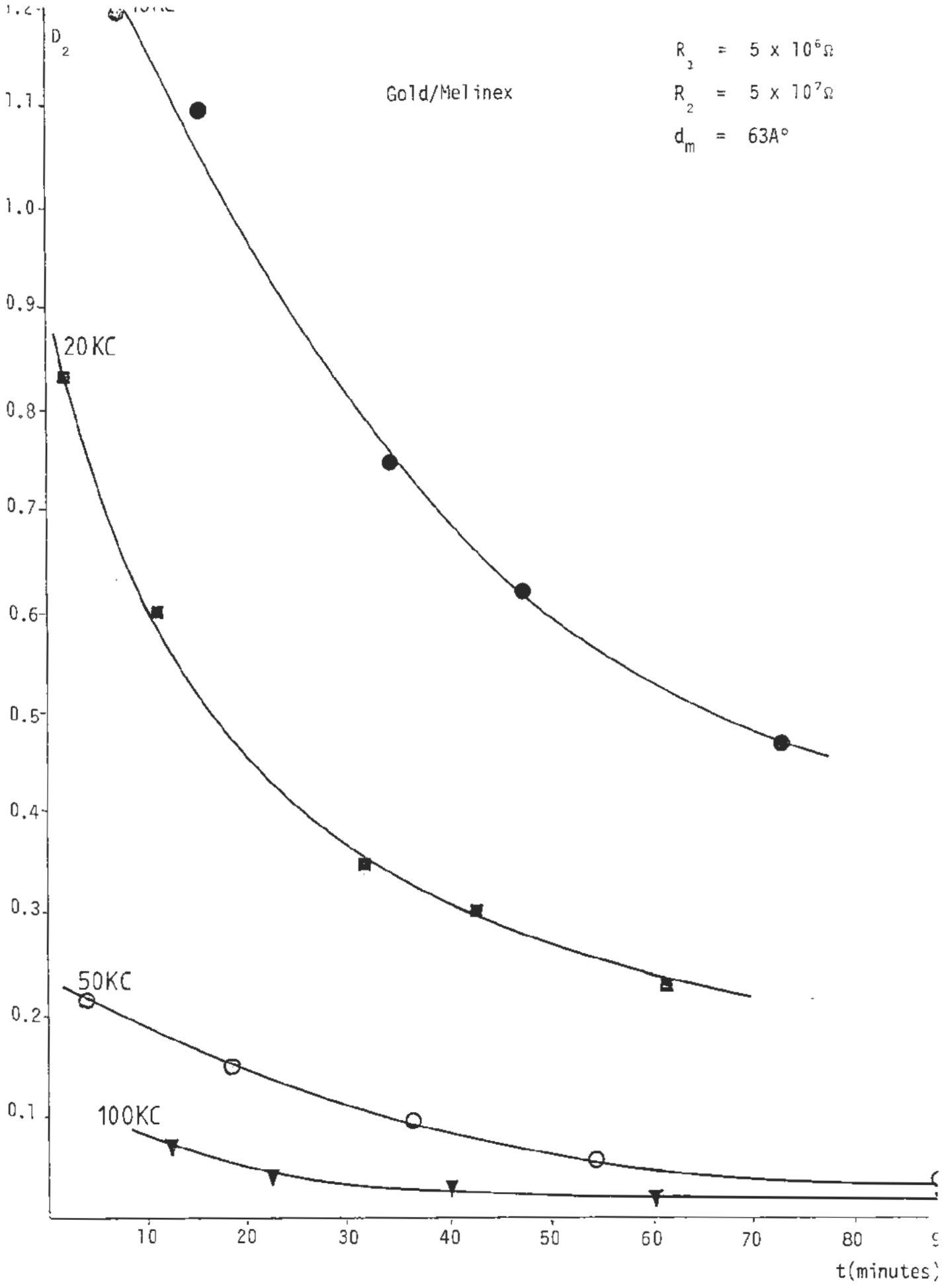

Fig. (3.9) Variation of the dissipation factor (D_2) with time in vacuum

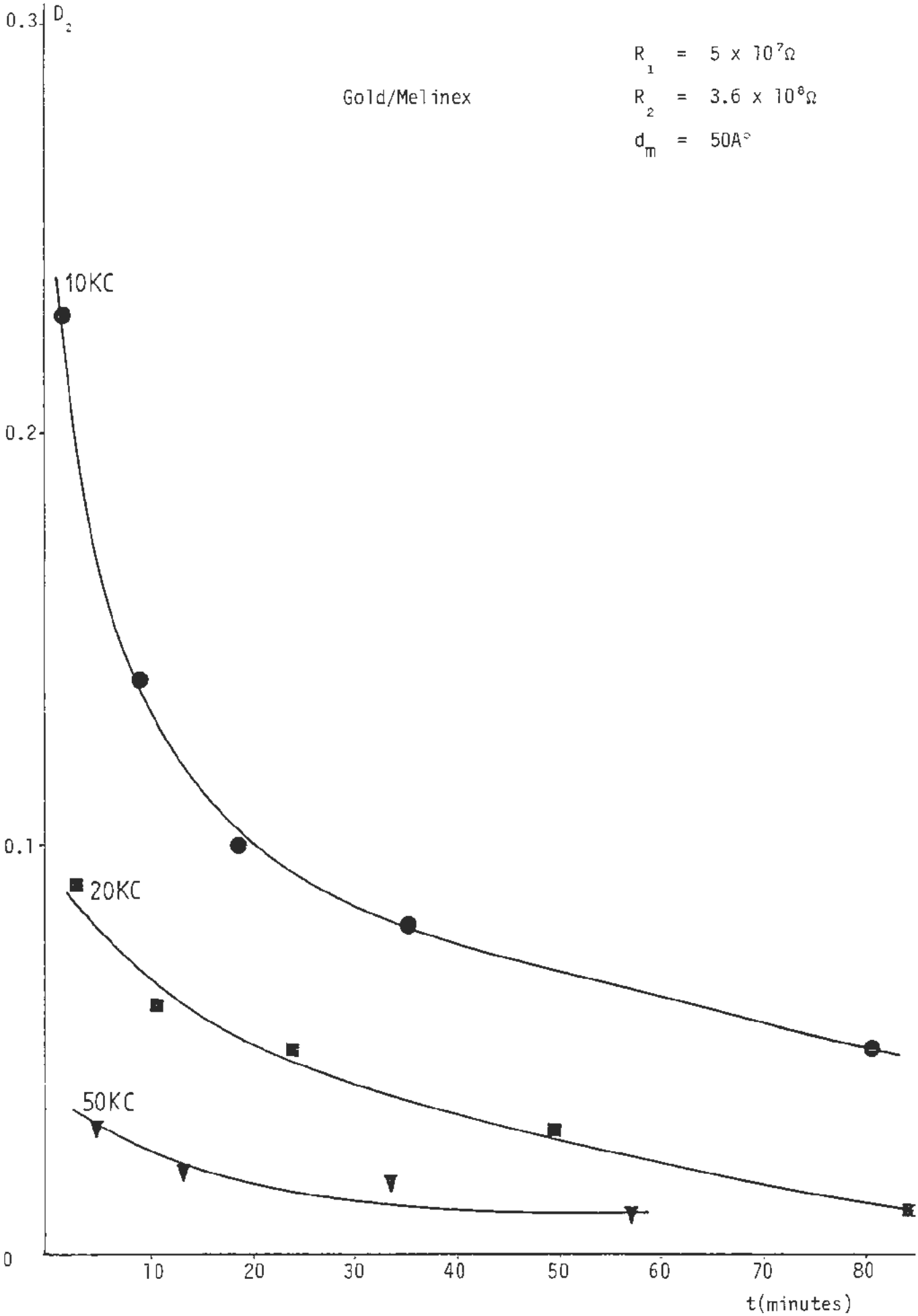

Fig. (3.10) Variation of the dissipation factor (D_2) with time in vacuum

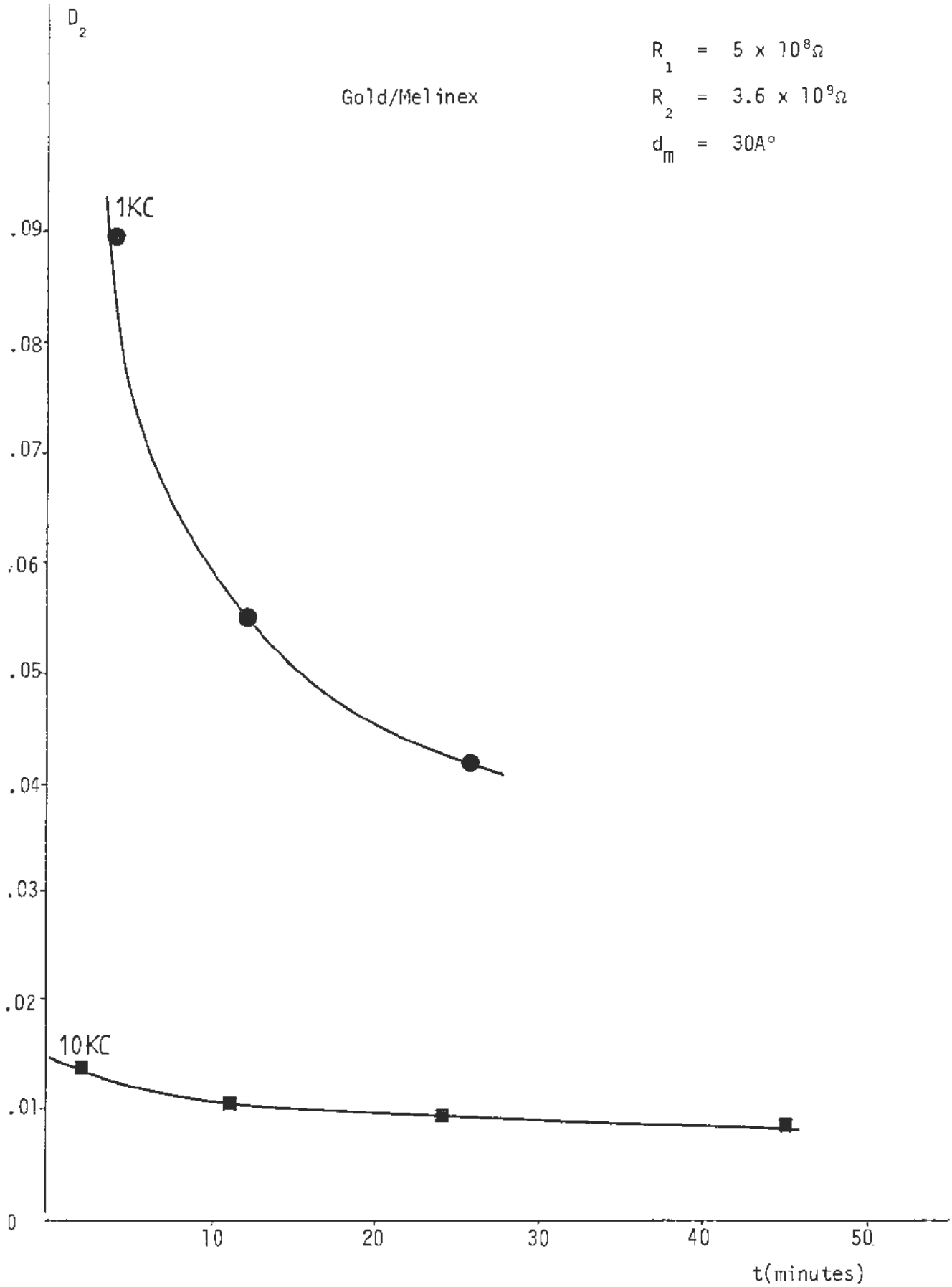

Fig. (3.11) Variation of the dissipation factor (D_2) with time in vacuum

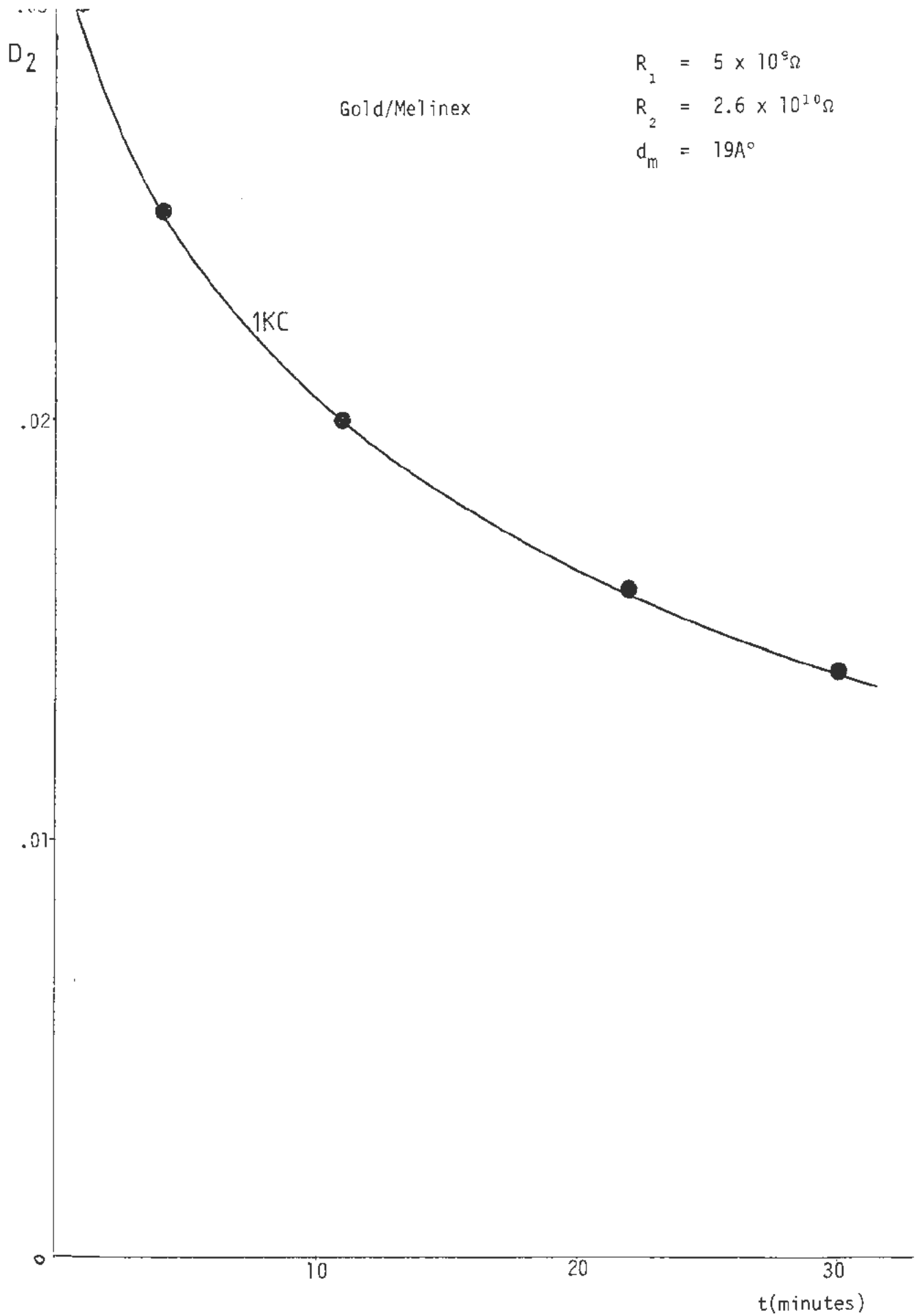

Fig. (3.12) Variation of the dissipation factor (D_2) with time in vacuum

3.5 The measured capacitance of discontinuous aluminium films deposited on glass and "Melinex"

Four different aluminium films were deposited on each substrate and by following the same procedure as in the case of gold films the relevant results were obtained as shown in Tables (3.13) to (3.18) and Figs. (3.13) to (3.18). No detectable change in (C_1) and (D_1) were observed after depositing the films with $R_1 = 5 \times 10^9 \Omega$, this could be attributed to the fact that although deposition took place in a residual air pressure as low as 7×10^{-6} torr there would still be sufficient oxygen molecules present to completely oxidize the islands (86).

3.6 Post-deposition resistance changes in discontinuous gold and aluminium films

It was not our intention to study the post-deposition drift in the d.c. resistance of our films because such item was tackled before by many investigators especially for gold films. Nevertheless it may be useful to see how the d.c. resistance of these films change with time, as shown in Figs. (3.19) and (3.20) for gold and aluminium films respectively. These may help in interpreting the variation of the dissipation factor (D_2) with time as well.

3.7 Calculation of the parallel capacitance of discontinuous metal films

The capacitance of island films can be calculated, in principle, if all the quantitites in the right hand side of eqn. (1.13) are known; but it is too difficult to have the values of (R_1), (R_2) and (C') for our films and this difficulty may be the reason why we cannot find any published values for the calculated capacitiance

so far. Accordingly, only the general characteristics of the capacitance and its value under certain conditions will be tried here. Eqn. (1.13) can be rewritten as

$$C_{p/C'} = \left(\frac{W}{\ell}\right)\left(\frac{R_1}{R_2}\right)^2 \left[\frac{1}{1 + 2\left(\frac{R_1}{R_2}\right) + \left(\frac{R_1}{R_2}\right)^2 + 4\pi^2 f^2 C'^2 R_1^2}\right] \quad (3.3)$$

such that for certain aspect ratio $\left(\frac{\ell}{W}\right)$, the ratio $C_{p/C'}$ will depend on fR_1C' as a variable and $\frac{R_1}{R_2}$ as a parameter. Figures (3.21) to (3.23) show a family of curves, obtained for different parameters, with the main following characteristics:

(a) For any given value of fR_1C', $C_{p/C'}$ increases with the increase of $\frac{R_1}{R_2}$

(b) The decrease of $C_{p/C'}$ with the increase of $(fC'R_1)$ is well demonstrated for $R_1/R_2 = 1$ while it is less pronounced for larger values of $\frac{R_1}{R_2}$.

It is evident from Fig. (3.23) that:

$$C_p = C' \qquad \left(\frac{W}{\ell} = 1\right) \quad (3.4)$$

$$C_p = 12.5C' \qquad \left(\frac{W}{\ell} = 12.5 \text{ for our films}\right) \quad (3.5)$$

It should be remembered that (C'), as given by eqn. (1.20), was deduced on the assumption that the two islands were of spherical shape and completely immersed in the dielectric. In fact a more realistic assumption is required which would be a disk-shaped or hemispherical islands with the dielectric on one side and vacuum on the other side as shown in Fig. (3.24). A notice must be given to the fact that when (R_1) goes to zero, namely, the metal film becomes physically continuous then the parallel capacitance (eqn. 1.13)

goes to zero as well. There is evidence that islands of discontinuous metal films may well be taller than wide and for the purpose of simple calculation they can be idealised as elongated boxes a shown in Fig. (3.25) and if the aspect ratio of the film is 10^{-6} then the following equation can be written

$$C' = \varepsilon_0 \frac{yZ}{x} \quad ; \text{ then taking } x = Z = 50A^\circ,\ y = 80A^\circ$$

$$C' = 7.1 \times 10^{-8} pF \tag{3.6}$$

$$C_p = 7.1 \times 10^{-2} pF \tag{3.7}$$

Table (3.13)

In situ monitoring of the changes in the capacitance and dissipation factor as a result of depositing aluminium film ($R_1 = 5 \times 10^6 \Omega$, $d_m = 55A°$) across the gap of planar capacitor having glass as a dielectric

Before deposition			Immediately after halting the deposition					
f(Kc)	C_1 (pF)	D_1	t(mins)	f(Kc)	D_2	C_2 (pF)	C_2'(pF)	$C_f = C_2' - C_1'$
1	0.8092	0.005	1	20	0.08	0.8760	0.8704	0.07
10	0.8032	0.005	1.5	20	0.04	0.8417	0.8404	0.04
20	0.8004	0.005	2	20	0.03	0.8311	0.8304	0.03
50	0.7987	0.005	3	20	0.024	0.8209	0.8204	0.02
100	0.7901	0.005	3.5	10	0.039	0.8265	0.8252	0.022
			4.5	10	0.034	0.8242	0.8232	0.02
			5	10	0.031	0.8210	0.8202	0.017
			6	10	0.028	0.8188	0.8182	0.015
			7	1	0.2	0.8624	0.8292	0.020
			8.5	20	0.014	0.8136	0.8134	0.013
			10	20	0.012	0.8105	0.8104	0.010
			12.5	10	0.017	0.8144	0.8142	0.011
			14	10	0.016	0.8124	0.8122	0.009
			16	1	0.08	0.8265	0.8212	0.012
			17.5	1	0.07	0.8232	0.8192	0.010
			20	1	0.06	0.8201	0.8172	0.008
			24	10	0.013	0.8103	0.8102	0.007
			28.5	1	0.05	0.8192	0.8172	0.008
			30	20	0.008	0.8035	0.8034	0.003

Table (3.14)

In situ monitoring of the changes in the capacitance and dissipation factor as a result of depositing aluminium film ($R_1 = 5 \times 10^7 \Omega$, $d_m = 46A°$) across the gap of planar capacitor having glass as a dielectric

Before deposition			Immediately after halting the deposition					
f(Kc)	C_1(pF)	D_1	t(mins)	f(Kc)	D_2	C_2(pF)	C_2'(pF)	$C_f = C_2' - C_1'$
1	0.8070	0.005	1	10	0.033	1.0363	1.0352	0.2342
10	0.8010	0.005	2	10	0.02	1.0046	1.0042	0.2032
20	0.7998	0.005	3	10	0.017	0.9737	0.9734	0.1724
50	0.7921	0.005	4	20	0.010	0.9530	0.9529	0.1531
100	0.7834	0.005	5.5	1	0.030	0.9404	0.9396	0.1326
			7.5	10	0.010	0.9373	0.9372	0.1362
			9.5	10	0.009	0.9038	0.9037	0.1027
			10.5	20	0.008	0.9130	0.9130	0.1132
			12	1	0.024	0.9157	0.9152	0.1082
			14.5	1	0.022	0.9080	0.9076	0.1006
			17	10	0.006	0.8931	0.8931	0.0921
			22	1	0.017	0.8949	0.8946	0.0876
			29	1	0.014	0.8593	0.8591	0.0521
			30	10	0.005	0.8336	0.8336	0.0326

Table (3.15)

In situ monitoring of the changes in the capacitance and dissipation factor as a result of depositing aluminium film ($R_1 = 5 \times 10^8 \Omega$, $d_m = 30A^c$) across the gap of planar capacitor having glass as a dielectric

Before deposition			Immediately after halting the deposition					
f(Kc)	C_1(pF)	D_1	t(mins)	f(Kc)	D_2	C_2(pF)	C_2'(pF)	$C_f = C_2' - C_1'$
1	0.8097	0.005	0.5	1	0.012	0.9530	0.9529	0.1432
10	0.8039	0.005	1	1	0.010	0.9219	0.9218	0.1121
20	0.8012	0.005	2	1	0.007	0.9109	0.9109	0.1012
50	0.7982	0.005	4	1	0.005	0.8923	0.8923	0.0826
100	0.7921	0.005	5	1	0.005	0.8097	0.8097	0.0000

Table (3.16)

In situ monitoring of the changes in the capacitance and dissipation factor as a result of depositing aluminium film ($R_1 = 5 \times 10^6 \Omega$, $d_m = 54A^c$) across the gap of planar capacitor having "Melinex" as a dielectric

Before deposition			Immediately after halting the deposition					
f(Kc)	C_1(pF)	D_1	t(mins)	f(Kc)	D_2	C_2(pF)	C_2'(pF)	$C_f = C_2' - C_1'$
1	0.6325	0.004	1	20	0.085	0.6995	0.6945	0.066
10	0.6301	0.005	1.5	20	0.043	0.6798	0.6785	0.050
20	0.6285	0.006	2	20	0.033	0.6702	0.6695	0.041
50	0.6233	0.007	3	20	0.027	0.6590	0.6585	0.03
100	0.6185	0.007	4	10	0.041	0.6642	0.6631	0.033
			5	10	0.033	0.6588	0.6581	0.028
			6	10	0.030	0.6527	0.6521	0.022
			7	1	0.22	0.6883	0.6565	0.024
			9	20	0.017	0.6487	0.6485	0.020
			10	20	0.015	0.6456	0.6455	0.017
			13	10	0.020	0.6464	0.6461	0.016
			15	1	0.115	0.6571	0.6485	0.016
			18	1	0.090	0.6507	0.6455	0.013
			20	1	0.080	0.6456	0.6415	0.009
			25	10	0.015	0.6392	0.6391	0.009
			29	1	0.06	0.6408	0.6385	0.006
			30	20	0.09	0.6417	0.6365	0.008

Table (3.17)

In situ monitoring of the changes in the capacitance and dissipation factor as a result of depositing aluminium film ($R_1 = 5 \times 10^7 \Omega$, $d_m = 48A°$) across the gap of planar capacitor having "Melinex" as a dielectric

Before deposition			Immediately after halting the deposition					
f(Kc)	C_1(pF)	D_1	t(mins)	f(Kc)	D_2	C_2(pF)	C_2'(pF)	$C_f = C_2' - C_1'$
1	0.6350	0.004	1	10	0.035	0.853	0.852	0.2212
10	0.6308	0.005	2	10	0.022	0.8405	0.8401	0.2093
20	0.6287	0.006	3	10	0.018	0.8147	0.8144	0.1836
50	0.6250	0.007	4	20	0.011	0.7911	0.7910	0.1623
100	0.6186	0.007	5	1	0.033	0.7781	0.7781	0.1431
			8	10	0.011	0.7834	0.7834	0.1526
			11	20	0.009	0.7599	0.7599	0.1312
			12	1	0.026	0.7473	0.7473	0.1123
			15	1	0.024	0.7276	0.7276	0.0926
			17	10	0.007	0.7412	0.7412	0.1104
			29	1	0.017	0.7072	0.7070	0.072
			30	10	0.005	0.7134	0.7134	0.0826

Table (3.18)

In situ monitoring of the changes in the capacitance and dissipation factor as a result of depositing aluminium film ($R_1 = 5 \times 10^8 \Omega$, $d_m = 28A°$) across the gap of planar capacitor having "Melinex" as a dielectric

Before deposition			Immediately after halting the deposition					
f(Kc)	C_1(pF)	D_1	t(mins)	f(Kc)	D_2	C_2(pF)	C_2'(pF)	$C_f = C_2' - C_1'$
1	0.636	0.004	0.5	1	0.014	0.7733	0.7732	0.1372
10	0.6315	0.005	1	1	0.011	0.7537	0.7536	0.1176
20	0.6289	0.006	2	1	0.008	0.7442	0.7442	0.1082
50	0.6244	0.007	4	1	0.005	0.7283	0.7283	0.0923
100	0.6188	0.007	5	1	0.004	0.636	0.636	0.0000

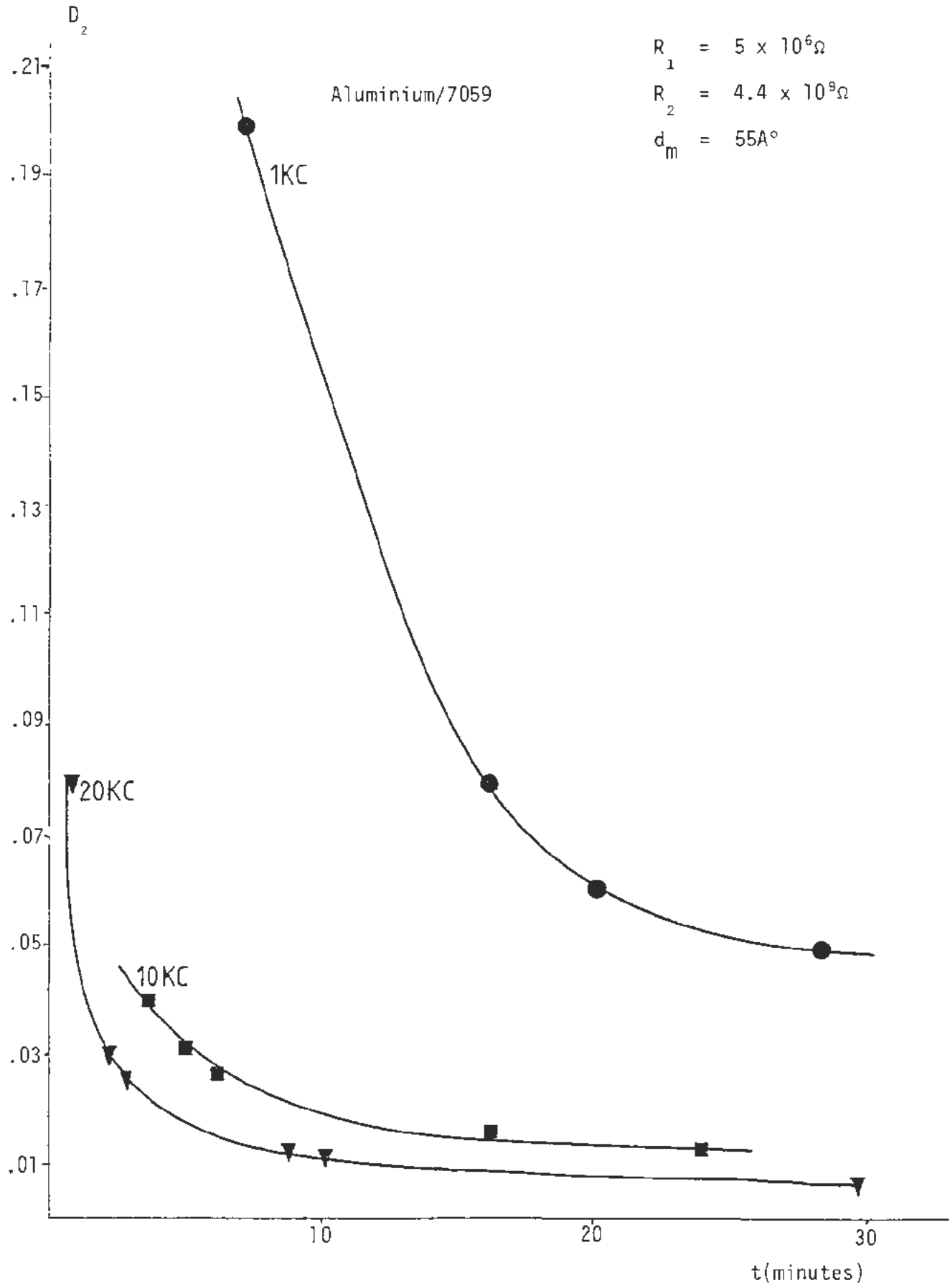

Fig. (3.13) Variation of the dissipation factor (D_2) with time in vacuum

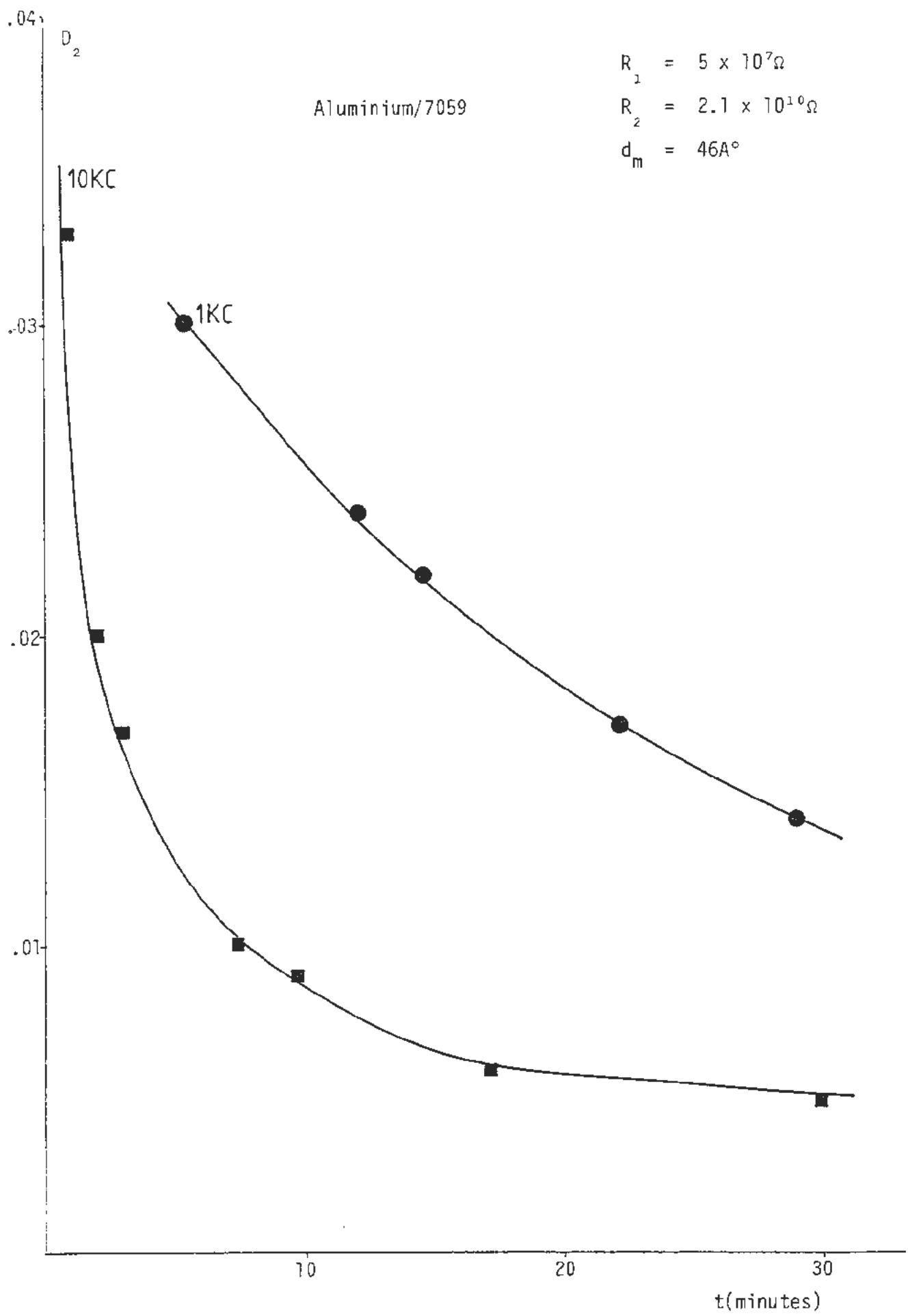

Fig. (3.14) Variation of the dissipation factor (D_2) with time in vacuum

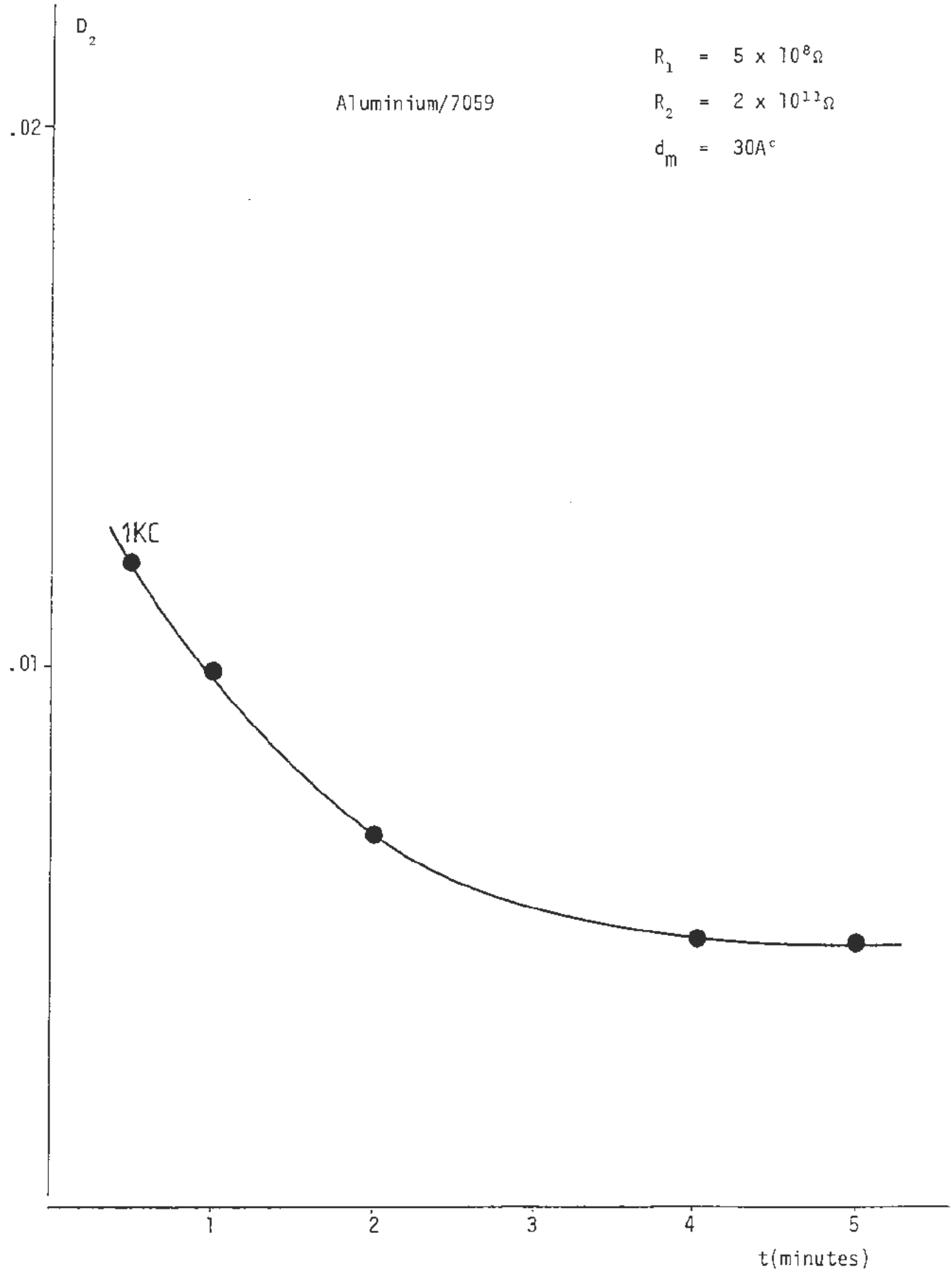

Fig. (3.15) Variation of the dissipation factor (D_2) with time in vacuum

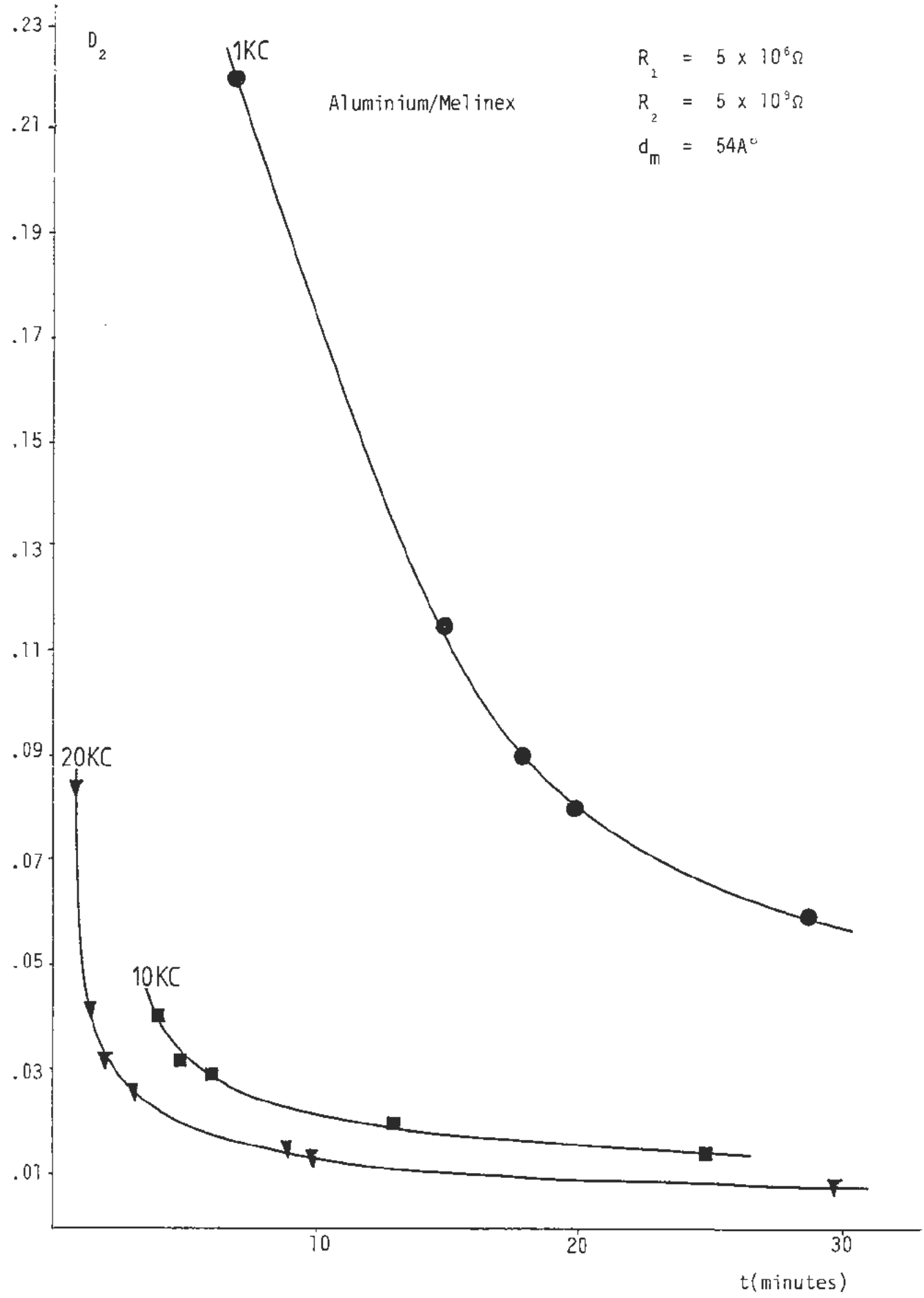

Fig. (3.16) Variation of the dissipation factor (D_2) with time in vacuum

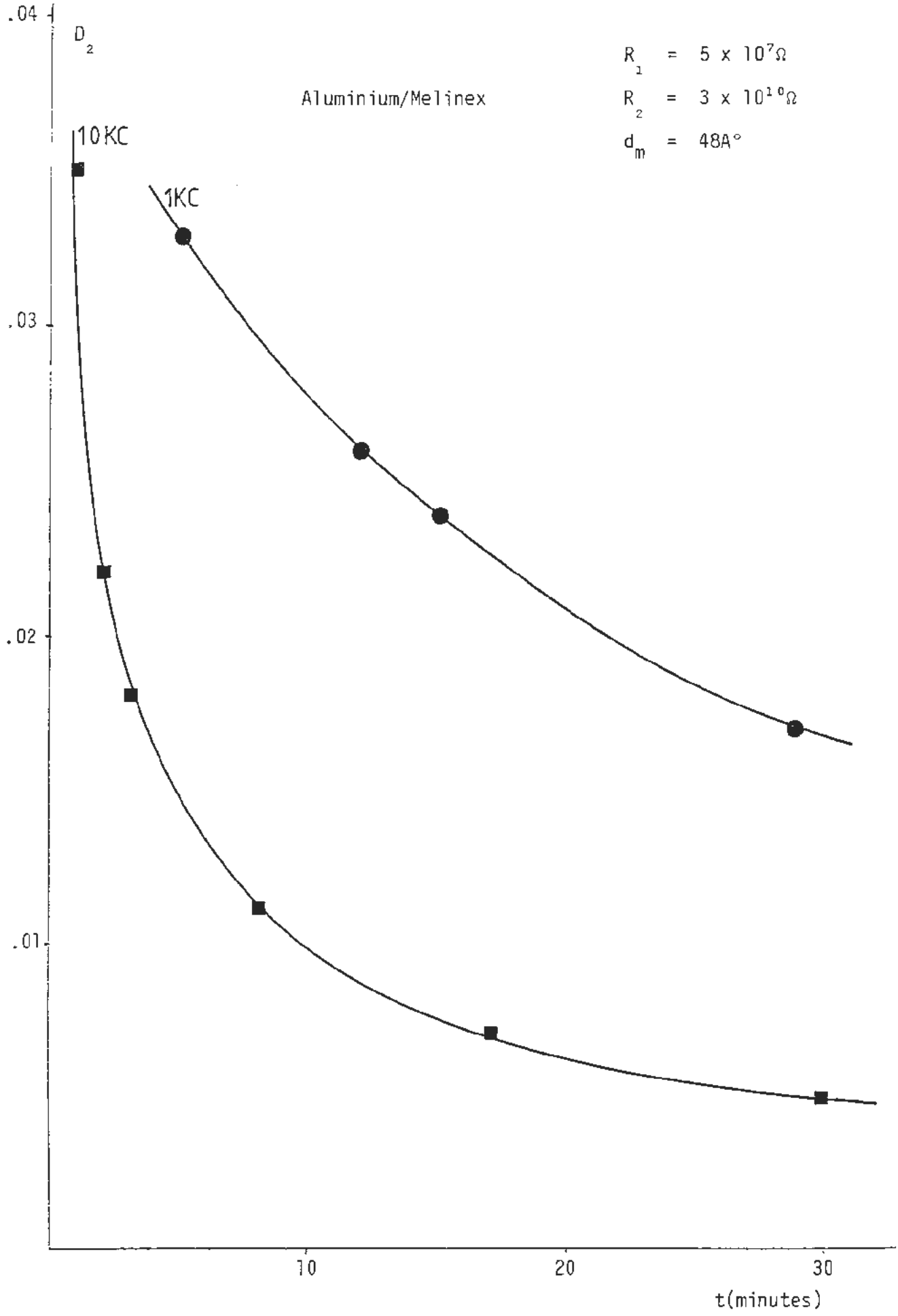

Fig. (3.17) Variation of the dissipation factor (D_2) with time in vacuum

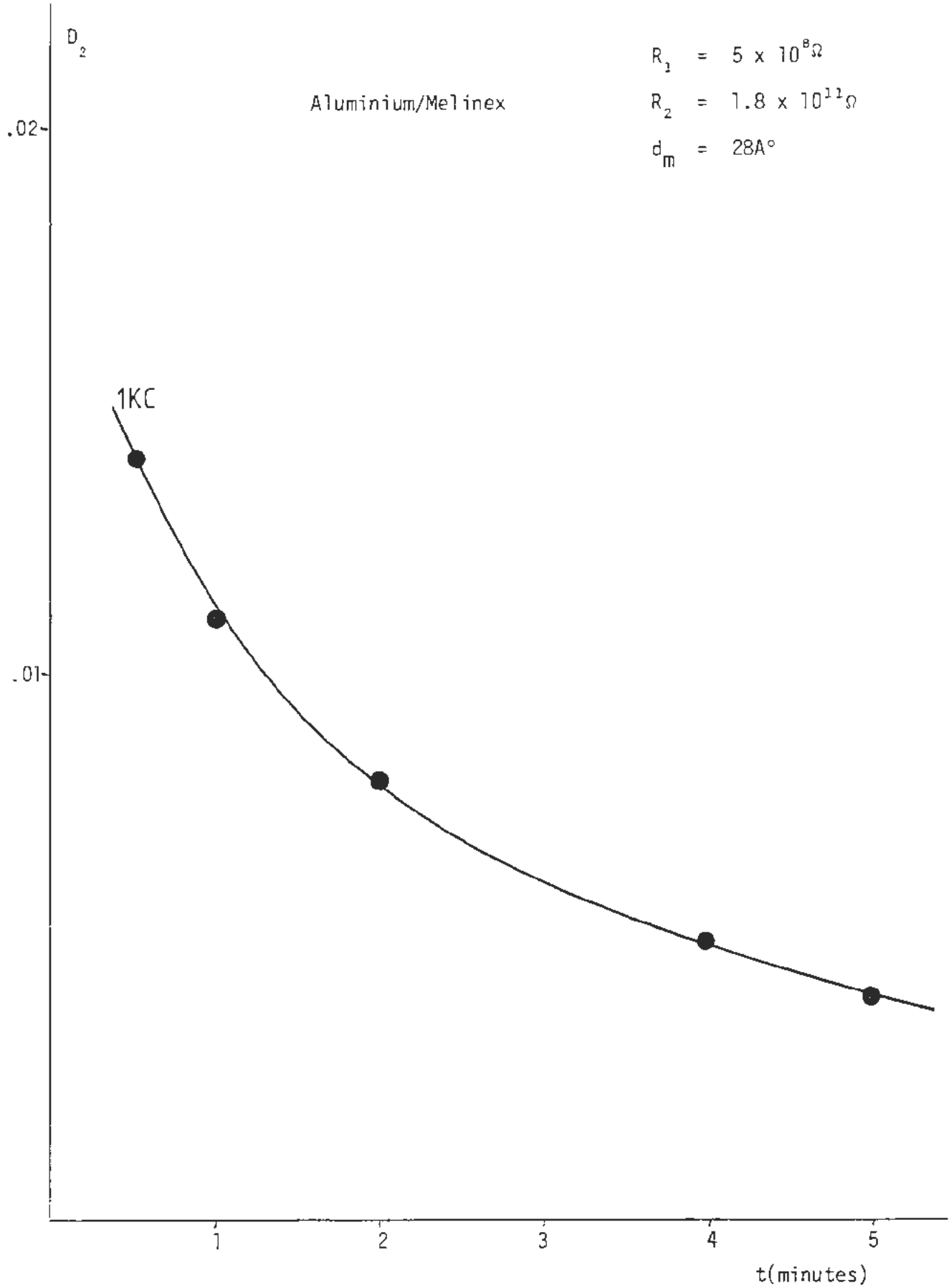

Fig. (3.18) Variation of the dissipation factor (D_2) with time in vacuum

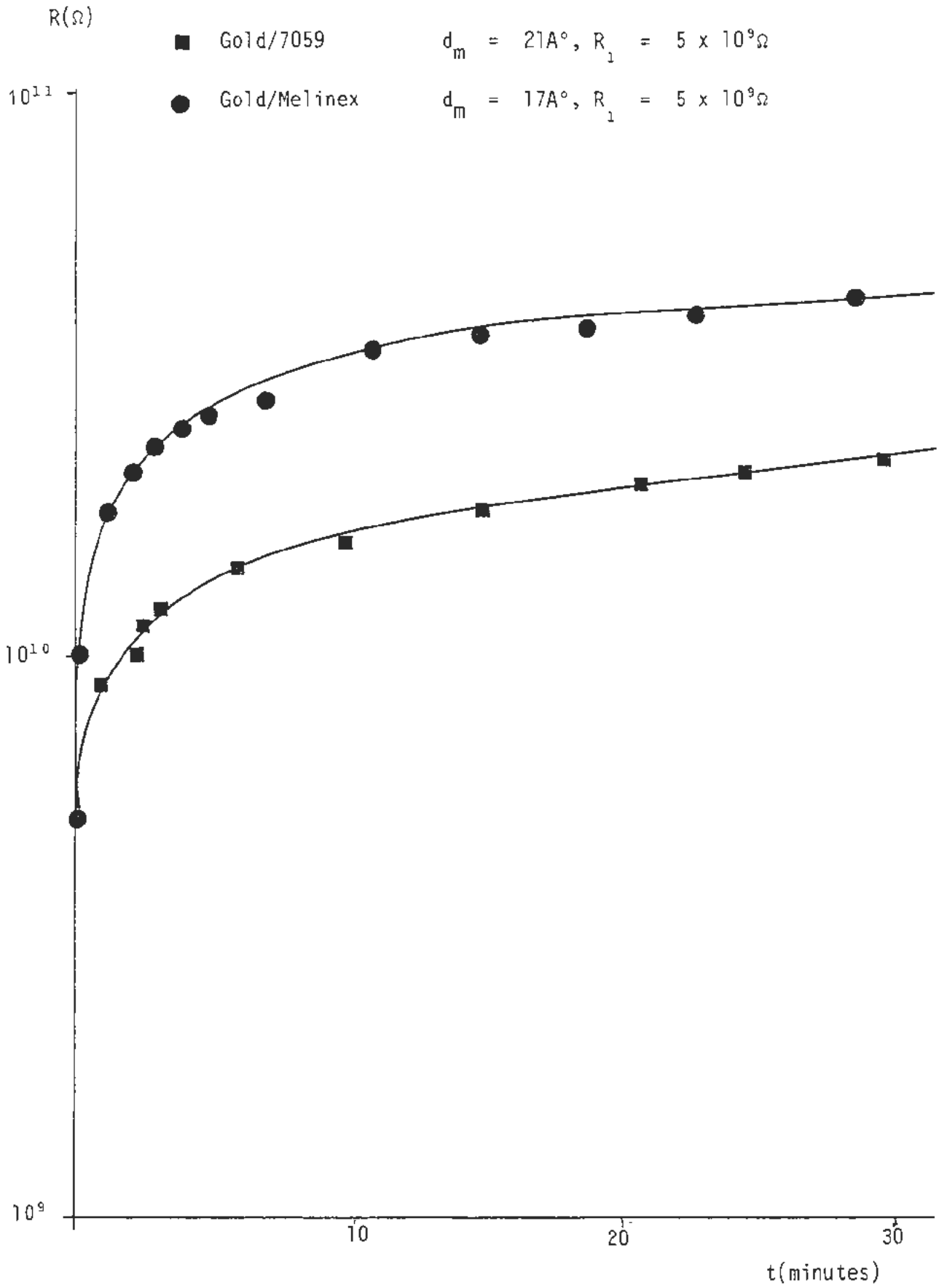

Fig. (3.19) Variation of the d.c. resistance of gold films with time in vacuum

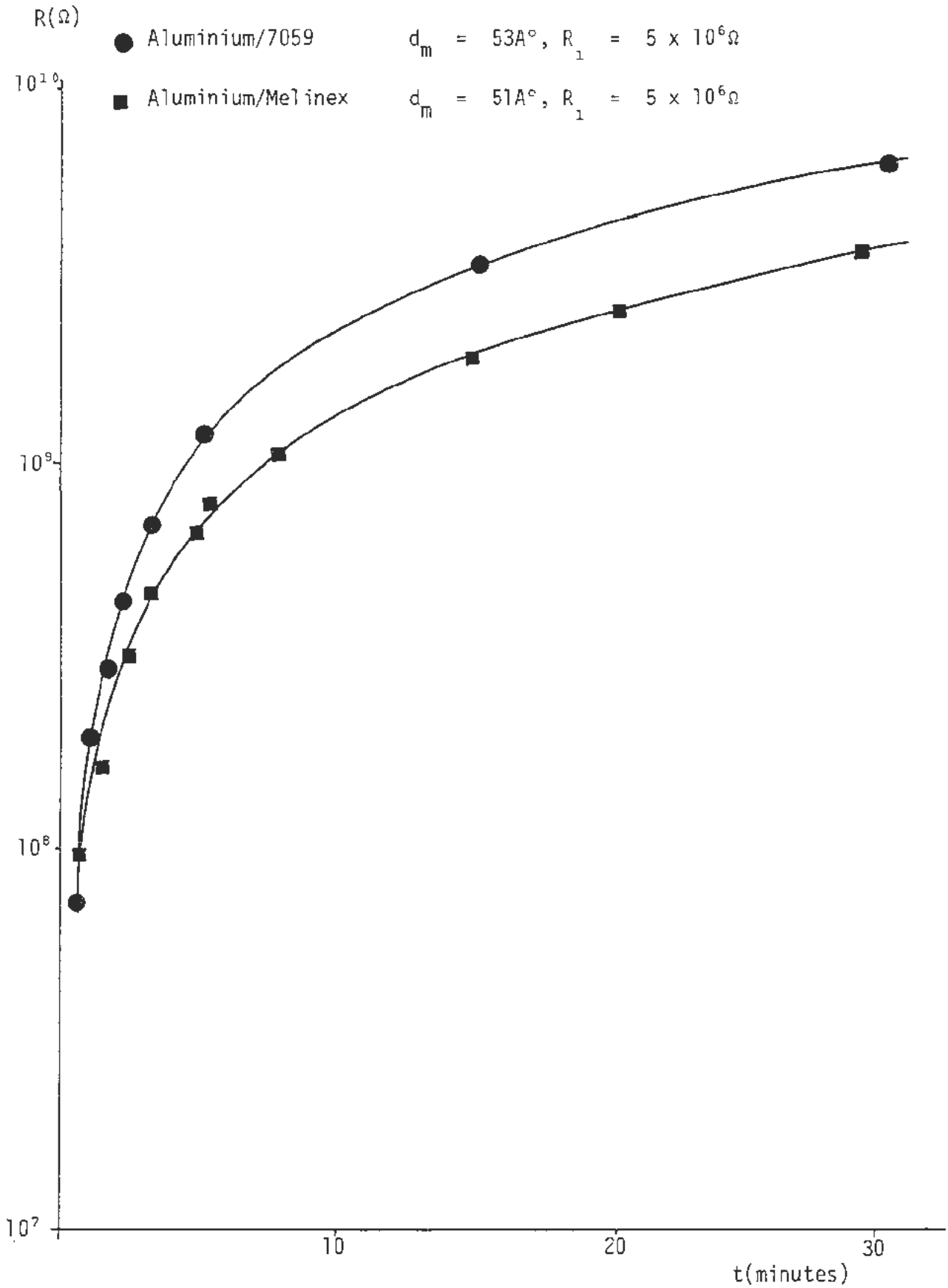

Fig. (3.20) Variation of the d.c. resistance of aluminium films with time in vacuur

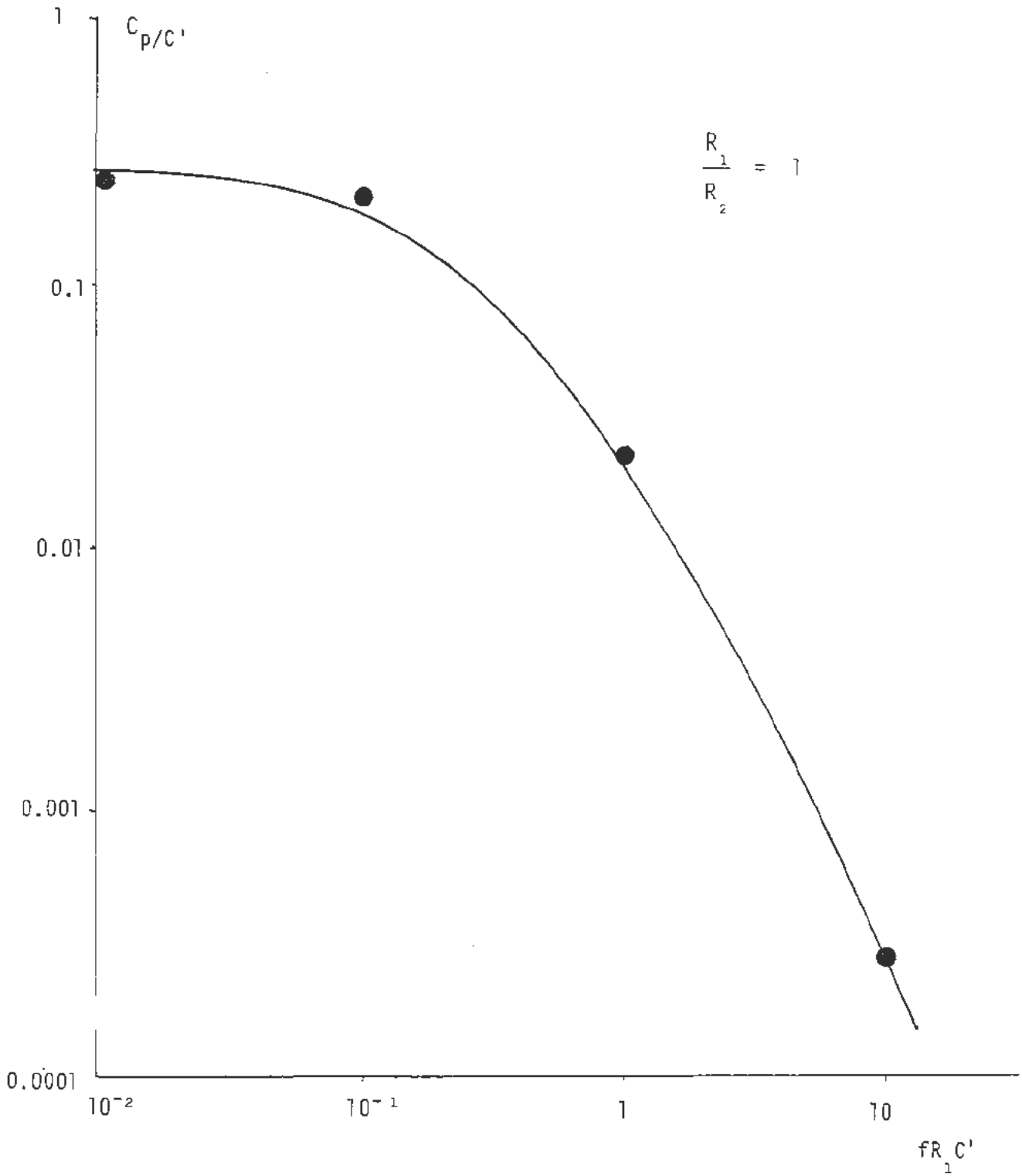

Fig. (3.21) Variation of $C_{p/C'}$ with $fC'R_1$ $(\frac{W}{\ell} = 1)$

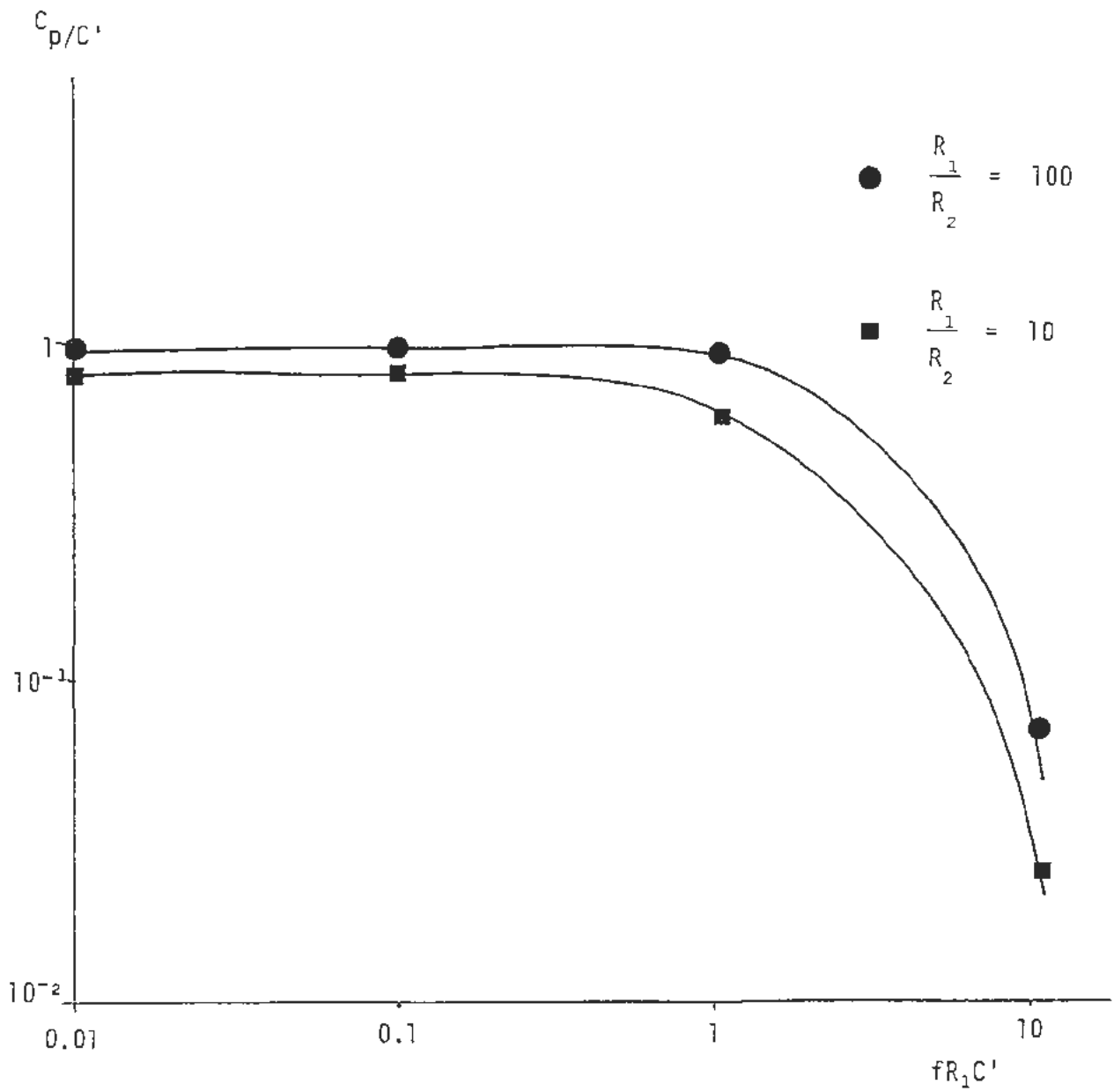

Fig. (3.22) Variation of $C_{p/C'}$ with $fC'R_1$ $\quad (\frac{W}{\ell} = 1)$

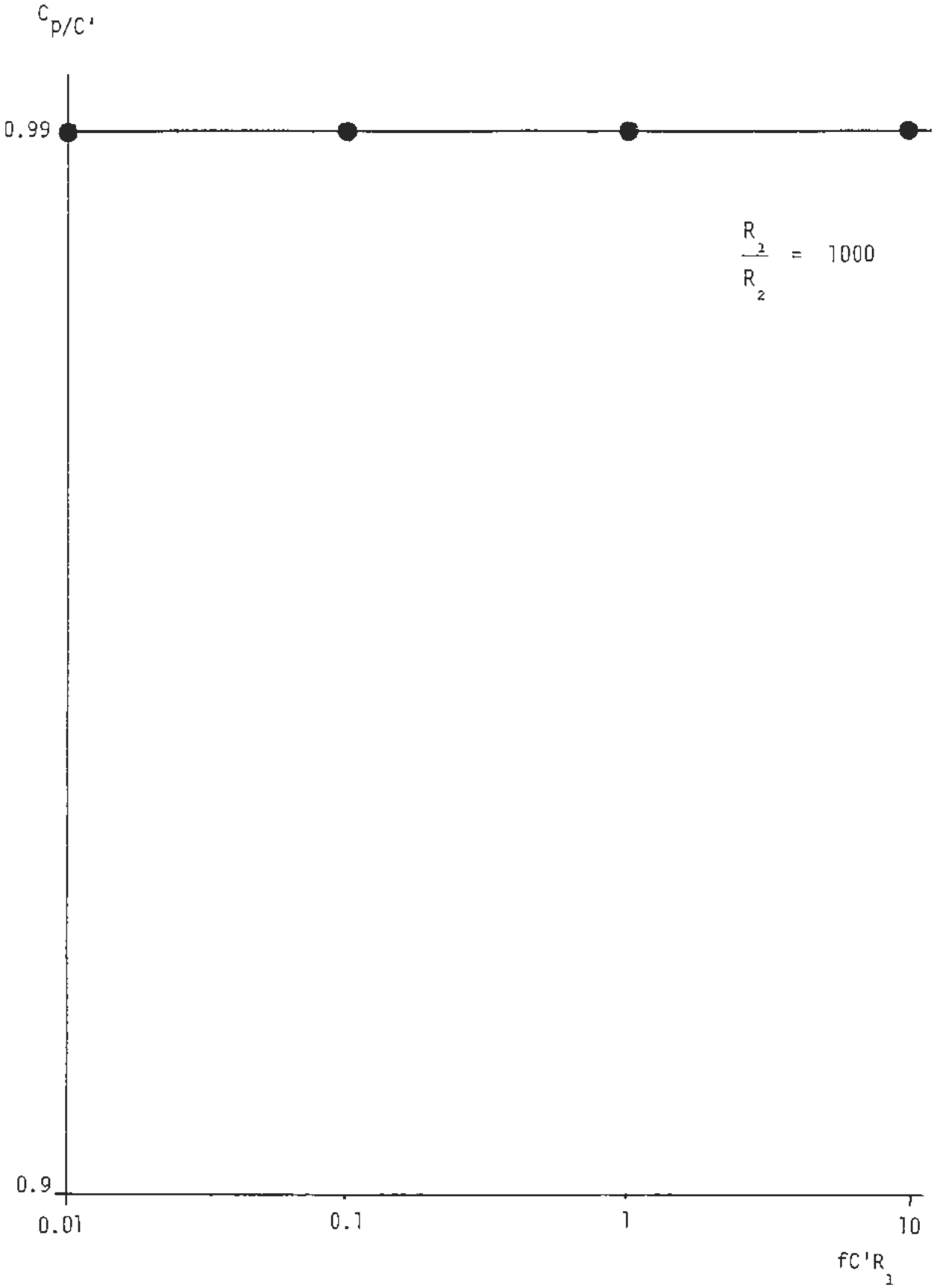

Fig. (3.23) Variation of $C_{p/C'}$ with $fC'R_1$ $(\frac{W}{\ell} = 1)$

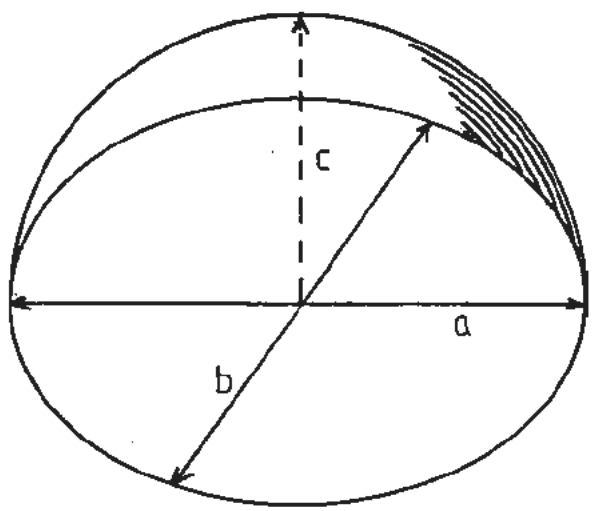

Fig. (3.24) Disc-shaped island

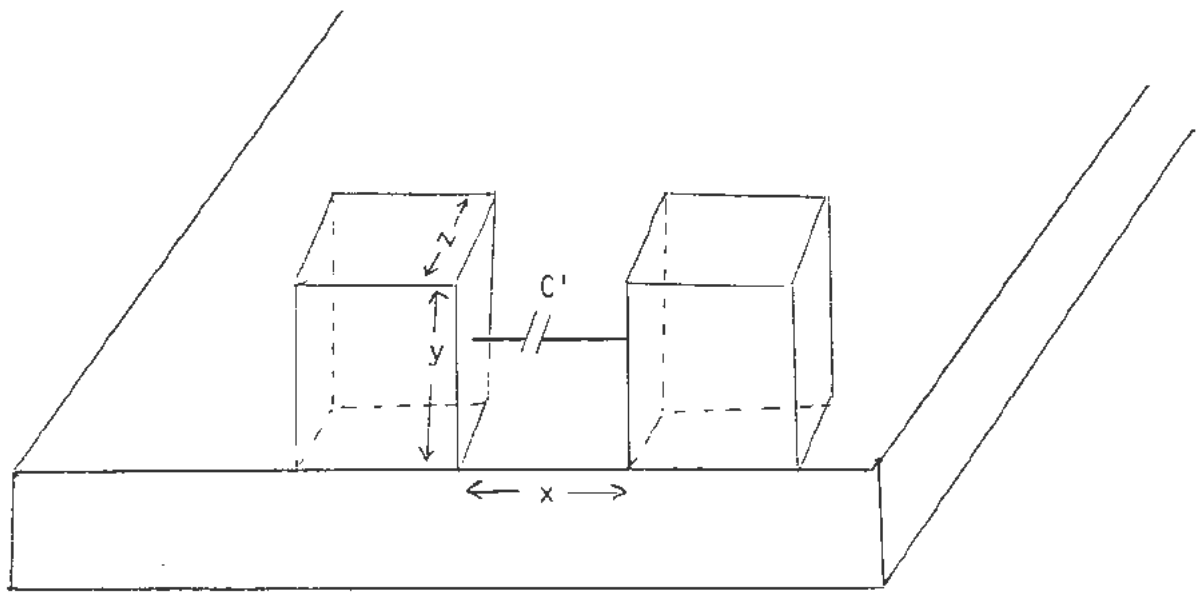

Fig. (3.25) Two elongated islands on surface of substrate

3.8 Determination of the film structure by transmission electron microscopy

The examination of the films by transmission electron microscopy requires the penetration of the beam through them and therefore it is necessary either to prepare films identical to those on which experiments were performed, but on sufficiently thin substrates, or to strip the actual films on which experiments were conducted. Generally, there are three possible methods to strip the film after backing it with thin layer of carbon (28) (i) to dissolve the substrate by the appropriate solvent, i.e, hydrofluoric and sulphuric acids for glass and Melinex respectively (60) (ii) mechanically with the aid of formavar and sellotape (iii) floating the film with carbon backing layer off by surface tension in a bath of water. It is well recognized that whatever the method of stripping is (87) it is never certain whether the structure observed is the same as that on the original substrate and it is probably not since if indeed the entire film does leave the substrate, then presumably this must be because the adhesion is greater to the carbon layer than to the substrate; in which case we would expect a change in the islands shape and in contact angle. In view of the disadvantages of the stripping methods, the films examined in the present work were deposited on electron microscope grids already loaded with thin carbon layer and located very close to the planar capacitors during the deposition of the discontinuous metal films. The micrographs shown in Figs. (3.26) to (3.29), which were taken with JEOL JEM100B transmission electron microscope at a magnification of 10,000X, reveal the discontinuity of the examined films.

3.9 Attempts to produce a larger enhancement in the planar capacitance

From the results presented in Tables (3.5) to (3.18) it is evident that the increase in the capacitance from (C_1) to (C_2) is small and associated with large dissipation factor (D_2). It is decided at this stage of research to explore some feasible approaches which may lead to a larger enhancement in the planar capacitance without profoundly affecting the original losses (D_1). The larger enhancement, if happened, will offer us the chance to study the effect of strain on capacitance hoping that a new capacitive transducer may be developed. Two approaches were tried (i) island films of Pd were first deposited because, as reported by other researchers (50), Pd nuclei provide nucleation sites for gold films and eventually larger and closer composite islands were formed. Discontinuous gold films were subsequently deposited but no advantageous effect of Pd nuclei was observed, (ii) by depositing aluminium with significant proportion of oxygen present (residual pressure 10^{-4}torr) there will be a possibility of laying down, at the moment of halting the deposition, aluminium islands separated from each other by an oxide layer and in that sense two-dimensional cermet may be obtained. In very rare number of experiments a larger enhancement was observed, i.e., the capacitance (C_2) and the dissipation factor (D_2) were 3pF and 0.027 respectively at 1Kc.

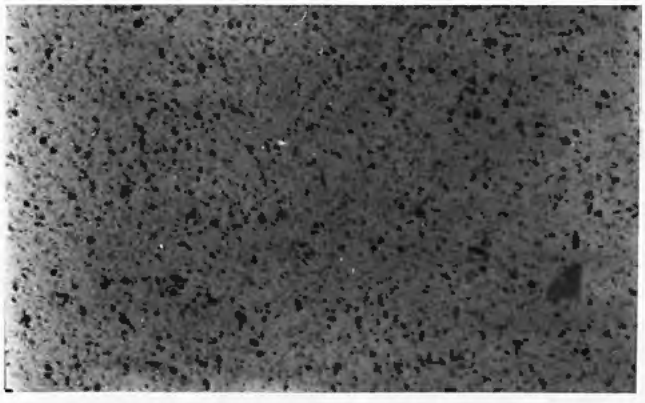

Fig. (3.26) Electron micrograph for aluminium film (d_m = 30A°)

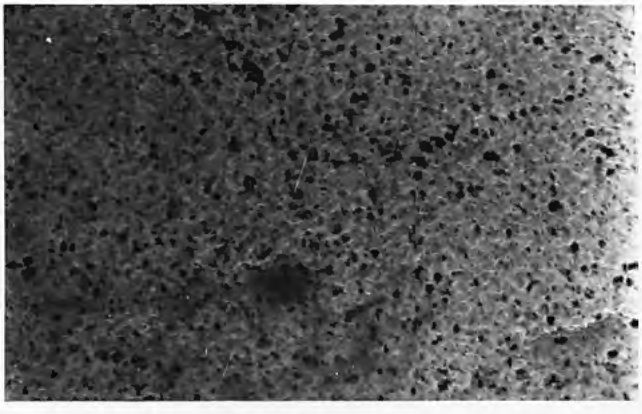

Fig. (3.27) Electron micrograph for aluminium film (d_m = 55A°)

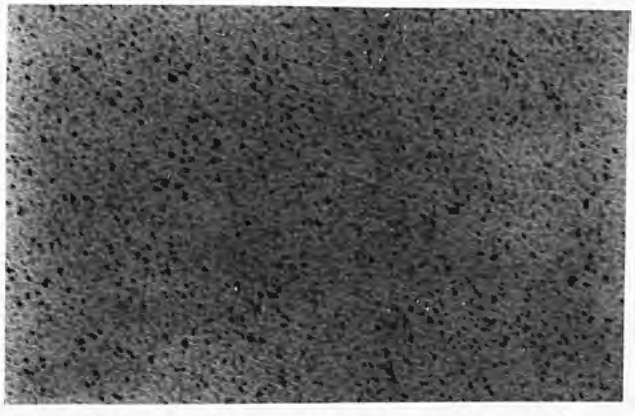

Fig. (3.28) Electron micrograph for gold film (d_m = 22A°)

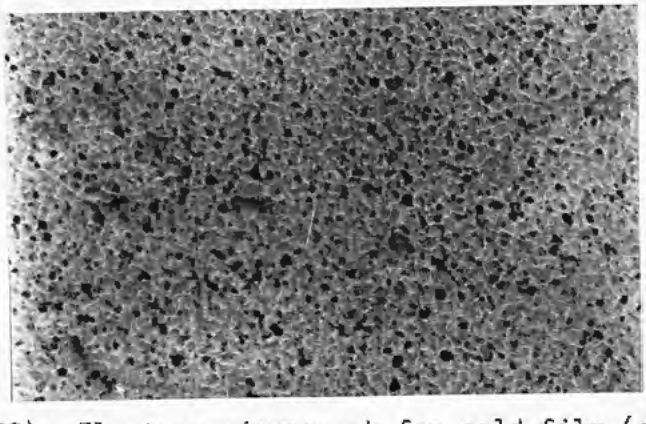

Fig. (3.29) Electron micrograph for gold film (d_m = 60A°)

CHAPTER 4 DISCUSSION AND CONCLUSIONS

4.1 Comments on the measured capacitance and dissipation factor of the planar capacitors

With reference to Tables (3.1) to (3.4), it can be seen that the measured capacitance is (i) larger in the case of open shield box and this will be explained in Section (4.3), (ii) decreases very slightly with the increase of frequency, perhaps, due to the reduction in the effective dielectric constant of the capacitor (88). Regarding the dissipation factor, it is independent of the frequency for glass substrates whilst it increases with frequency for Melinex. Generally speaking, the planar capacitor losses are of two types (89): those attributed to the dielectric substrate and those attributed to the thin film metallic electrodes. Once the base material (substrate) is chosen, nothing can be done in the planar capacitor design to materially reduce the losses due to this material. On the other hand, the second type of losses depends on the sheet resistance of the deposited electrodes and on the operating frequency. A lower value of the sheet resistance obviously will produce lower dissipation factor while higher frequencies cause larger losses (90,91). In view of the frequency range (1-100)Kc used in the present work, it is more likely to consider that the losses are due to the dielectric base and to justify this conjecture, the experimental values of the losses were compared with those reported for bulk glass (7059) and Melinex where reasonable agreement was found.

4.2 Comparison between the calculated and the measured planar capacitance

The calculated values of the planar capacitance, given by equations (3.1) and (3.2), are slightly larger than the measured ones as displayed in Tables (3.1) to (3.4); for glass as a dielectric the

differences are 0.0217pF and 0.0390pF in case of open and closed box respectively while for Melinex the differences are 0.0435pF and 0.0566pF. The measured values at 1Kc are chosen to find the differences. In fact the presence of the lid and the bottom of the shield box will reduce the contributions (C_I) and (C_{IV}) respectively; this reduction is well demonstrated in Figs. (3.1) to (3.4). Since the thickness of glass and Melinex are 0.8mm and 0.036mm respectively, the effect of the bottom on (C_{IV}) will be more pronounced in case of planar capacitors having Melinex as a dielectric. To sum up, allowing for the reduction caused by the shield box, the calculated values of the planar capacitance are in reasonable agreement with the measured ones.

4.3 Why the measured capacitance changes as a result of moving earthed sheet over and under the capacitor

The most striking points in Figs. (3.1) to (3.4) are (i) the decrease in the capacitance as the earthed metallic sheet approaches the capacitor from either directions (ii) the decrease in the capacitance is non-linear and more prononounced at lower values of y_1, y_2 [Fig. (2.3)]. The first remark could be explained by the fact that the electric field between two equipotentials (92) is equivalent to a capacitance which may tend to zero (70) if an earthed sheet completely surrounds one of the equipotentials and accordingly the measured planar capacitance should be a bit larger in the case of open shield box because in such a situation there will be more lines of force in the medium above the electrodes. The implication of the second remark is that the distribution of the electric lines of force around the capacitor is not uniform as shown in Fig. (4.1). Different practical devices have been

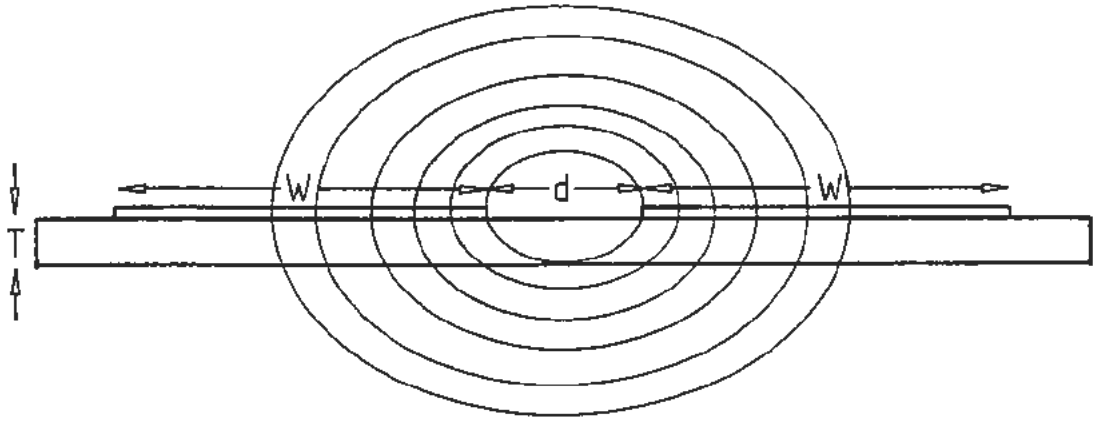

Fig. (4.1) Distribution of the electric lines of force when the condition T >> 2W + d is not valid

developed which utilize the principle of varying the planar capacitance as a consequence of changing the number of lines of force around the electrodes, like the capacitance altitude (93,94) and transducers (95) for determining the water content in wet soil. In the first, there is a direct capacitance between two insulated electrodes mounted on the aircraft and this capacitance will be affected by the proximity of the earth, which behaves as a conducting sheet, during taking off and landing. The variation of the capacitance could be used to determine the altitude of the aircraft. In the second, the number of electric lines of force above two interdigitated electrodes will partially depend on the effective dielectric constant of the medium containing the lines, for example, the dielectric constant of water is about 80 at 120Hz while that of normal completely dry soil is about 2.6 and so the presence of even small amount of water in the soil causes a drastic change in the effective dielectric constant providing that the wet soil forms the medium above the electrodes. The corresponding change in the planar capacitance could be calibrated to give the water content by weight in the soil.

4.4 Why the d.c. resistance of discontinuous gold and aluminium films increases after halting the deposition

Figures (3.19) and (3.20) show the remarkable increase in the resistance with time especially for aluminium films where after 30 minutes in vacuum the resistance became one thousand times the original one [$R_2 = 10^3 R_1$] while for gold films $\frac{R_2}{R_1}$ is nearly 10 for the same period of time. The immense increase in the resistance of aluminium films will be more appreciated if we remembered that (R_1) is $5 \times 10^6 \Omega$ and $5 \times 10^9 \Omega$ for aluminium and gold respectively.

In general the resistance of any film will vary after deposition, for low resistance films the resistance decreases with time and for higher resistance samples it increases (96-98) and it has been assumed that the two types of behaviour identify the films as continuous or discontinuous. For discontinuous films the rate of resistance variation with time (i) is great for large film resistance, (ii) is less for refractory metals and (iii) may be decreased by overcoating with silicon monoxide. Three types of explanation have been offered; the simplest of these is the temperature effect (99) where the film is heated during deposition by radiation from the source and as the deposition ceases the film cools freely to ambient. For discontinuous metal films the falling temperature will lead to an increasing resistance since such films possess negative temperature coefficient of resistance. The second explanation is based on the shape changes that are undergone by fixed islands. Nishiura and Kinbara (83) assumed the islands to have an oblate spheroidal shape and regarded this as variable with time after deposition. Their proposition was that the inter-island gap, and hence the tunnelling resistance, would increase as the islands tend to more spherical form. The final category of explanation is also the most complex, namely, the agglomeration effect (100-102). According to this category, the films are assumed to be composed of islands some of which are in thermally activated motion and so the formation, by coalescence, of larger islands is possible. The mobility of the islands on the substrate and the number of islands with sufficient energy to move is determined from an assumed thermal activation process. The activated islands are allowed to move, collide and combine with other islands, analogous to two dimensional gas. As the islands combine, the mean

gap increases with the implication of increasing the resistance. The aforementioned three explanations could possibly account for the increase in the resistance of aluminium and gold films. In order to account for the immense increase in the resistance of aluminium films, another important effect should be taken into consideration which is the susceptibility of these films to oxidation after deposition due to the presence of oxygen in the residual air atmosphere. To understand how the oxidation of the islands could lead to additional increase in the resistance, it will be assumed that tunnelling occurs from the surface of the metal island (77) and not from the surface of the oxide layer and consequently the tunnelling distance will increase by twice the oxide thickness as shown in Fig. (4.2).

4.5 Why the dissipation factor, after depositing the discontinuous films, changes with time and frequency

It is found that the dissipation factor (D_2) decreases with the increase of the operating frequency, the passage of time and the increase of the initial resistance of the films (R_1) as revealed in Figs. (3.5) to (3.18). In order to account for these findings, it will be appropriate to see the implications of laying down discontinuous metal films across the gap of the planar capacitor on its dissipation factor and capacitance. Regarding the impact on the dissipation factor, the conduction current between the two electrodes should increase as a result of reducing the d.c. resistance between them and consequently eqn. (1.10) can be used to account, qualitatively, for the present findings. The impact on the capacitance will be handled in the next section.

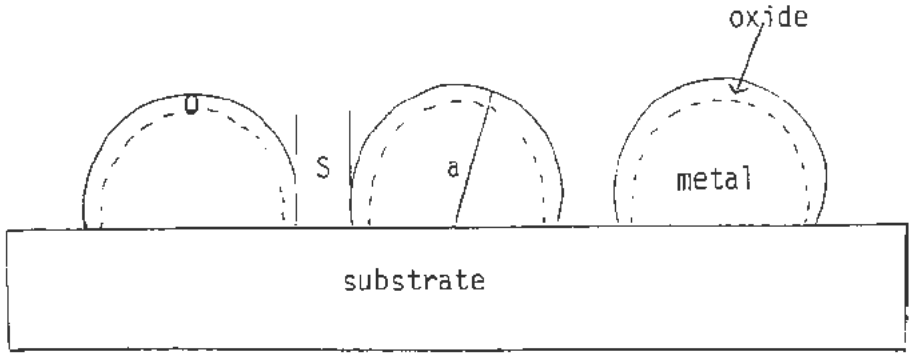

Fig. (4.2) Cross-section of discontinuous film;
S-inter-island spacing, a-island radius,
O-oxide thickness

4.6 Why the deposition of discontinuous metal films enhance the planar capacitance

The increase in the capacitance from (C_1) to (C_2') as indicated in Tables (3.5) to (3.18) is attributed to the fact that the films possess inherent parallel capacitiance $C_f = C_2' - C_1'$ (103). In theory, the increase in planar capacitance can be, qualitatively, tackled from another point of view, namely, the effect of the film (islands) on the different contributions to the planar capacitance. According to what has been stated in Section (1.5), the presence of the islands will increase (i) the dielectric constant of the substrate (eqn. 1.23) as shown in Fig. (4.3) and consequently enhance the substrate contribution (eqn. 1.3) to the planar capacitance. (ii) the dielectric constant of the medium separating the two faces 1,2 in Fig. (1.3) and hence promote the contribution c_{III} (eqn. 1.4); if the thickness (t_e) of the electrodes, in our planar capacitors, is assumed to be 10^3A° then c_{III} will be 0.1×10^{-4}pF which is indeed extremely small compared with the other two contributions as calculated in Section (3.3). It is evident from Fig. (4.3) and eqn. (1.22) that the larger the surface coverage of the islands the larger the enhancement in both the substrate contribution and c_{III}; this can be achieved by depositing films having large islands (a) and narrow gaps (s) but it has always been found too difficult to produce such films because of the structural changes caused by surface mobility and island coalescence (104).

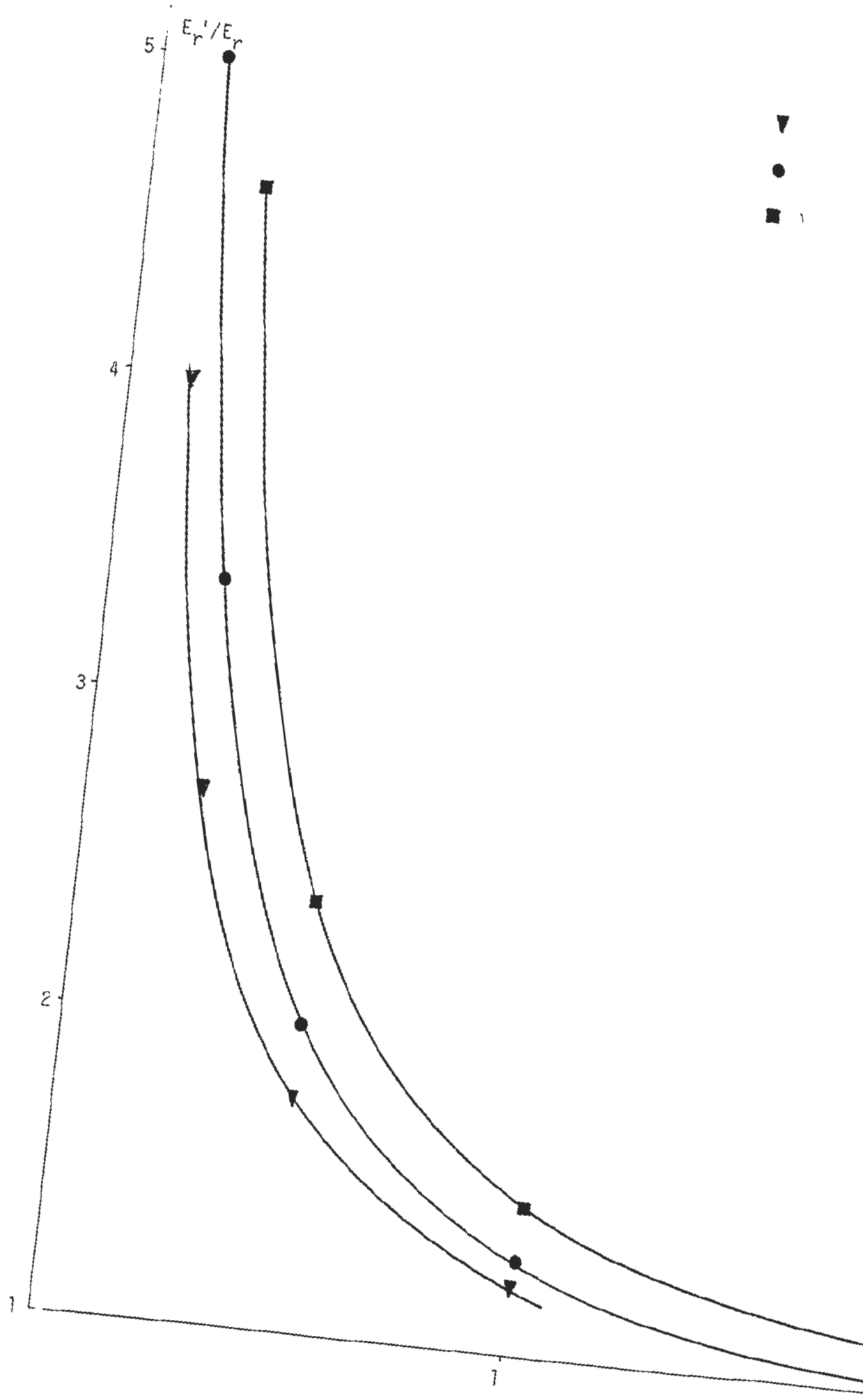

Fig. (4.3) Dependence of $\frac{E_r'}{E_r}$

4.7 Comments on the measured capacitance of discontinuous gold and aluminium films

Regarding the measured capacitance of the films (C_f), the following remarks are relevant: (1) it increases with the increase of (R_1), (2) it increases with lowering the operating frequency, (3) it decreases with the elapse of time especially for aluminium films perhaps due to the growth of the oxide layer on the surface of the islands, (4) the type of the substrate has not any appreciable effect on (C_f). Remarks 1 and 2 are reasonably comply with the predicted behaviour of the capacitance as shown in Figs. (3.21) and (3.22). In fact it is necessary to compare the values of the measured capacitance for our films with (i) the calculated capacitance as described in Section (3.3), (ii) the values of the measured capacitance already reported in the literature, namely, the capacitance of Pd and Mn films. The comparison has revealed that, in the first case the measured values are larger than the calculated ones and which can be attributed to the drawback of the model used in Section (1.4.b) which is too simplified since it neglects the capacitance between non adjacent islands (105), i.e., the capacitance between each island and every other island in the film. While in the second case our measured values are much smaller than those supposed to be for Pd and Mn films (Section 1.4.d). From the experience gained in the present work we think that the allocation of the measured capacitance, by the other investigators (49,50) to be only for the studied films (Pd, Mn) was inappropriate because apart from the films capacitance, the presence of the planar capacitance between the electrodes, the capacitance between the leads and more likely the parasitic capacitance would naturally contribute to the measured capacitance.

4.8 Conclusions

The following conclusions can be stated:

1- The calculated values of the planar capacitance are slightly larger than the measured ones; but they could be in reasonable agreement if we allow, qualitatiively, for the reduction in the contributions (C_I) and (C_{IV}) from the media above the electrodes and underneath the substrate respectively. The reduction is due to the presence of the lid and the bottom of the shield box which enclosed the capacitors during the measurements.

2- The measured planar capacitance decreases as a result of moving an earthed metallic sheet towards the capacitor since the number of the electric lines of force will diminish as the sheet approaches the electrodes or the back of the substrate.

3- Within the used range of operating frequency (1-100)Kc, the measured dissipation factor of the planar capacitors is due to the losses in glass or Melinex.

4- The dissipation factor of the planar capacitor is attenuated, as a result of depositing discontinuous metal film across the gap between the two electrodes, such that it decreases with (i) the increase of the operating frequency (ii) the increase of the initial d.c. resistance of the film (iii) the passage of time after halting the deposition.

5- The measured parallel capacitance (C_f) of discontinuous gold and aluminium films decreases with (i) the decrease of the initial d.c. resistance of the films (ii) the increase of the operating frequency (iii) the elapse of time especially for aluminium films due to the growth of the oxide layer on

the surface of the islands.

6- The type of the substrate (glass or Melinex) has not any apprecial effect on the capacitance of the films.

7- The measured parallel capacitances (C_f) of our films are much smaller than those reported and supposed to be for Pd and Mn films whilst the values of (C_f) are larger than the calculated ones (C_p).

4.9 Suggestions for further research

1- The enhancement of the dielectric constant of a substrate (E_r) can be predicted from eqn. (1.23) as deduced by Leaver (54). In fact an independent experimental evidence is required to endorse Leaver's view and this can be achieved by the in situ monitoring of the planar capacitance as a result of laying down discontinuous metal films on the back of the substrate and not across the gap between the two electrodes. The advantage of this situation is to avoid any changes in the dissipation factor and to concentrate the attention on the expected increase in the planar capacitance only.

2- The determination of the films structure will be ideally relevant to our objectives, as stated in Section (1.6), if a correlation between the expected increase in planar capacitance and the surface coverage (106) of the islands can be confirmed. There is no reason, in principle, why an entire deposition of discontinuous metal films, measurement of the changes in the planar capacitance and determination of the surface coverage should not be carried

out within an electron microscope. Similar experiments (107) have been performed in studies of nucleation of metals, and the only additional complication would be that of providing electrical contacts.

3- No attempt has been undertaken so far to measure the capacitance of thin film cermets. The capacitance of these films can be measured by the in situ monitoring of the changes in the planar capacitance as a consequence of:

(i) simultaneous deposition of metal and insulator films across the gap of the capacitor,

(ii) depositing several different layers on top of each other such that any second layer is discontinuous metal film whilst the rest of the sample is composed of insulating continuous films.

REFERENCES

1. R.W. Berry, R.M. Hall and M.T. Harris, "Thin Film Technology", Van Nostrand Reinhold Co., New York (1968)

2. W.W. Happ, Electronic Industries E4 (1962)

3. H.R. Kaiser and P.S Castro, Lockheed Tech. Rept. 6-59-61-2 (1961)

4. Y. Song, J. Appl. Phys. 47, 2651 (1976)

5. F.Z. Keister and R.W. Scapple. Trans. Nat. Vac. Symp. 116 (1962)

6. L. Binotto and G.F. Piacentini, Thin Solid Films 12, 325 (1972)

7. N.D. Channon and P.G. Barnwell, IERE Conference Proceedings No. 31 Conference on Hybrid Microelectronics - University of Technology Loughborough (1975)

8. R.G. Bennett and J.H. Calderwood, "Complex Permittivity", The English University Press (1971)

9. B.A. Gregory, "An Introduction to Electrical Instrumentation and Measurement Systems", second ed., Macmillan, (1981)

10. F.E. Terman, "Radio Engineers Handbook", McGraw-Hill, (1943)

11. A.T. Dover and F.T. Chapman, "Electrical Engineering", Longmans, (1961)

12. P.J. Harrop, "Dielectrics", Butterworths (1972)

13. B. Hague, "Alternating Current Bridge Methods", 6th ed., Pitman Press (1971)

14. M.G. Evers, Philips Res. Repts. 1, 161 (1946)

15. K.L. Horovitz and V.A. Johnson, "Methods of Experimental Physics", Vol. 6, part 13 (1959)

16. W.F. Swann, Phil. Mag. 28, 467 (1914)

17. Z.H. Meiksin, in "Physics of Thin Films" (G. Hass, M.H. Francombe and R.W. Hoffman, eds.) Vol. 8, Academic Press (1975)

18. C.A. Neugebauer and M.B. Webb, J. Appl. Phys. 33, 74 (1962)

19. T.E. Hartman, J. Appl. Phys. 34, 943 (1963)

20. K.V. Van Steensel, Philips Res. Repts. 22, 246 (1967)

21. N. Mostovetch and B. Vodar, in "Semiconducting Material" (H.K. Henick, ed.) (1951)

22. C.A. Neugebauer and R.H. Wilson, Proc. Intern. Symp. Thin Films, Clausthal 579 (1965)

23. N.M. Bashara and L.A. Weitzenkamp, J. Appl. Phys. 35, 1893 (1964)

24. R.M. Hill, Nature 204, 35 (1964)

25. A.A. Milgram and C.S. Lu, J. Appl. Phys. 37, 4773 (1966)

26. C.A. Neugebauer, Trans. 9th Natl. Vac. Symp. Am. Vac. Soc. 149 (1962)

27. R.M. Hill, Proc. Roy. Soc. A309, 377 (1969)

28. R.M. Hill, Proc. Roy. Soc. A309, 397 (1969)

29. J.L. Vassen, in "Physics of Thin Films" (G. Hass, M.H. Francombe and R.W. Hoffman, eds.) Vol. 9, Academic Press, (1977)

30. L. Kasprzak, R. Laibowitz, S. Herd and M. Ohring, Thin Solid Films 22, 189 (1974)

31. K.L. Chopra, Appl. Phys. Letters 7, 140 (1965)

32. K.L. Chopra, J. Appl. Phys. 37, 2249 (1966)

33. O.I. Kennedy, R.E. Hayes and R.W. Alsford, J. Appl. Phys. 38, 1986 (1967)

34. J. Lebas, C.R. Acad. Sci., Ser. B268, 1393 (1969)

35. E. Ahilea and A.A. Hirsch, J. Appl. Phys. 42, 5601 (1971)

36. L. E. Murr and H.P. Singh, Appl. Phys. Letters 20, 512 (1972)

37. M. Koedam, Philips Res. Repts. 16, 266 (1961)

38. A.V. Joglekar, J. Phys. (D) 7, 1270 (1974)

39. P. Datta and H. Kawamoto, RCA Review 43, 212 (1982)

40. W.R. Smyth, "Static and Dynamic Electricity", 2nd ed., McGraw-Hill, (1950)

41. Ibid., p. 118

42. J.E. Swanson, D.S. Campell and J.C. Anderson, Thin Solid Films 1, 325 (1967)

43. A.A. Hirsch and S. Bazian, Physica 30, 258 (1964)

44. M.A. Angadi and P.V. Ashrit, J. Mater. Sci. 16, 3513 (1981)

45. M.A. Angadi and S.M. Shivaprasad, J. Mater. Sci. Letters 2, 207 (1983)

46. S.M. Deshpand and A.D. Crowell, J. Vac. Sci. Technol. 9, 97 (1972)

47. B.W. Wlicznerski, Thin Solid Films 55, 361 (1978)

48. J.E. Morris, Thin Solid Films 36, 29 (1976)

49. E.M. Castro and J. Beynon. Thin Solid Films 66, L21 (1980)

50. P.A. Tick and F.P. Fehlner, J. Appl. Phys. 43, 362 (1972)

51. W.E. Kock, Bell System Technical Journal 27, 58 (1948)

52. G.C. Riddle, Proceedings of the Symposium of Electron Beam Technology, p. 351 (1962)

53. M.M.Z. Kharadly and W. Jackson, J.I.E.E. 100, 199 (1953)

54. K.D. Leaver, J. Phys. (C) 10, 249 (1977)

55. M.S. Raven, Phys. Rev. B 29, 6218 (1984)

56. P. Lloyd, Brit. J. Appl. Phys. 15, 1349 (1946)

57. G.A. Johand and S.W. Chaikin, I.E.E.E. Trans. on parts, material and packaging PMP-2, 29 (1966)

58. J. Fridrich, Thin Solid Films 7, 277 (1971)

59. F.W. Schenkel, I.E.E.E. Trans. Components parts CP-11, 194 (1964)

60. M.J. Knight and K.N. Jha, Thin Solid Films 2, 131 (1968)

61. M.J. Knight, J. Vac. Sci. Technol. 6, 706 (1969)

62. J. Beynon, Electronic Eng. 40, 609 (1968)

63. R. Brown in "Handbook of Thin Film Technology" (L. I. Maissel and R. Glang, eds.), McGraw-Hill, (1970)

64. L. Holland, "The properties of Glass Surfaces" Chapman and Hall (1964)

65. F.K. Harris, "Electrical Measurements", John Wiely, (1952)

66. W. Alexander, "Electrical Instruments and Measurements", 2nd ed., Cleaver-Hame (1962)

67. P.K. Weimer, in "Physics of Thin Films" (G. Hass and R.E. Thun, eds.), Vol. 2, Academic Press (1964)

68. J.E. Dryer, Ph.D. thesis, Ohio State University (1972)

69. J.F. Hersh, General Radio Experimenter 33, 7 (1959)

70. A.M. Thompson, I.R.E. Trans. Instrument I-7, 245 (1958)

71. J.F. Hersh, General Radio Experimenter 36, 3 (1962)

72. S.M. Boyer, B.H. Claussen, Third European Hybride Microelectronics Conference, p. 345 (1981), Avignon

73. R.N. Gupta and M. Misra, Indian J. Pure and Applied Phys. 19, 1151 (1981)

74. C.M. Huggins and A.H. Sharbaugh, J. Chem. Phys. 38, 393 (1963)

75. R.M. Hill, Contemp. Phys. 10, 221 (1969)

76. H. Fredriksoon, B. Persoon and L. Ystrom, Phys. Scr. 3, 169 (1971)

77. F.P. Fehlner, Advances in Vacuum Science and Technology, Vol. 2, part 3, 691 (1965)

78. S.L. McCarthy. J. Vac. Sci. Technol. 13, 135 (1976)

79. H.K. Chaurasia and W.A. Voss, Nature 244, 28 (1974)

80. W.R. Holland and D.G. Hall, Phys. Rev. Letters 52, 1041 (1984)

81. G. Sauerbrey, Z. Physik 155, 206 (1959)

82. M.P. Lostis, J. Phys. Radium 20, 25 (1959)

83. M. Nishiura and A. Kinbara, Thin Solid Films 24, 79 (1974)

84. T. Andersoon, J. Appl. Phys. 47, 1752 (1976)

85. T. Andersoon. Thin Solid Films 29, L21 (1975)

86. C.G. Granqvist and R.A. Buhrman. J. Appl. Phys. 47, 2200 (1976)

87. J.E. Morris and T.J. Coutts, Thin Solid Films 47, 3 (1977)

88. C.G. Koops, Philips Tech. Rev. 5, 300 (1940)

89. R.W. Scapple, Proceeding of the 24th of electronic components conference, p. 203 (1974)

90. P.K. Reddy, Thin Solid Films 109, 339 (1983)

91. T. Wiktorczyk and C. Wesolowska, Thin Solid Films 120, 171 (1984)

92 F. Futschik, Proc. Electronic Components Conference, p. 278 (1968)

93. W.L. Walton and M.E. Pemberton. Proc. I.E.E. 96, 379 (1949)

94. T.S. Mcleod and C.M. Deavin, Proc. I.E.E. 110, 1505 (1963)

95. S.P. Lucas, M.R. Casey, R.K. Blacksome and W.H. Dawes, Proc. of the 24th Electronic Components Conference, p. 130 (1974)

96. M.R. Neumann and W.G. Sutton, J. Vac. Sci. Technol. 6, 710 (1969)

97. C.A. Neugebauer, Trans. 9th Natl. Vac. Symp., p. 45 (1962)

98. T. Andersoon, J. Phys. (D) 9, 76 (1976)

99. J.E. Morris, Vacuum 22, 153 (1972)

100. W.B. Philips, E.A. Desloge and J.G. Skofronick, J. Appl. Phys. 39, 3210 (1968)

101. J.G. Skofronick and W.B. Philips, J. Appl. Phys. 38, 4791 (1967)

102. J.G. Skofronick and W.B. Philips, in "Basic Problems in Thin Film Physics" (R. Niedermeyer and H. Mayer, eds.), P. 591, Van den Hoeck and Rupprecht (1966)

103. R. Broudy and H. Levinstein, Phys. Rev. 94, 285 (1954)

104. T.J. Coutts, "Active and Passive Thin Film Devices", Academic Press, (1978)

105. R.J. Weber, I.E.E.E. Trans. on Parts, Materials and Packaging PMP3, 14 (1967)

106. P.P.L. Regtien, Solid State Sensors, p. 109 (1980)

107. H. Poppa, Thin Solid Films 34, 94 (1976)